‘GREEN’ HYDROPHOBIC TREATMENT FOR COTTON FABRICS

A Thesis

Presented to the Faculty of the Graduate School

of Cornell University

In Partial Fulfillment of the Requirements for the Degree of

Master of Science

by

Yidong Zhong

August 2014

ABSTRACT

Greener approaches for hydrophobic treatment of cotton fabric were studied. In the first method, fatty acid was grafted onto cotton (cellulose) fiber surface to decrease the surface energy. Acetic anhydride was used to facilitate the reactivity. Microwave heating, an energy efficient method, was used to reach the reaction temperature. The 'green' method developed here resulted in hydrophobic cotton fabric with a water contact angle of 137.48^{o} (± 2.79). In addition, it was shown that the hydrophobicity lasted for 37 cycles of laboratory laundry washes.

A second method involved using of amine-silica nanoparticles to increase the surface roughness of cotton fabric. The effects of attaching single or dual size nanoparticles as well as chemical and physical attachment of particles onto cotton fiber surface were studied. Cotton fabric with deposited particles was further crosslinked to obtain possible 'permanent' surface topography. Different crosslinkers were used to test wash durability of final products. Resulting cotton fabrics were treated by fatty acid hydrophobic treatment, water contact angle as high as 153.41^{o} (± 2.33) was achieved. These fabrics with water contact angles of greater than 150^{o} can be considered as superhydrophobic. Resulting crosslinked and hydrophobic cotton fabric allowed 24 cycles of laboratory laundering without the loss of hydrophobicity.

BIOGRAPHICAL SKETCH

Yidong Zhong was born in Shangyu, Zhejiang Province, China on Nov. 11th of 1988. He participated in a joint degree program for undergraduate study. In June 2012, he graduated from Humboldt State University (Arcata, California) and Hefei University of Technology (Hefei, China), with Bachelor of Science degree in Chemistry and Bachelor of Engineering degree in Chemical Engineering, respectively.

In Aug. 2012, he enrolled in Fiber Science program at Cornell University. In Aug. 2014 he graduated after working with Prof. Anil N. Netravali and his ‘Green Materials’ group with a Master of Science degree. After graduation, he will start his career in industry.

Dedicated to My Family

ACKNOWLEDGMENTS

I would like to thank my thesis advisor, Prof. Anil N. Netravali, for his suggestions and encouragement. Also, I would like to thank my minor advisor, Prof. Minglin Ma, for valuable discussion.

I had fortune to do research with talented colleagues in the Department of Fiber Science & Apparel Design. I thank our department and CCMR for the use of instruments.

TABLE OF CONTENTS

LIST OF FIGURES

LIST OF TABLES

1 LITERATURE REVIEW

With increased awareness of sustainability from academia, industry and governments, finding alternative to petroleum derived products has been a key research goal for the past couple of decades. Most plant derived natural biopolymers are considered renewable materials and some of them exhibit properties comparable to petroleum based products. For thousands of years biopolymers have been used based upon their natural properties. With modern advances in science and technology, it has been possible to modify biopolymers to improve their properties and even render many novel and/or desired properties that the nature has not bestowed upon them (Heinze and Wagenknecht, 1988); (Heinze and Liebert, 2001).

Cotton fibers are inherently hydrophilic because of their chemistry consisting of glucose units, each consisting of 3 hydroxyl groups. Making their surface hydrophobic would make it useful in a wide range of applications including self-cleaning textiles, water/oil separation, anti-biofouling, friction reduction etc. (Lai *et al.*, 2011); (Klemm *et al.*, 2005), As a result, there have been many efforts to give cotton fiber surfaces hydrophobicity (Heinze and Wagenknecht, 1988). None of them, however, have used or developed green technologies, need of the current day. The present study focuses on the development of novel greener methods to impart hydrophobic characteristics to cotton fabrics which could be useful in developing water repellent apparel.

1.1 Cellulose

Cotton mainly consists of cellulose, one of the most abundant polymers on earth, and being produced yearly, it is considered as an inexhaustible material (Klemm *et al.*, 2005). Chemical composition of cotton can be varied with different origin with proximate composition as listed in Table

1.1 (Hon *et al.*, 1998). Cellulose is a linear homopolymer consisting of β- (1→4) linked D-glucose units as shown in Figure 1.1. Within each glucose unit, number 2, 3, and 6 carbons have hydroxyl groups, respectively, giving the cellulose molecule its highly hydrophilic characteristic and thus limiting its applications. Most chemical modifications of cellulose have used these three hydroxyl groups because of their polar/reactive nature compared to the rest of the molecule.

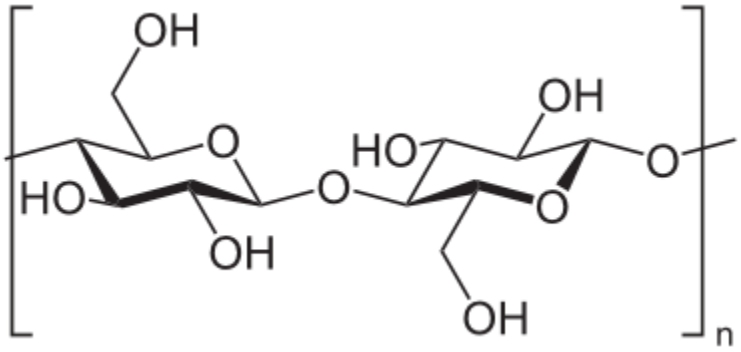

Figure 1.1: Molecular repeat unit (cellobiose) of cellulose (Klemm *et al.*, 2005)

Cellulose esters have been successfully applied in industrial applications for more than 50 years, especially in the form of short chain cellulose ester (i.e. acetic, propionic and butyric) (Heinze and Glasser, 1998). The application fields for cellulose esters include cosmetics, food, construction materials, paper and so on. (Heinze and Wagenknecht, 1988); (Heinze and Liebert, 2001): (Navard, 2012).

Table 1.1: Chemical composition of cotton (Hon *et al.*, 1998)

	Composition (%)			
	Cellulose	Hemicellulose	Lignin	Ash
Cotton	95	2	0.9	0.4

Naturally occurring fatty acids are biocompatible and biodegradable, the long alkyl backbone chain has much lower surface tension compared to the hydroxyl groups on cellulose. By grafting fatty chain onto cellulose surface the hydrophobicity of cellulose surface can be increased. However, fatty acids

show extremely low reactivity toward the cellulosic hydroxyl groups (Jansura *et al.*, 2000).

Up to date, numerous methods have been published to facilitate the fatty acid reactivity toward cellulose (Wang and Tao, 1994); (Vaca-Garcia *et al.*, 1998); (Chaucelon *et al.*, 1999). Most of these reactions have been performed in homogenous solutions, which require proper solvent to dissolve the cellulose. On the other hand, some researchers have put an emphasis on enhancing the reactivity of the fatty acids, thus, making their reaction with cellulose easy. Some outstanding representatives include *in-situ* activation of carboxylic/fatty acids by *N,N'*-Dicyclohexylcarbodiimide (DCC), *N,N'*-Carbonyl -diimidazole (CDI) and *p*-Toluenesulfonyl chloride (Navard, 2012).

1.2 Structure and accessibility

Cellulose can be regarded as a polyalcohol. However, the reactivity of cellulose with organic acids towards esterification is much lower than common alcohols (Heinze and Wagenknecht, 1988). The reasons can be explained by the low accessibility of cellulosic hydroxyl groups and weak electrophilic nature of the fatty acids.

As mentioned earlier in the introduction, each anhydroglucose unit contains three hydroxyl groups, and they are extensively involved in both intra- and inter-molecular hydrogen bonding as shown in Figure 1.2 (Navard, 2012). These hydrogen bonds allow molecules to be pulled together facilitating crystallization. The formed crystalline regions are highly aligned and packed structure (Heinze and Liebert, 2001). This is helped by the linear nature of the cellulose molecule. Without breaking of the hydrogen bonding, the lone pair electron on hydroxyl oxygen can only have low affinity towards nucleophilic attack. Which means that in order to achieve the maximized hydroxyl group's accessibility, the hydrogen bonding network has to be destroyed.

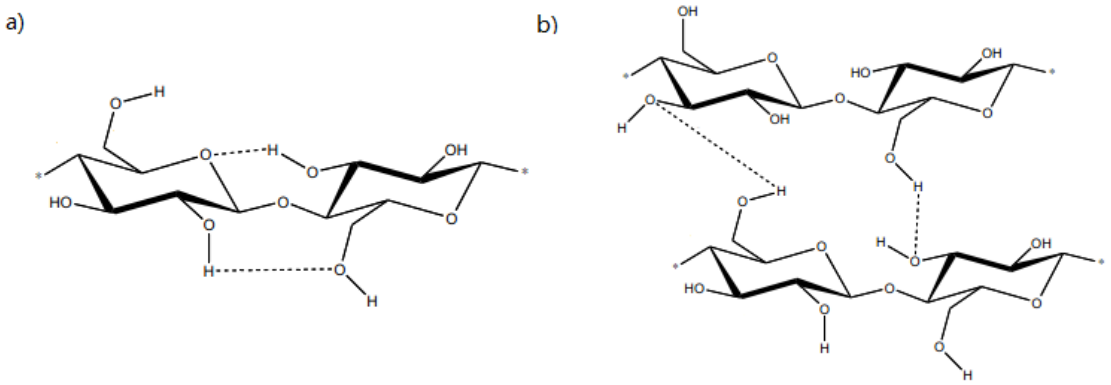

Figure 1.2: a) Intramolecular bonds; b) intermolecular bonds in cellulose structure (Navard, 2012)

1.3 Fatty acid

In nature, fatty acids are mostly found in the ester form, linked with glycerol, cholesterol or aliphatic alcohols (Christie, 1993). The chemical structure of a typical fatty acid contains a carboxylic group on one end of its backbone chain and the rest are hydrocarbons. Based on the degree of saturation, fatty acids can be divided into three groups; monounsaturated (only one double bond), polyunsaturated (more than one double bonds), and saturated (no double bond).

Esterification reaction between the hydroxyl group on cellulose and the carboxyl group on the short-chain carboxylic acid has been extensively studied (Satge *et al.*, 2002); (We *et al.*, 2004); (Edgar *et al.*, 2001); (Maim *et al.*, 1951). However, few reports have shown the esterification between long-chain fatty acid and cellulose. Since the speed of esterification reaction is determined by the step where lone pair of electron on hydroxyl group attack carbonyl carbon, the reactivity of a carboxyl group has a positive correlation with electron deficiency of carbonyl carbon. The low reactivity of fatty acid is caused by electron donating property of fatty acid chain. Longer fatty acid chain will result in attenuating the positive characteristic of carbonyl carbon, thus reduce the chance for reaction to take place.

1.4 Activation of fatty acid

From above discussion it is clear that the fatty acids need activation for the esterification reaction with cellulose. Such activation can be accomplished by reacting the fatty acid with desired chemicals to form more reactive intermediates. Usually, this intermediate molecule has an electron withdrawing group attached to the carbonyl carbon, which enhances the electron deficiency characteristic of carbonyl carbon. More positive character of carbonyl carbon means higher affinity for a nucleophile to attack and hence better chance of reaction.

1.4.1 Fatty halides

Fatty acids can react with sulphonic acid chloride (TosCl), and the reaction products are fatty chloride, fatty anhydride and sulphonic acid as shown in Figure 1.3 (Heinze, 2006). The esterification mechanism of fatty acid in the presence of TosCl is still being debated, however, based on ^{1}H NMR results of acetic acid and TosCl reaction, the formation of acetic anhydride and acetyl chloride is believed to cause the esterification with cellulose.

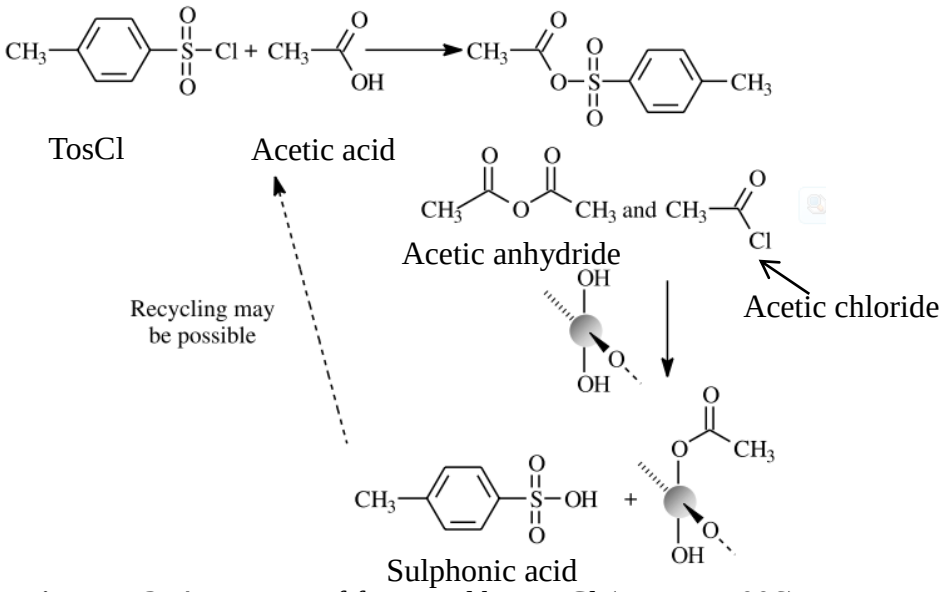

Figure 1.3: Activation of fatty acid by TosCl (Heinze, 2006)

Lithium chloride/*N*,*N*-dimethylacetamide (LiCl/DMAc) is the preferred solvent for this reaction, and pyridine is recommended to be present in the reaction mixture (Heinze, 2006). It's believed that pyridine can neutralize the by-product, hydrochloric acid. However, fatty halides method will always cause the degradation of cellulose.

1.4.2 Anhydride

Vaca-Garcia pioneered the use of acetic anhydride as co-reactant to facilitate the graft of fatty chain on cellulosic material (Vaca-Garcia *et al.*, 1998). Cellulose mixed triesters was synthesized with an average of 2.2 acetyl groups and 0.8 fatty substituents per anhydroglucose unit. Based on their published method, LiCl/DMAc was used as homogeneous solvent system and 130^{o}C thermal heating for 5 hrs was required to achieve full substitution.

1.4.3 Others activation methods

N,*N*-dicyclohexylcarbodiimide (DCC) is another powerful chemical that can transform fatty acid into more reactive intermediate. Samaranayake *et al.* studied the acylation of cellulose in homogeneous solution using DMAc/LiCl as solvent (Samaranayake and Glasser, 1993). In their study fatty acid was activated by DCC and 4-pyrrolidinopyridine (PP) as catalyst, the results show that by changing the reaction conditions, degree of substitution (DS) can vary from 0 to 2.5 (from acetic to stearic acid). The mechanism for this reaction is illustrated in Figure 1.4. The major drawback of this method is the high toxicity of DCC, especially through skin contact, the LD_{50} of DCC is 71 mg/kg (Samaranayake and Glasser, 1993).

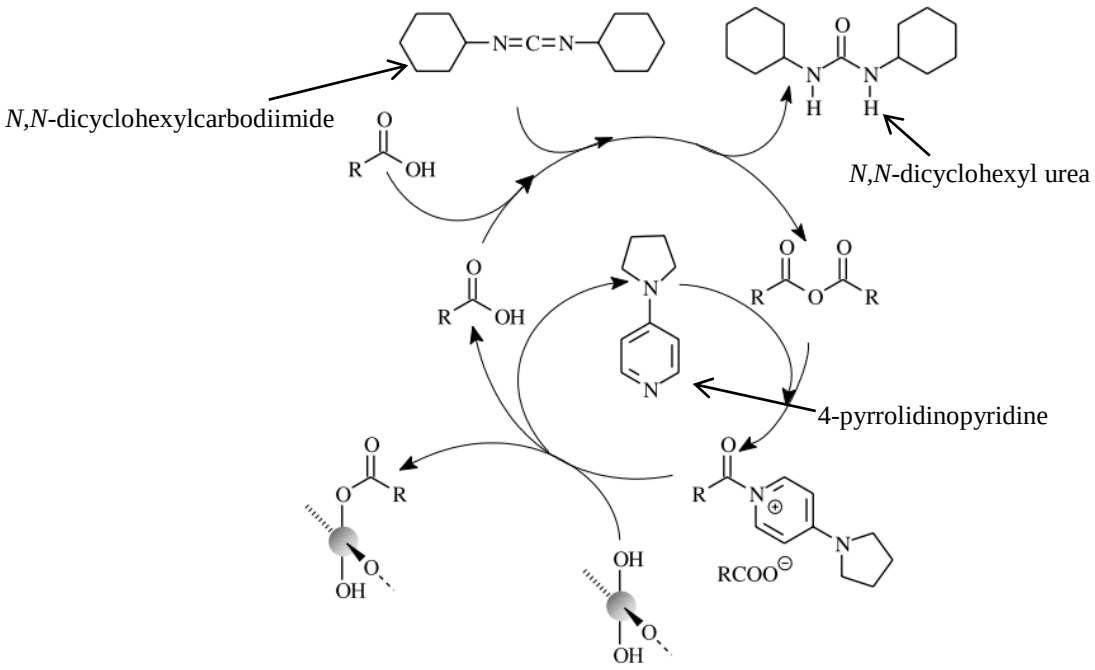

Figure 1.4: Activation of fatty acid by DCC/PP (Samaranayake and Glasser, 1993)

N,*N*-Carbonyldiimidazole (CDI) has become an alternative for DCC, because it is less toxic compared to DCC. The by-products of CDI method are carbon dioxide and imidazole as shown in Figure 1.5 (Heinze, 2006). Imidazole can be readily removed by dissolving in water and other common solvents. CDI is soluble in water and alcohol, and can be removed from the mixture easily. To author's knowledge, CDI hasn't been applied to the activation of fatty acid, but it has successfully been used to activate wide range of carboxylic acids with chiral [(-)-menthyloxy acetic acid], unsaturated [3-(2-furyl)-acryl carboxylic acid], heterocyclic [liponic acid], and cyclodextrin [carboxymethyl-ß -cyclodextrin] containing moieties (Liebert and Heinze, 2005). Once activated, carboxyl group will be in its more active form, a higher tendency will be observed when reacting with hydroxyl group.

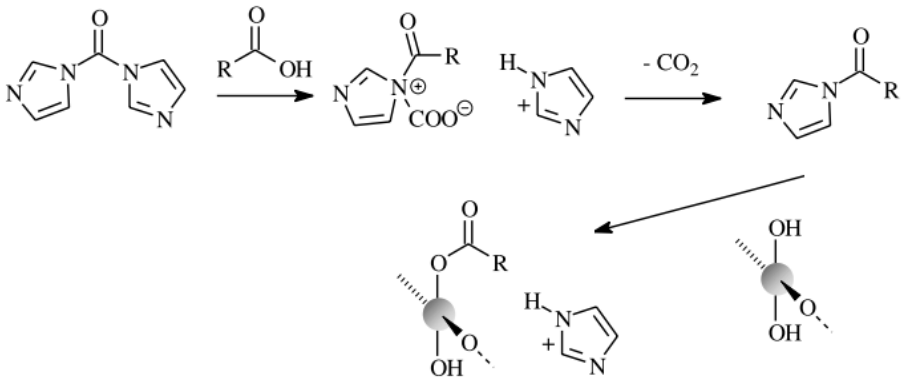

Figure 1.5: Activation of fatty acid by CDI (Heinze, 2006)

1.5 Challenges and greener attempts

To author's knowledge, no fully green, durable and hydrophobic cotton surface has been reported in the open literature. A permanent or durable hydrophobic surface usually requires covalent attachment of low surface energy compounds or molecules onto cotton. Nevertheless, there are several greener attempts with the minimal use of petroleum based chemicals to achieve durable and hydrophobic cotton surface.

Antova *et al.* synthesized cellulosic stearate through transesterification reaction between methyl stearate with low-molecular microcrystalline cellulose under microwave heating (Antova *et al.*, 2004). Their results show that when cellulose and methylstearate mixed with a mole ratio of 1:3, and *p*-toluene sulphonic acid as catalyst after 10 min of microwave heating, a degree of substitution of 0.95 can be obtained (Antova *et al.*, 2004).

Another interesting report also used the transesterification reaction but between cellulose and triglyceride (Dankovich and Hsieh, 2007). Dankovich and Hsieh obtained hydrophobic cotton surface by reacting bleached cotton with 1% triglyceride in acetone. In this process solvent was first evaporated and followed by heating for 1 hr at 120^{o}C. While they claimed that their modified product as hydrophobic

cotton, the water contact angle of their modified cotton was only 80^o, which may still be considered as hydrophilic (Dankovich and Hsieh, 2007).

In the present study, fatty acids were grafted onto cellulose to decrease the surface energy. Fatty acid is considered as natural and abundant and can be easily obtained by hydrolysis of triglycerides. In order to avoid the use or toxic chemicals, *e.g.* TosCl and DCC, acetic anhydride, was used to facilitate the reactivity of fatty acid.

Microwave heating as an energy efficient way to increase temperature was used replacing the conventional hydrothermal (oil bath) heating.

1.6 Theory of superhydrophobicity

From thermodynamic point of view, the water contact angle on a flat surface is determined by interfacial surface tension of solid, liquid and vapor phases. It can be calculated by Young's equation:

$$\cos\ \theta\ =\ \frac{\gamma_{sv}-\gamma_{sl}}{\gamma_{lv}} \qquad (1)$$

where θ is the apparent contact on a flat surface, γ_{sv}, γ_{sl} and γ_{lv} stand for the interfacial surface tension values for solid-vapor, solid-liquid and liquid-vapor, respectively (Bellanger *et al.*, 2014).

By definition, superhydrophobicity refers to a surface with static water contact angle larger than 150^o as well as low (usually lower than 10^o) water contact angle hysteresis (the difference between the advancing and receding water contact angles) (Tuteja *et al.*, 2007). It's widely accepted that surface wetting property is governed by two key parameters, surface topography and surface energy (Ma and Hill, 2006). With a fixed surface topography, lower surface energy can be expected to result in a higher water contact angle. Also, by altering the surface morphology for a specific surface energy material, the water contact angle will change based on roughness.

It's worth to mention that a true flat surface with lowest known surface energy, 6.7 mJ/m^2, can only achieve water contact angle of 119^o (Nishino *et al.*, 1999). With the limited improvement of hydrophobicity by reducing surface energy of materials, tremendous efforts have to be made to tailor the surface morphology. Several comprehensive reviews are available for this subject, they summarize different strategies to fabricate superhydrophobic surface with hierarchical structure, especially micro and nanometer scale roughness (Ma and Hill, 2006); (Bellanger *et al.*, 2014); (Li *et al.*, 2007); (Yan *et al.*, 2011); (Roach *et al.*, 2008).

Two theoretical models have been widely accepted to explain the superhydrophobic phenomenon, they are Wenzel model and Cassie-Baxter model (Wenzel, 1936); (Cassie and Baxter, 1944). The Wenzel model suggests that the liquid follows the contours of a rough surface as shown in Figure 1.6a. The water contact angle on this type of surface can be calculated by Wenzel's equation:

$$\cos \theta^W = r\cos \theta \tag{2}$$

where r is roughness factor for solid phase and represents the ratio of the actual surface area to its horizontal projection (r should always be larger than 1). θ^W is the water contact angle under Wenzel state and θ is the apparent water contact angle on a flat surface of that same material (Wenzel, 1936).

Based on this model, a hydrophobic surface should have $\theta^W > \theta > 90^o$, and for a hydrophilic surface, $\theta^W < \theta < 90^o$. In other words, based on the nature of material, hydrophobicity or hydrophilicity can be enhanced with increase of surface roughness. Moreover, due to the strong attraction between water and solid, a water droplet in Wenzel state is described as "sticky" (Bellanger *et al.*, 2014).

However, Cassie-Baxter model suggests that water will only contact with the top of asperities and there will be air trapped between water droplet and solid phase, as shown in Figure 1.6b. The

Cassie-Baxter's water contact angle can be calculated as following:

$$\cos \theta^C = f\cos \theta\text{-}(1\text{-}f) \quad (3)$$

where f is the fraction of the solid/liquid interphase and (1-f) is the fraction of the vapor/liquid interface. θ^C is the water contact angle under Cassie-Baxter state, θ is the apparent water contact angle on a flat surface of that same material (Cassie and Baxter, 1944).

Under Cassie-Baxter state, liquid has less contact area with solid phase than Wenzel state, which means a weaker adhesion between them. Thus, a water droplet under Cassie-Baxter state is often described as "non-sticky" and it will fall off from the solid surface with a slight inclination (Bellanger *et al.*, 2014).

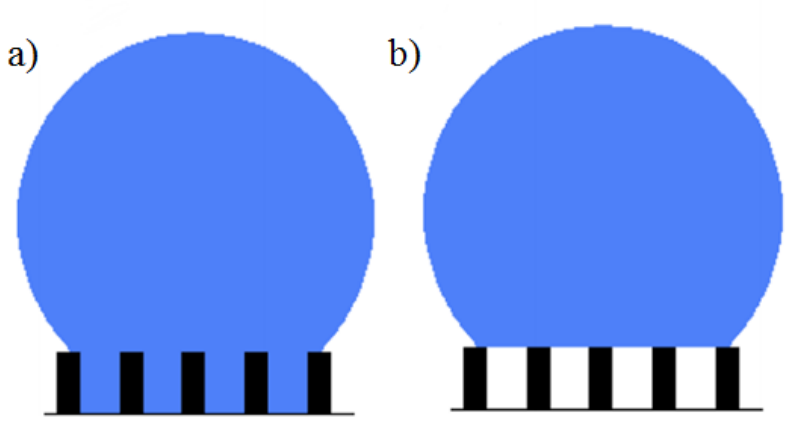

Figure 1.6: Liquid droplet deposited on rough surface a) Wenzel state; b) Cassie-Baxter state (Bellanger *et al.*, 2014)

Researchers further developed these two models by introducing critical angle, θ_c, for transition from Wenzel to Cassie-Baxter state, θ_c can be calculated by following equation:

$$\cos \theta_c = \frac{f-1}{r-f} \quad (4)$$

A water contact angle larger than θ_c meaning the liquid droplet is in Wenzel state; otherwise, the liquid droplet will be in Cassie-Baxter state (Bico and Quéré, 2002); (Bellanger *et al.*, 2014).

1.7 Lotus effect and biomimicry

Lotus leaf (*Nelumbo nucifera*) is the most well-known plant that exhibits superhydrophobicity. It has a water contact angle of 161.0 ± 2.7^{o} and sliding angle as low as 2^{o}. According to Barthlott and Neinhuis, such high water contact angle is contributed by the epicuticula wax and the micro and nanometer scale papillae structure on the leaf (Barthlott and Neinhuis, 1997). The epicuticula wax provides a low surface energy (but the wax on its own has a water contact angle of 110^{o}) (Li *et al.*, 2007). More importantly; the surface of lotus leaf consists of both micro and nanometer scale roughnesses: one around 10 μm and the other around 100 nm, as shown in Figure 1.7 (Li *et al.*, 2007); (Guo and Liu, 2007). This dual-size roughness allows air trapped underneath liquid phase, which significantly improves the hydrophobicity (Sun *et al.*, 2005). The ability that lotus leaf causes water droplets roll off and take away undesired contaminants is called "lotus effect", therefore, surfaces with lotus effect always exhibit self-cleaning (Li *et al.*, 2007).

Beside lotus there are other plants and insects that have dual-size roughness that exhibit superhydrophobicity. Some examples for plants are rice leaf (*Oryza sativa L.*) (θ = 157.0 ± 2^{o}), purple setcreasea (*Setcreasea purpurea boom*) (θ = 167.0 ± 2^{o}) and perfoliate knotweed (*Polygonum perroliatum L.*) (Wolfs *et al.*, 2013). Water strider's leg is a great example for insect, Gao and Lei reported that water strider's leg has remarkable water repellence (Gao and Jiang, 2004). They revealed that water strider's leg is covered by large numbers of oriented spindle-like microsetae as well as finer nanogrooves on setas as shown in Figure 1.8 (Gao and Jiang, 2004).

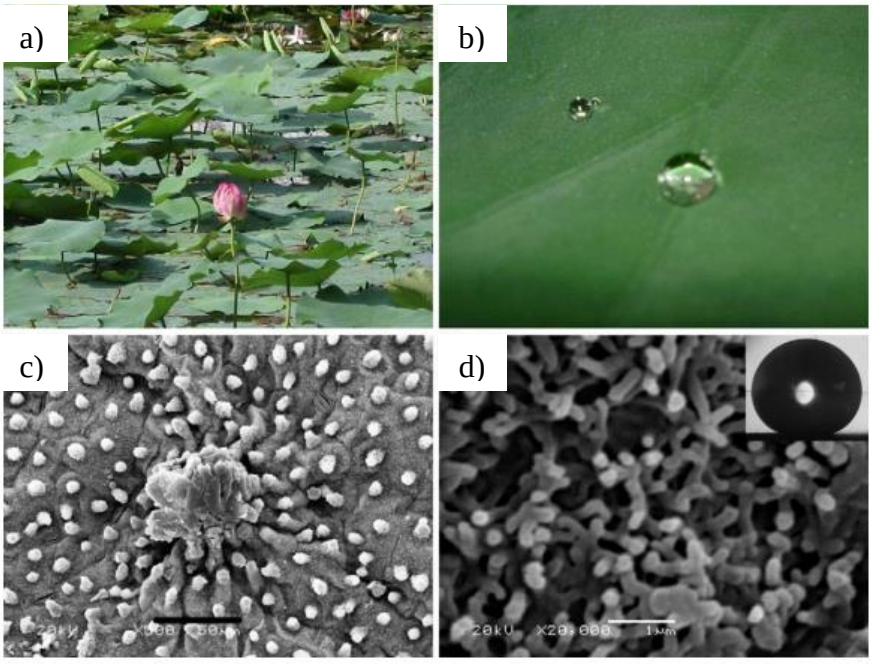

Figure 1.7: a) Lotus leaves on a pond; b) a water droplet floating on a lotus leaf; c) and d) SEM images of lotus leaves with different magnification (the bar of c and d are 50 μm and 1μm, respectively); The inset in d) is shows a water contact angle of 161 ± 2^{o} (Guo and Liu, 2007)

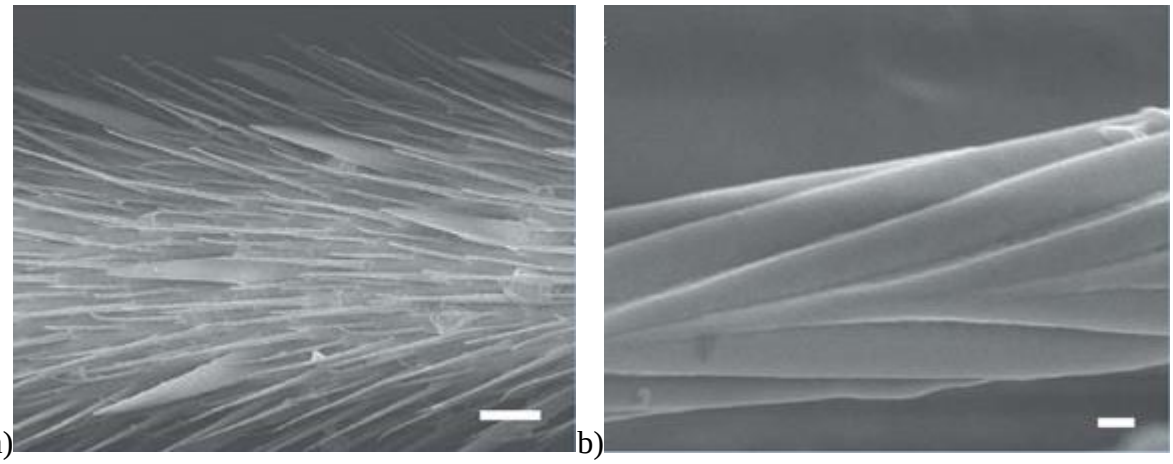

Figure 1.8: SEM images of a leg showing a) numerous oriented spindly microsetae; b) the fine nanoscale grooved structures on a seta. (the bar of a and b are 20 μm and 200 nm, respectively) (Gao and Jiang, 2004)

Other examples for insects are gecko foot, Homoptera (*Meimuna opalifera*) wing and Diptera (*Tabanus chrysusrus*) wing (Hansen and Autumn, 2005); (Wolfs *et al.*, 2013); (Byun *et al.*, 2009). All of them contain dual size hierarchical structures. Their SEM images are shown in Figure 1.9. These

naturally occurring structures have sparked scientist interest and enthusiasm for biomimicry and several ground breaking technologies have been made based on the knowledge learned from nature. Some outstanding examples are aircraft wing inspired by bird, improved digital displays from light refracting properties of butterfly wings, superhydrophobic or self-cleaning surface mimicking the lotus leaf (Romei, 2008); (Saito, 2011); (Blossey, 2003).

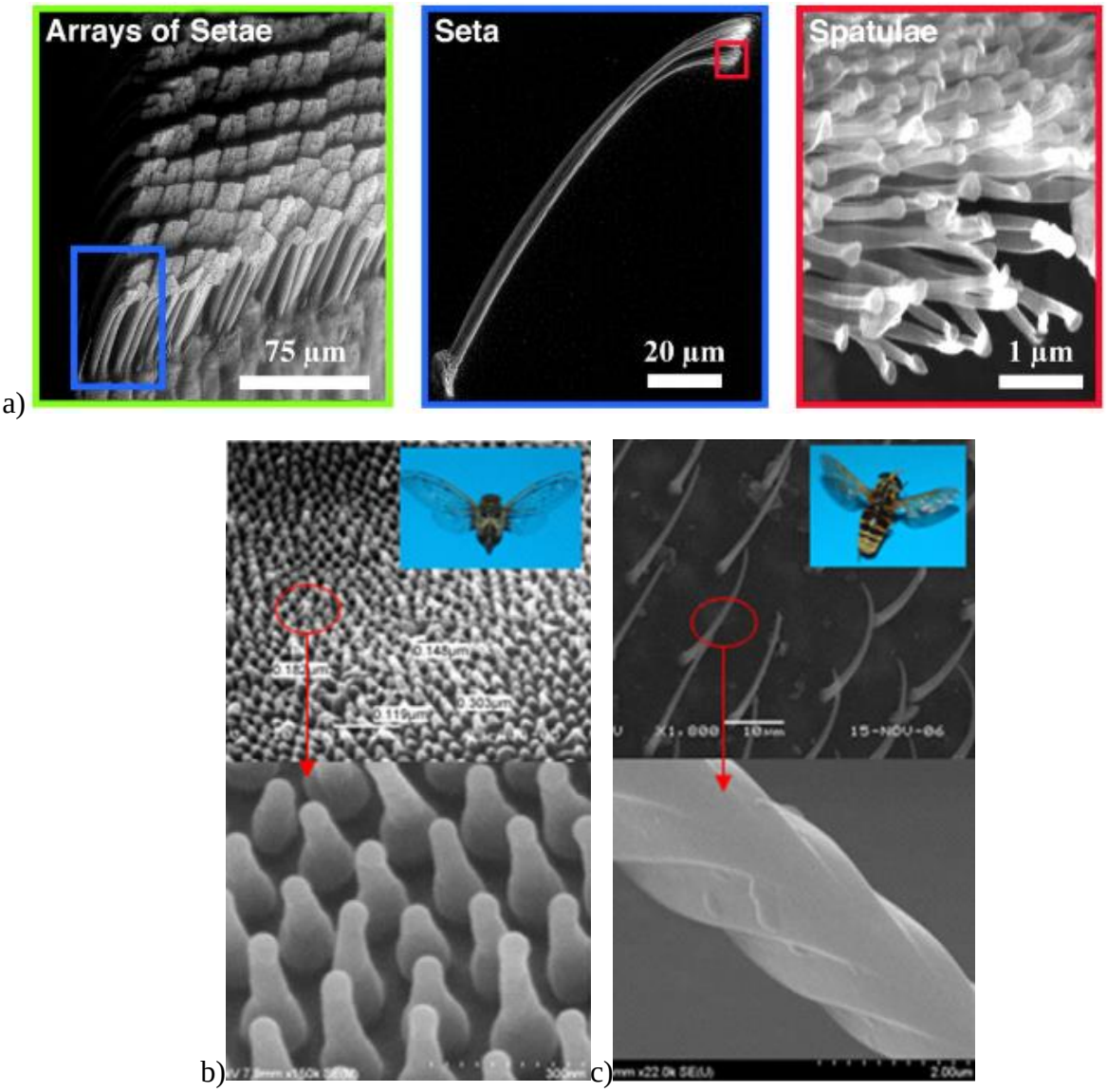

Figure 1.9: SEM images of hierarchical Structure a) micro and nanostructure of seta in the gecko feet; b) Homoptera (*Meimuna opalifera*) wing; c) Diptera (*Tabanus chrysusrus*) wing (Hansen and Autumn, 2005) (Byun *et al.*, 2009)

1.8 Current methods to fabricate superhydrophobic surface

On the basis of Wenzel and Cassie-Baxter theories, designing specific surface roughness has been the current research focus for fabricating superhydrophobic surface. Different fabrication methods have been published, and they can be classified into two categories: top-down and bottom-up approaches (Li *et al.*, 2007).

Top-down approach usually involves roughening a flat surface by etching and lithography. Bhat *et al.* used dichlorodifluoromethane (DCFM) plasmas to produce highly water-repellent and hydrophobic cotton surface (Bhat *et al.*, 2011). Their results also showed that after DCFM plasma treatment, fibril-like structures appeared on the fiber surface increasing the surface roughness. The SEM images of their DCFM plasma treat fibers are shown in Figure 1.10.

a) 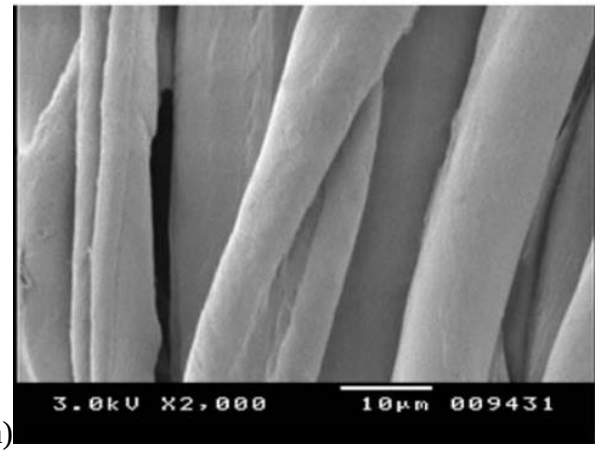

b) 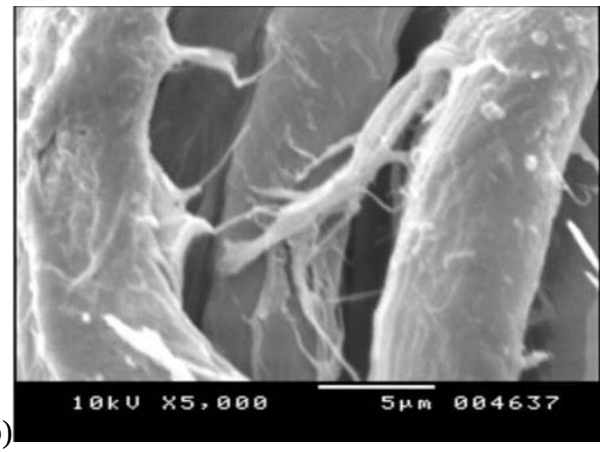

Figure 1.10: SEM images of a) control (desized and scoured cotton); b) DCFM plasma-treated cotton fiber showing fibril-like structures on the surface (Bhat *et al.*, 2011)

Etching is mainly used to create superhydrophobic surface for metal substrate. Qian and Shen reported a simple chemical etching method to fabricate superhydrophobic surface on polycrystalline metals, aluminum, copper and zinc (Qian and Shen, 2005). They used dislocation etchant that selectively dissolved the dislocation sites in the grains. The etched surfaces were followed by fluoroalkylsilane

treatment, and the final products exhibited a superhydrophobic water contact angle of 155^{o}.

Lithography is a versatile technique to obtain large scale controlled micro/nanometer pattern. Martines *et al.* fabricated regular nanopatterns (nanopillars and nanopits) in silicon wafers (Martines *et al.*, 2005). Their process involved electron beam lithography and plasma etching to obtain nanopatterns, and same patterns were subsequently coated with octadecyltrichlorosilane. Their final products showed a water contact angle of 164^{o}.

Bottom-up approach includes sol-gel, layer-by-layer assembly and chemical deposition methods. Sol-gel methods have been used to fabricate superhydrophobic surface for variety substrates (Ma and Hill, 2006). The major advantage of this method is that it does not require a post hydrophobic treatment, since the roughness can be fabricated by intrinsically hydrophobic materials. Organoalkylsilane and fluoroalkylsilane are frequently used to fabricate hydrophobic silica particles (Shirtcliffe *et al.*, 2005); (Hikita *et al.*, 2005). By tailoring the size, size distribution and surface chemistry of silica particles, different surfaces with specific hydrophobic properties can be made. For example, Hikita *et al.* used the sol-gel method to fabricate super water repellent surface by colloidal silica particles and fluoroalkylsilane (Hikita *et al.*, 2005). With an optimized particle to fluoroalkylsilane ratio, final product surface was able to repel both water and oil.

Layer-by-layer assembly method can be used to precisely control the thickness of film by vary amount of layers. Usually, these layers are self-assembled through electrostatic interaction and hydrogen bonding (Ma and Hill, 2006). Ji *et al.* constructed multilayers by alternately depositing polyethyleneimine (PEI) and poly(acrylic acid) (PAA) onto 3-aminopropyltriethoxysilane coated substrates (Ji *et al.*, 2006). After crosslinking at 180^{o}C for 2 hrs, fluoroalkylsilane was deposited on the

surface through chemical vapor deposition. Multilayered film shown hierarchical structure and its surface morphology is shown in Figure 1.11. Their final product exhibited a water contact angle of 172^{o} $\pm 1.5^{o}$.

a) 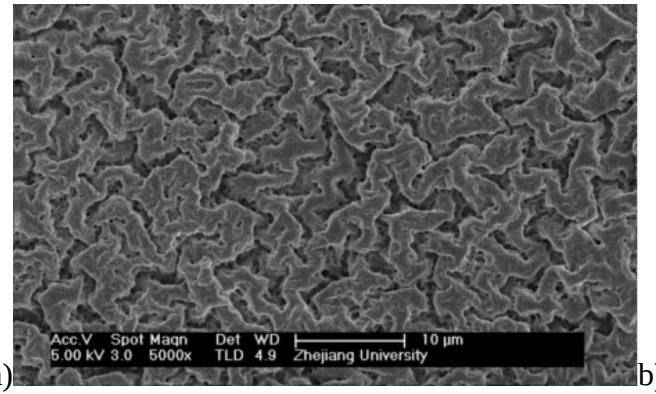

b) 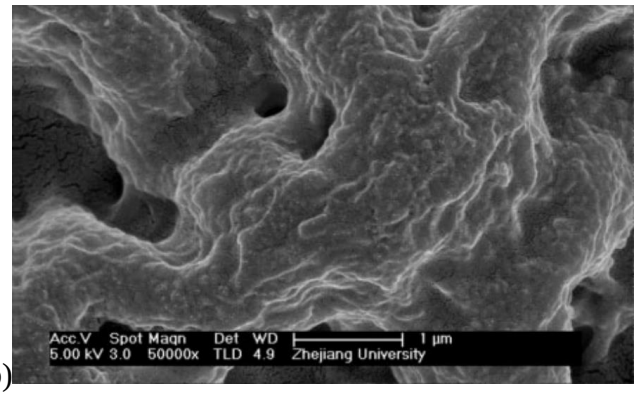

Figure 1.11: SEM images of PAA/PEI film. (the bar of a and b are 10 µm and 1 µm, respectively) (Ji *et al.*, 2006)

1.9 Superhydrophobic modifications of cotton fabrics

Numerous publications have shown the successful superhydrophobic modifications of cotton fabrics. Most of these methods involve fabrication of rough surface using nanoparticles (SiO2, TiO_2) and then followed by low surface chemical treatment, e.g. fluoroalkylsilane (Athauda *et al.*, 2013); (Xue *et al.*, 2009); (Xue *et al.*, 2008); (Ramaratnam *et al.*, 2007); (Yu *et al.*, 2007).

Deng *et al.* grafted *1H,1H,2H,2H*-nonafluorohexyl-1-acrylate onto cotton fabric under γ-ray radiation (Deng *et al.*, 2010). After covalently attaching this fluoropolymer onto cotton fiber, the resulting modified cotton fabric exhibited a water contact angle of 155^{o}.

Athauda *et al.* prepared two size of functionalized silica nanoparticle (40 nm and 7 nm) (Athauda *et al.*, 2013). By changing the order of deposition, followed by same hydrophobic treatment, different water contact angles were obtained. Figure 1.12a shows SEM image where 7 nm nanoparticles were

deposited first and followed by 40 nm nanoparticles. In this situation, the corresponding water contact angle was 149.6^{o}. Figure 1.12b shows SEM image where 40 nm nanoparticles were deposited first and followed by 7 nm nanoparticles. In this case, the corresponding water contact angle was 110.1^{o}. Athauda *et al.* pointed out that the difference in water contact angle values is caused by different surface roughness (Athauda *et al.*, 2013).

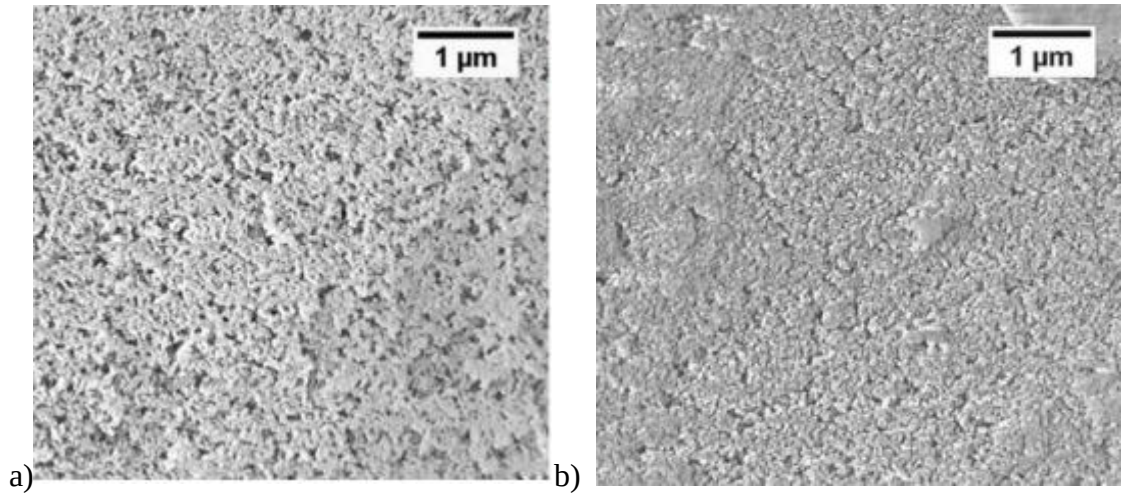

Figure 1.12: SEM images of a) bottom layer is consists of 7 nm silica nanoparticles top layer is consists of 40 nm silica nanoparticles; b) bottom layer is consists of 40 nm silica nanoparticles top layer is consists of 7 nm silica nanoparticles (Athauda *et al.*, 2013)

Zimmermann *et al.* described a simple approach to fabricate superhydrophobic cotton fabric. Their method involved grown a layer of polymethylsilsesquioxane (PMSQ) nanofilaments onto cotton fibers (Zimmermann *et al.*, 2008). As shown in Figure 1.13, PMSQ nanofilaments provided both lower surface energy and roughness to cotton fiber. Final hydrophobic cotton fabric showed a water sliding angle of 25^{o}. However, water contact angle value was not reported.

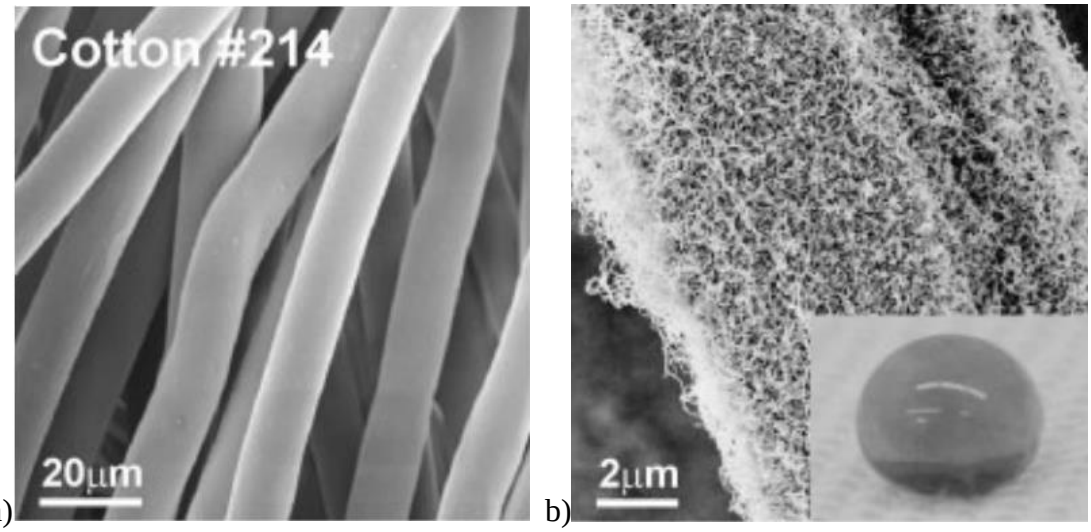

a) b)

Figure 1.13: SEM images of a) uncoated cotton fibers; b) PMSQ nanofilaments coated cotton fibers (Zimmermann *et al.*, 2008)

Hoefnagels *et al.* prepared superhydrophobic cotton fabric by *in situ* introducing silica particles onto cotton fibers, followed by hydrophobic treatment with polydimethylsiloxane (PDMS) (Hoefnagels *et al.*, 2007). Amine-silica particles were *in situ* formed by Stöber method (Hoefnagels *et al.*, 2007). Their optimized Amine-Silica particles formation condition showed a water contact angle of 155°. The particles covered surface morphology is shown in Figure 1.14.

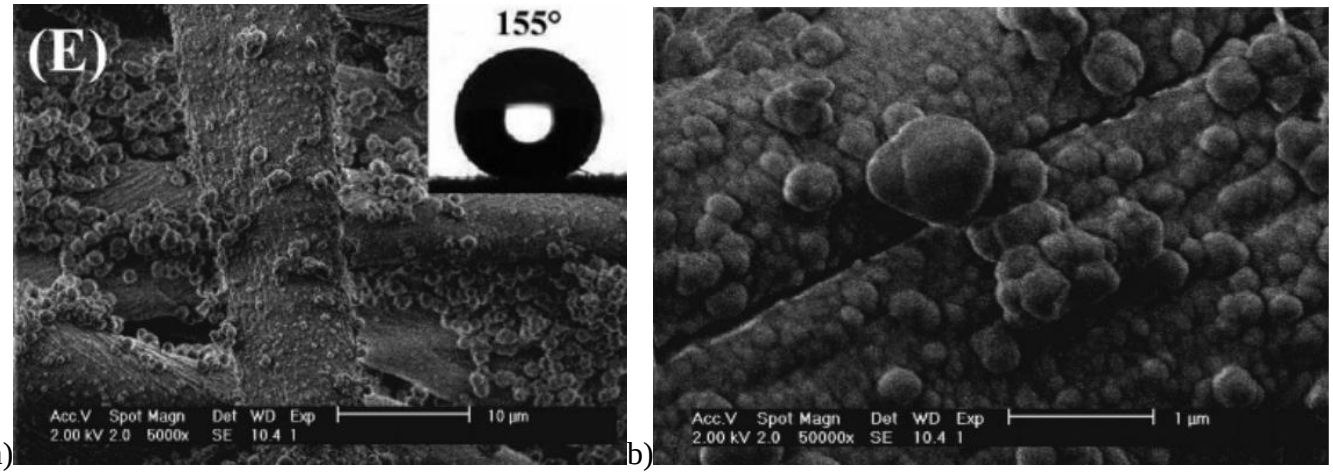

a) b)

Figure 1.14: SEM images of cotton fibers covered by in situ prepared Amine-Silica nanoparticles, followed by PMDS hydrophobic treatment. a) low magnification; b) high magnification (Hoefnagels *et al.*, 2007)

Zhou *et al.* used an alternative procedure, as Hoefnagels *et al.*'s (Hoefnagels *et al.*, 2007), to fabricate superhydrophobic surface for polyester fabric (Zhou *et al.*, 2012). Fluoroalkylsilane modified silica particles were first prepared, and then deposited onto fiber through dip-coating. After that the modified fabric was cured at 135^{o} for 30 min. They reported the resulting fabric to have a water contact angle of 171^{o}. Their preparation procedures and surface morphology are illustrated in Figure 1.15. SEM image clearly showed the roughness at 200 nm scale, however, at micrometer scale, the surface roughness is not obvious.

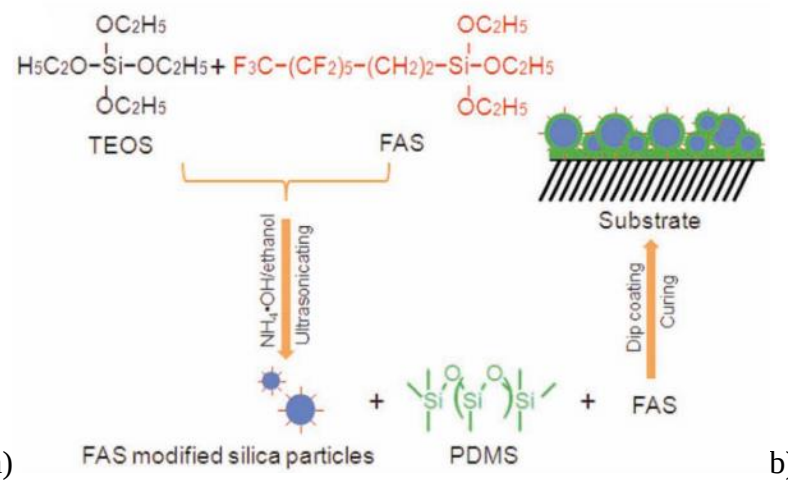

a)

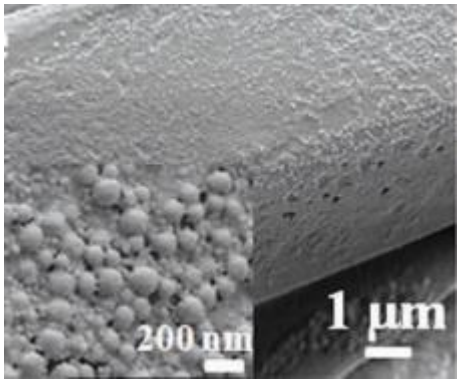

b)

Figure 1.15: a) Procedures for coating solution preparation; b) SEM images hydrophobic treated polyester fiber with different magnifications (Zhou *et al.*, 2012)

1.10 'Greening' of the superhydrophobic treatment

Inspired by superhydrophobic and self-cleaning nature of lotus leaf, numerous methods have been published to imitate its surface structure. Hydrophobic surface with different water contact angle values can be made by tailoring specific surface morphology and coating with low surface energy chemicals. However, to author's knowledge, no publication has been reported in open literature aimed to use greener or environment-friendly method for superhydrophobic surface fabrication. There are several

technical challenges that need to be resolved before such green method can be achieved:

1) Few naturally occurring chemicals exhibit low surface tension property. Fatty acids are considered having a low surface tension among natural chemicals. However, their surface tension values are around 40 mJ/m^2. Fluorinated chemicals, on the other hand, can achieve surface tension as low as 6.7 mJ/m^2 (Nishino *et al.*, 1999). Because of the significantly low surface tension of fluorinated chemicals they are still dominantly being used with several recent superhydrophobicity related publications (Wooh *et al.*, 2014); (Li *et al.*, 2014); (Yang *et al.*, 2014).
2) Lithographic or plasma etching techniques require expensive instruments and are only capable to fabricate small scale superhydrophobic surface. These processes only utilize limited amount of chemicals. It's not so meaningful to debate whether they can be considered as green processes. In addition, these methods only create rough surface, if the initial material or substrate does not have low surface energy, a hydrophobic treatment is still required.
3) Bottom-up approaches to fabricate artificial rough surface as described earlier in section 1.7, usually require extensive use of petroleum based chemicals. Few naturally existing materials have been found that have the versatility to be used for hierarchical structure fabrication.

Never the less, there are some interesting published results; their procedures can be further investigated for a green superhydrophobic treatment (Oliveira *et al.*, 2013); (Wang *et al.*, 2012). Oliveira *et al.* used inexpensive and natural occurring diatomaceous earth, siliceous exoskeleton of diatoms, to fabricate micro and nanometer scale roughness on a glass surface (Oliveira *et al.*, 2013). Figure 1.16 shows SEM images of diatomaceous earth coated glass surface. The size of diatomaceous earth range from 5 μm to 20 μm, and the nanotexture of diatomaceous earth provide nanoscale roughness. The

resulting surface exhibited a water contact angle of 151.0 ± 0.9^{o} after fluoroalkylsilane treatment.

a) 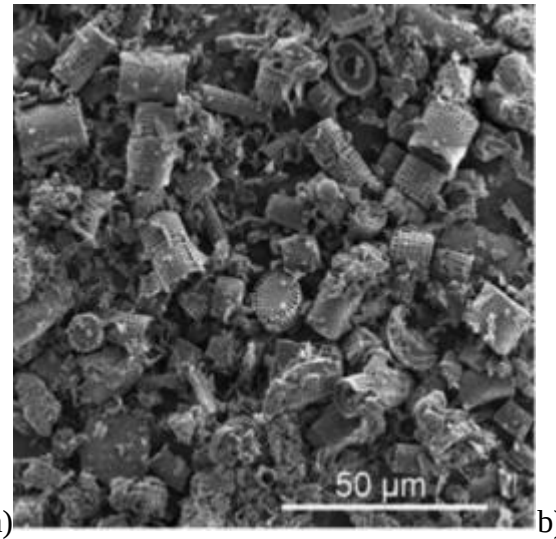

b) 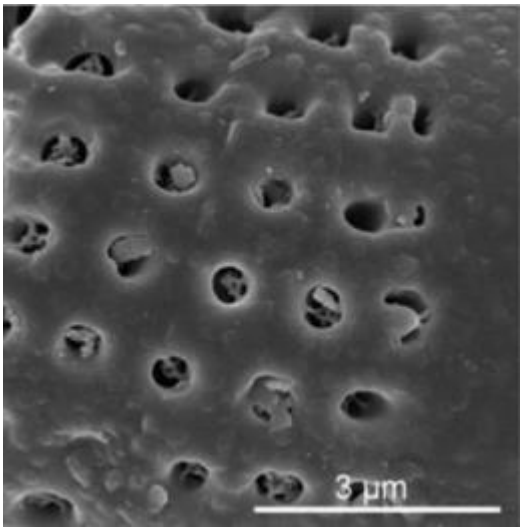

Figure 1.16: SEM images of diatomaceous earth a) micrometer size structure; b) nanotexture of diatomaceous earth (Oliveira *et al.*, 2013)

Wang *et al.* prepared silica nanoparticles (25 – 30 nm in diameter) from rice husks, an inexpensive and yearly renewable resource (Wang *et al.*, 2012). This biogenic silica nanoparticle has same properties and can be used as a green substrate to replace Stöber method based silica nanoparticles.

The present study aims to develop greener approach for superhydrophobic surface fabrication. Since the silica particle from rice husk still needs further investigation for controlled size and morphology. Stöber method based silica particle were used to increase surface roughness. Fluorinated compounds were avoided in this study, due to the fact that most of them are hazardous to the environment and toxic to human beings and other living creatures (Hekster *et al.*, 2003). A greener method utilizing fatty acid was used to decrease the surface energy of cotton.

A novel method to crosslink particles onto surface was developed. The purpose of this was to avoid particles falling off from substrate surface during washing or during use, and thus, decreasing the environmental concerns.

2. EXPERIMENTAL METHODS

2.1 Materials

Table 2.1 summarizes the chemicals used for this study, Sunbeam microwave with 0.9 Cu. ft chamber and 900 Watts power was used in this study.

Table 2.1: Chemicals used for study

Specimens	Formula	Chemical structure	Melting temperature	Boiling temperature
Acetic anhydride	$C_4H_6O_3$	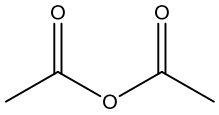	-73.1 ℃	139.8 ℃
Heptanoic acid	$C_7H_{14}O_2$	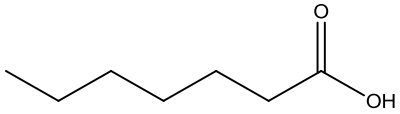	−7.5°C	223.0 ℃
Octanoic acid	$C_8H_{16}O_2$	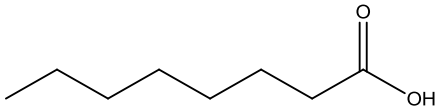	16.7 ℃	239.7 ℃
Dodecanoic acid	$C_{12}H_{24}O_2$	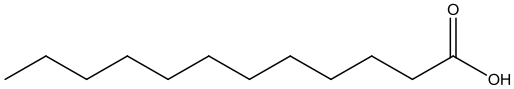	43.2 ℃	298.9 ℃
stearic acid	$C_{18}H_{36}O_2$	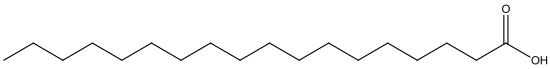	69.8 ℃	382.0 ℃

2.2 Pretreatment of cotton fabric

Desized, scoured and bleached woven cotton fabric was used as raw material in this study. Fabric was cut into 10 cm × 10 cm size specimens and purified using 300 ml ethanol solution (ethanol to water volume ratio = 8:2) in 500 mL Erlenmeyer flask at 50^{o}C for 20 min. The purpose of this pretreatment was to partially remove any remaining ash, hemicellulose and lignin and obtain as high cellulose content as possible.

2.3 Preparation of fatty anhydrides

A mixture of 26 g of heptanoic acid and 20 g of acetic anhydride were introduced in a Petri dish. After they were thoroughly mixed, petri dish was covered and placed into a microwave oven (900W). The mixture was microwave heated at different power levels and for desired durations. Every time after the reaction was completed, the petri dish was taken out from the microwave oven and both the chemical mixture and the microwave oven were allowed to cool to room temperature. During the microwave heating, proposed chemical reaction as illustrated in Figure 2.1 is expected to take place. The resulting mixture was characterized using HPLC to confirm its chemical composition, detailed test procedures are described in the characterization section 2.8.

Fatty acid with a melting point higher than room temperature was used, e.g. dodecanoic acid (melting point: 43.2^{o}C) in this study. First, the fatty acid was first completely melted by heating 5^{o}C above its melting point. After that acetic anhydride was added and stirred for 5 min to form a uniform mixture.

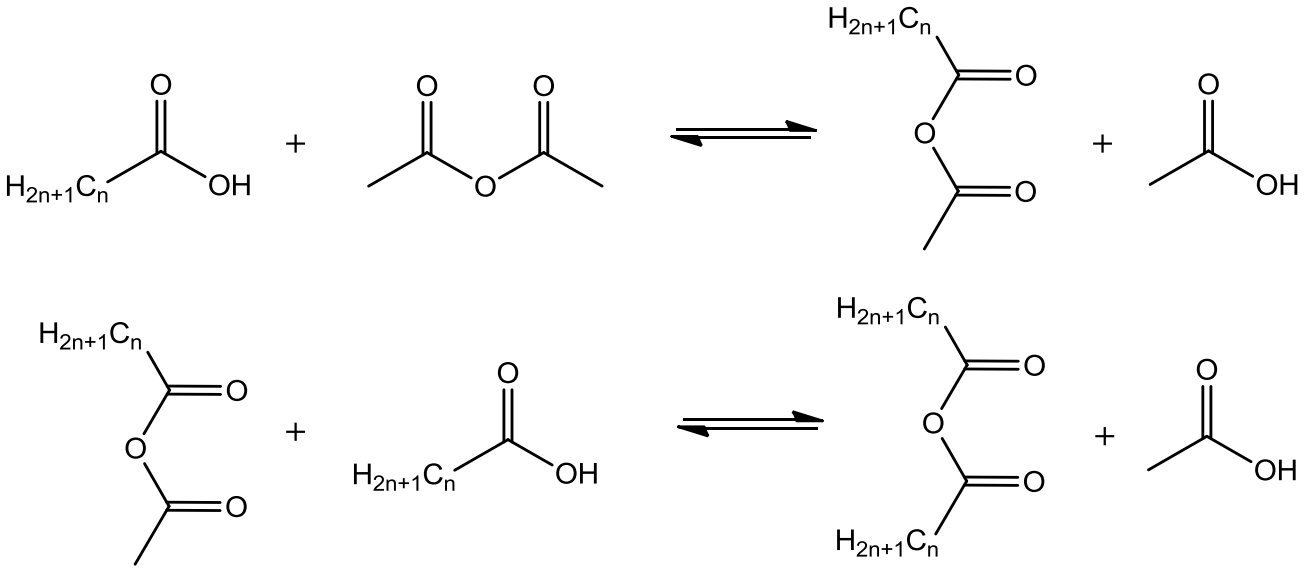

Figure 2.1: Chemical process of fatty anhydride preparation

2.4 Hydrophobic treatment of cotton fabric

Purified cotton fabric specimen was placed in the petri dish containing as-prepared fatty-acetic anhydride solution, making sure that the fabric is completely immersed in reaction mixture. Petri dish was then covered and placed in the microwave oven and the mixture was heated at different predetermined power levels and for different durations. During the microwave heating, the chemical reaction illustrated in Figure 2.2 was expected to take place, where fatty anhydride reacts with hydroxyl groups on cellulose backbone forming an ester bond and fatty acid as byproduct. Every time after the reaction was completed, the petri dish was removed from the microwave oven and the microwave oven was cooled to room temperature. The treated fabric was purified by Soxhlet extraction with ethanol to remove unreacted chemical residues for at least 12 hrs. The treated and purified fabric was dried in oven at 60^{o}C overnight.

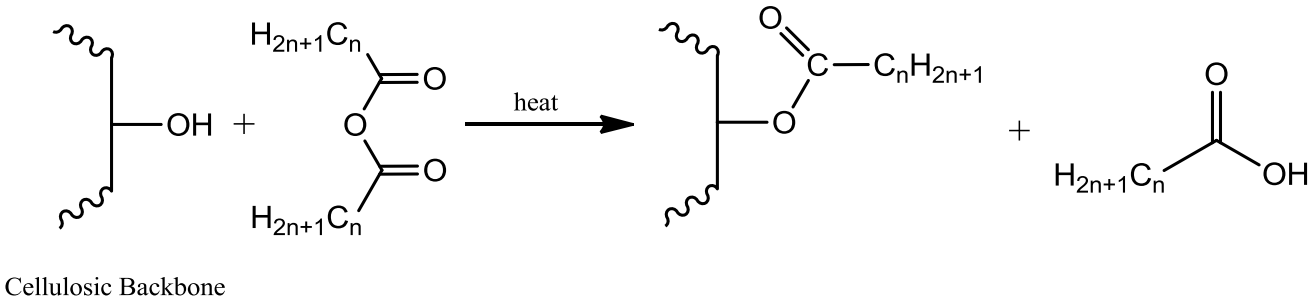

Figure 2.2: Chemical reaction between cellulose and fatty anhydride

2.5 Preparation of amine-silica particles

Amine-silica nanoparticles were prepared by modified Stöber method, procedures are described as following (Stöber *et al.*, 1968): 50 mL absolute ethanol, 1 mL water and 1 mL NH_4OH (concentration: 28%) were mixed together in 125 mL Erlenmeyer flask. The mixture was stirred for 5 min to form a uniform solution. After that 4 mL Tetraethyl orthosilicate (TEOS) was quickly added to the solution

while stirring at 500 RPM at room temperature. After 30 min, different predetermined amounts of (3-Aminopropyl) triethoxysilane (APTES) were added to the solution. Same stirring speed was maintained and the reaction was allowed to go on for 12 hrs at room temperature. By changing the ratio of the reactants, amine-silica particles with different sizes were obtained. Amine-silica particles were purified using several cycles of centrifuging and dispersing in ethanol until supernatant didn't show purple color when heated together with ninhydrin. The purple color indicates the presence of amine group.

2.6 Deposition of amine-silica particles onto cotton fabric

Several strategies were used to deposit amine-silica particle onto cotton fiber surface. 'Physical deposition method' involves physical deposition of amine-silica particles onto the cotton fiber surface. Amine-silica particle dispersions with desired concentrations were prepared. Absolute ethanol was used as solvent. At least 1 hr of ultrasonication was performed to uniformly disperse particles. Ethanol washed cotton fabric was cut into specimens with 5 × 5 cm dimension which were immersed in amine-silica particle dispersion for desired lengths of time. The fabric specimens were then dried in an air circulating oven at 130^{o}C for 30 min.

'Covalent bonding method' involves covalently bonding amine-silica particles onto cotton fiber surface. Cotton fabric was first treated with 1,2,3,4-Butanetetracarboxylic acid (BTCA). BTCA treated cotton with free carboxyl group on surface can be further reacted with amine-silica particle for covalent bonding. The detailed BTCA treatment was described as followings:

In the next step, a 50 mL solution containing 10% (w/v) BTCA and 5% (w/v) sodium hypophosphite (SHP), as catalyst, was prepared. Ethanol washed cotton fabric specimens cut into 5 × 5 cm dimension

were immersed in the BTCA solution at 50^{o}C with stir speed at 80 RPM. After 10 min, the fabric was squeezed and dried at 130^{o}C for 30 min. During this process, crosslinking in the bulk of cotton fabric was allowed to occur. The fabric was then immersed into BTCA solution once more to allow more BTCA to penetrate into the fabric structure. Finally, the cotton fabric was cured (dried) at 130^{o}C for 30 min to allow the reaction to be completed. BTCA treated cotton fabric was extensively washed with tap wash to remove any residual chemicals and dried in an air circulating oven for at least 12 hrs at 60^{o}C.

Next step involved activation of carboxyl group by Ethyl (dimethylaminopropyl) carbodiimide/ *N*-Hydroxysuccinimide (EDC/NHS) coupling reaction. For this fifty (50) mL 10 mM MES buffer solution containing 0.1 mM EDC and 0.4 mM NHS was prepared.

After that, the carboxyl group activated cotton fabric was transferred into dispersed amine-silica particles dispersion of desired concentration. The reaction was allowed to complete for 3 hrs. Resulting cotton fabric was washed with tap water to remove any chemical residuals, and again, dried in oven.

'Crosslinking method' also involves covalently bonding amine-silica particles onto the cotton fabric surface. To achieve covalent bonding the cotton fabric was first immersed in well dispersed amine-silica particles dispersion with predetermined concentration. Mixture was stirred for 30 min to allow amine-silica particles to be physically adsorbed onto the cotton fabric surface. Cotton fabric was then dried in an air circulating oven at 130^{o}C for 30 min and followed by BTCA treatment. Same treatment procedure was used as described earlier in "Covalent bonding method". During the finally curing step, crosslinking reaction was expected to happen within cellulose, between top layer of cellulose and amine-silica particles, as well as within agglomerated amine-silica particles. Resulting treated cotton fabric was washed with tap water to remove any chemical residuals, and again, dried in the oven.

‘Green crosslinking method’ used similar procedures as those for ‘Crosslinking method’ except different crosslinking agents can be used. Dastidar and Netravali reported that oxidized sugar can be potentially used as a green crosslinker. After further investigation, following method was developed in this study to prepare green crosslinker (Dastidar and Netravali, 2013):

Twenty (20) g sucrose was added to 150 mL distilled water in a 500-mL flask, stirred for 5 min to completely dissolve the sucrose. After this 50 mL of hydrogen peroxide (30%) was added to the solution, which made the final hydrogen peroxide concentration to be 7.5%. The sucrose oxidation reaction was allowed to continue at 60^{o}C for 12 hrs. These conditions may be varied depending on the needs and to optimize the reaction. The oxidized sucrose was dried in an air circulating oven at 50^{o}C for at least 2 days to obtain highly viscous liquid or even solid. In order to remove any residual hydrogen peroxide, oxidized sucrose can be re-dissolved and dried one or more times.

Upon oxidation, the primary hydroxyl groups are converted (oxidized) to aldehyde or carboxyl groups. The oxidized sucrose that has two or more aldehyde groups can be used as a crosslinker. This sucrose based green crosslinker was expected to crosslink amine-silica particles as well as to covalently bond the nanoparticles onto cotton surface. Procedures used in BTCA treatment (crosslinking) were used for this green crosslinker.

2.7 ATR-FTIR spectroscopy

Attenuated total reflectance-Fourier transform infrared spectroscopy (ATR-FTIR) is the most straight forward technique that can be used to confirm the successful esterification between cellulose and fatty acid. The ester carbonyl has stretch band around 1745 cm^{-1}. Besides the obvious carbonyl band, the peaks induced by long alkyl chain can be identified as well. For example, peak around 2950 cm^{-1} is

assigned to CH_2 anti-symmetric stretch, 2880 cm^{-1} is assigned to CH_2 symmetric stretch, and 1280 cm^{-1} is assigned to CH deformation such as bending and stretching (Heinze *et al.*, 2006). While ATR-FITR spectra with these peaks present can be used to confirm the successful grafting of acyl chain, this technique is qualitative, and cannot be used to quantitatively determine the amount of acyl chains present on each anhydroglucose unit. In addition, this technique is not so sensitive. Even if the aldehyde and carboxyl groups are present if the concentration is low, this technique may not be useful.

In this study all specimens were characterized using an FTIR spectrophotometer (Nicolet Magna-IR 560, Thermo Scientific, Waltham, MA). ATR-FTIR spectra were taken in the range of 4000-550 cm^{-1} wavenumbers using a split pea accessory. The spectra were recorded as an average of 64 scans obtained at a resolution of 4 cm^{-1}.

2.8 High performance liquid chromatography

High performance liquid chromatography (HPLC, Agilent Technologies, 1200 Series) was used to study the chemical reaction between fatty acid and acetic anhydride. A Eclipse XDS-C_{18} 5μ 4.6 mm × 150 mm Agilent column was used for analysis. Flow rate was set at 1.5 mL/min with an eluent gradient starting at t=0 from 75% acetonitrile/25% water with 0.02 wt% phosphoric acid in water to 100% acetonitrile in 5 min and then keeping at 100% acetonitrile until the end of the analysis. Specimens measuring 10 μL were injected. Wavelength of 214 nm was used to quantitative analysis of the mixture using a UV detector (Peydecastaing *et al.*, 2009).

2.9 Scanning electron microscopy

Scanning electron microscope (SEM, Tescan-Mira3-FESEM) was used to characterize the surface topography of fibers. Specimens were oven dried in an air circulating oven and sputter coated with gold

prior to obtaining SEM images. Images were captured at an accelerating voltage of 5 kV.

2.10 Tensile testing of yarn

Effects of chemical treatment conditions on yarn (both weft and warp) removed from the fabric specimens were studied for their tensile properties using Instron universal testing machine (Model 5566). Due to the limitation of the specimen size (5 cm × 5 cm), modified version of ASTM D2256, Standard Test Method for Tensile Properties of Yarns by the Single-Strand Method, was used in these tests. Gauge length for all test specimens was 30 mm and the crosshead speed was set to 13 mm/min. Under these conditions the breakage of yarn was expected to take place in about 20 ± 3 s. Specimens were oven dried prior to testing using the same air circulating oven. At least 15 specimens were tested to obtain accuracy and reproducibility and their average values are reported. All tests were performed in standard ASTM conditions of 65% relative humidity and 21^{o}C.

2.11 Laundering durability test

Laundering durability evaluation was carried out in a modified version according to the American Association of Textile Chemists and Colorists (AATCC) Test Method 61–2003. The test was performed using a 500 mL flask containing 150 mL aqueous solution of Tide® laundry detergent (0.15%, w/w) and 50 stainless steel balls (diameter = 6 mm), the test was performed at 49 ℃, 40 rpm for 45 min. The size of the fabric specimens was 5 cm × 5 cm for the test. Each cycle in this study was considered to be equivalent to five hand or home launderings (Deng *et al.*, 2010).

2.12 X-ray photoelectron spectroscopy

X-ray photoelectron spectroscopy (XPS, Model: SSX-100, Manufacturer: Surface Science Instruments) was used to analysis the surface elemental composition of cotton fabric. XPS equipped

with Aluminum Kα X-rays and all binding energies were referenced to the carbon C1s energy peak at 284.63 eV. Photoemission electrons were collected at a 55 degree emission angle and the hemispherical analyzer used a 150V pass energy for survey scans and 50V pass energy for high resolution scans.

2.13 Aldehyde group content determination

Two grams of oxidized sucrose was dissolved in 100 mL distilled water in a 500 mL flask. The solution was adjusted to pH 3.2 with 0.5 N NaOH (or HCl, depending on the pH of solution) and 15 mL of hydroxylamine reagent was added. The flask was capped (using cork stopper) and placed in a 40 ℃ water bath for 4 hrs with slow stirring. The excess hydroxylamine was determined by rapidly back titrating the reaction mixture to pH 3.2 with standardized 0.5 N HCl. A blank (without oxidized sucrose) determination with only hydroxylamine reagent was performed in the same manner. The hydroxylamine reagent was prepared by first dissolving 30 g of hydroxylamine hydrochloride in 100 mL of 5 N NaOH before the final volume was adjusted to 500 mL with distilled water.

Carbonyl group content was calculated as follows:

$$\text{Aldehyde content (\%)} = \frac{[\text{blank}-\text{sample})\ \text{mL} \times \text{acid normality} \times 0.028 \times 100]}{\text{sample weight in g (dry basis)}} \quad (5)$$

% hydroxyl group converted to aldehyde was calculated as follows:

$$\text{\% Conversion} = \frac{\text{aldehyde content} \times \text{molecular weight}}{100 \times 28 \times 3} \quad (6)$$

2.14 Ninhydrin test for amine content determination.

A 0.35% (w/v) ninhydrin solution in absolute ethanol was freshly prepared. APTES solutions with different concentrations were used to build the calibration curve. Amine-silica nanoparticle specimen was dried at 120°C for 4−6 h, and then 0.2 g of specimen was placed in a capped vial containing 4 mL of absolute ethanol. The mixture was placed in a bath ultrasonicator for 30 min at room temperature.

Then, 1 mL of ninhydrin solution was added to the vial containing the sample and was ultrasonicated for 10 more minutes. The ninhydrin-specimen dispersion was then placed in a water bath at 65 ℃ for 30 min. The sample was centrifuged at 10,000 RPM for 15 min. Approximately 1 mL of supernatant was pipetted out and the absorbance at 568.11 nm was measured using an Ultraviolet–visible spectrometer (Model: Lamdba 35, Manufacture: PerkinElmer). Measurements were repeated three times and average number was used to construct the calibration curve (Soto-Cantu *et al.*, 2012).

3. RESULTS AND DISCUSSION

3.1 Chemical composition analysis by HPLC

The HPLC was used to track chemical composition change during the reaction as illustrated in Figure 3.1. Figure 3.1a shows the HPLC chromatogram of as-mixed equal moles of heptanoic acid and acetic anhydride where peaks #2 and #3 are assigned to acetic anhydride and heptanoic acid, respectively. The peak intensity difference is due to the difference in detector sensitivity between these two chemicals. Figure 3.1b shows the HPLC chromatogram of microwave treated mixture containing equal moles of heptanoic acid and acetic anhydride at 70% power level for 5 min. The newly emerged peaks seen after microwave treatment were assigned to acetic acid (#1), acetic-fatty anhydride (# 3) and fatty anhydride (# 4), respectively.

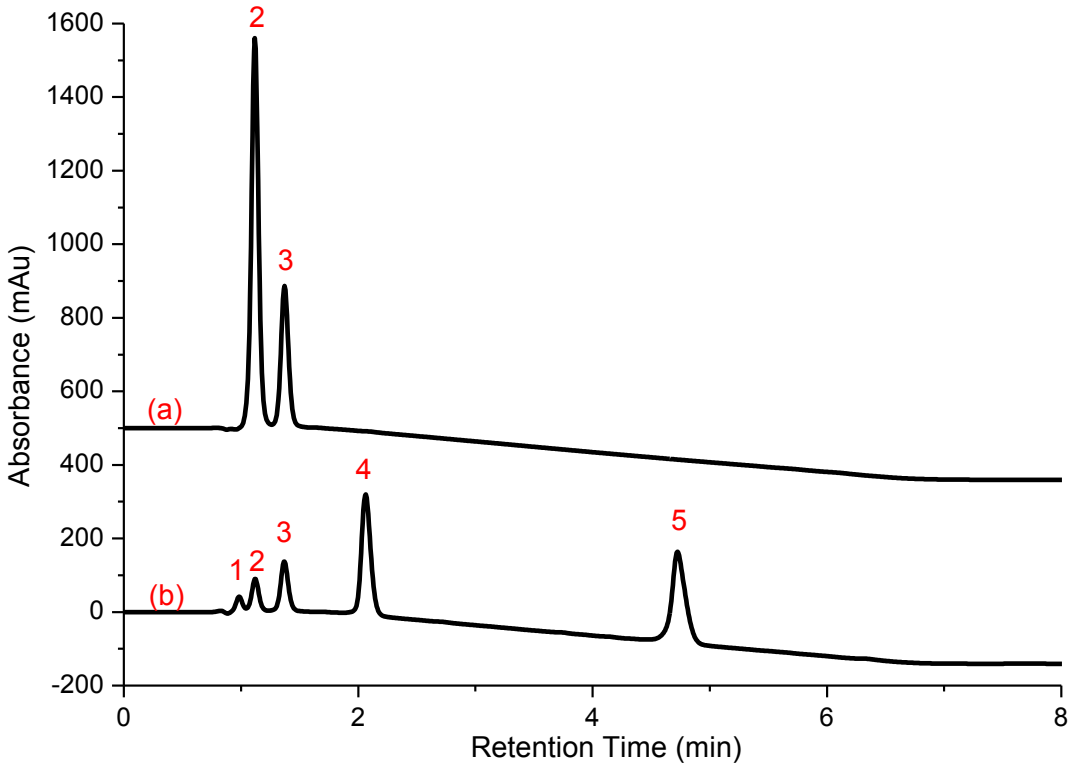

Figure 3.1: HPLC chromatograms a) as-mixed equal mole of heptanoic acid and acetic anhydride; b) 70% power/5 min microwave treated equal mole of heptanoic acid and acetic anhydride

Further investigation was carried out to maximize conversion of fatty acid into fatty anhydride form. Figure 3.2 shows chromatograms of microwave treated mixtures of equal moles of heptanoic acid and acetic anhydride heated at 100% power level for different times. After analyzing the peaks, it's clear that after 10 min of microwave heating, acetic anhydride peak (#2) disappeared. This is due to both being consumed by the reaction and/or evaporation. After 15 min of microwave heating, heptanoic acid peak (#3) disappeared. However, in the absence of acetic anhydride, the reaction proposed in Figure 2.1 can no longer propagate, so the appropriate explanation for the disappearance of heptanoic acid peak (#3) would be evaporation. When the reaction mixture was further heated in the microwave for 30 min, no significant difference was observed compared to the spectrum obtained for 15 min heating, except for the slight decrease in intensity observed for heptanoic-acetic anhydride. The reason for this minor change after 15 min is because of the high boiling point of both heptanoic-acetic anhydride and heptanoic anhydride. This suggests that the additional 15 min of microwave heating did not reach the boiling point of heptanoic-acetic anhydride and heptanoic anhydride.

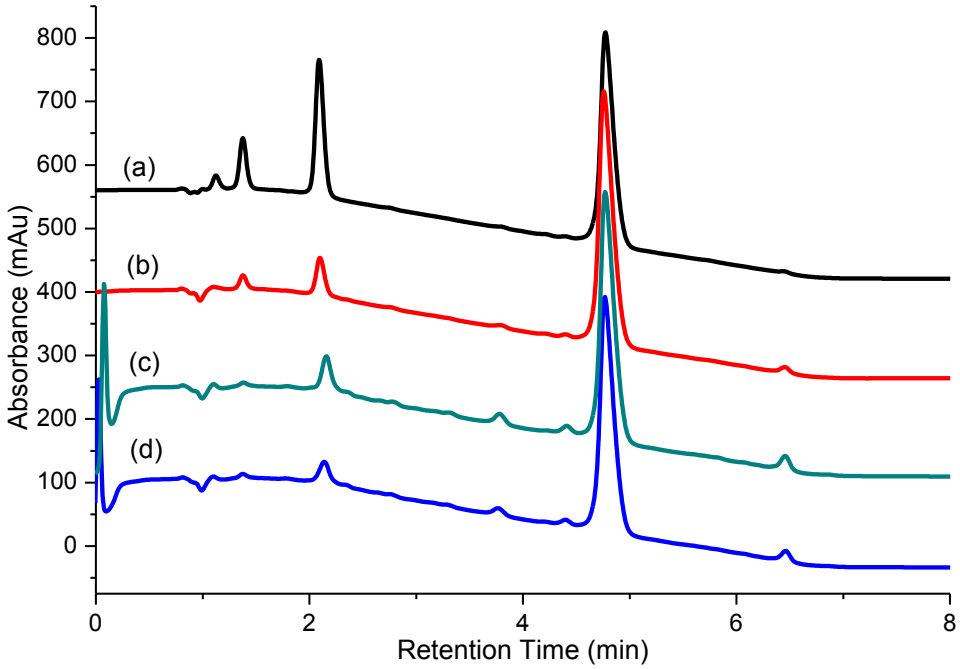

Figure 3.2: HPLC chromatograms a) 100% power/5 min; b) 100% power/10 min; c) 100% power/15 min; d) 100% power/30 min

Based on these chromatograms, optimized condition for preparation of heptanoic anhydride was decided to be between 10 to 15 min heating at 100% microwave power level. Since after 10 min of heating, heptanoic-acetic anhydride content was minimized, the majority present in treated mixture was heptanoic anhydride, thus, only heptanoic acyl grafting needs to be considered for later degree of substitution calculation. For microwaves with different wattages, the time as well as the power levels would be expected to be different and will need to be optimized.

Figure 3.3 shows chromatograms of microwave heated mixtures containing equal moles of heptanoic acid and acetic anhydride heated for different times at 70% power level. A lower power level is expected to result in a lower reaction temperature, since the same amount of the reaction mixture was used. Under these conditions heptanoic acid was completely reacted and/or evaporated after 20 min of heating. However, significant amount of heptanoic-acetic anhydride was still present even after 30 min

of microwave heating.

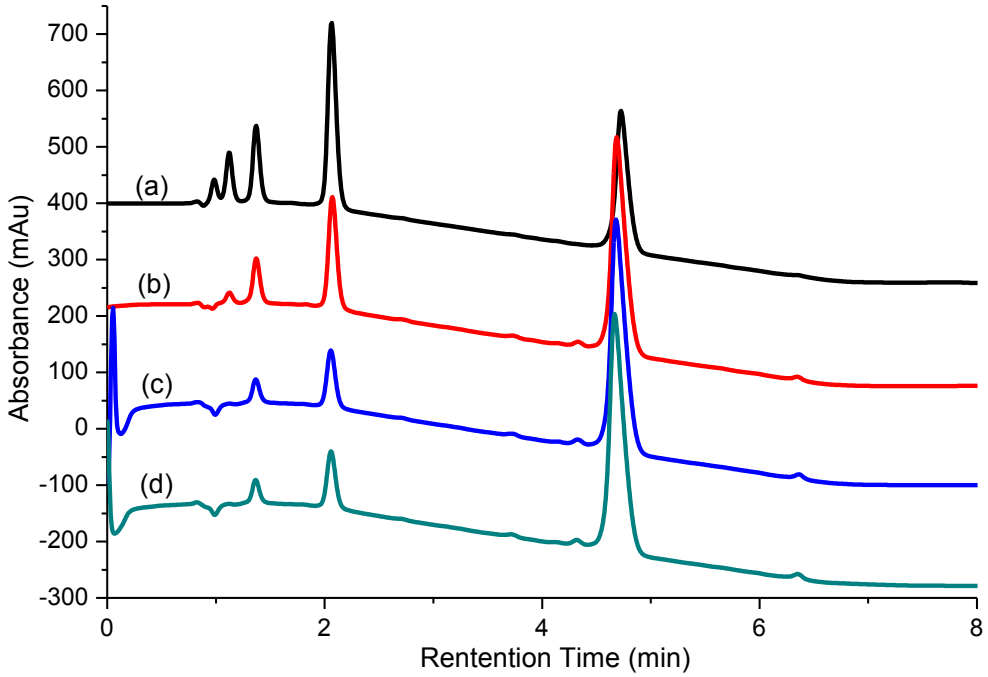

Figure 3.3: HPLC chromatograms a) 70% power/5 min; b) 70% power/10 min; c) 70% power/20 min; d) 70% power/30 min

These results suggest that HPLC can be a powerful technique to optimize the end point of acetic anhydride-heptanoic acid reaction and when the heptanoic acid is consumed. However, when a higher fatty acid (with larger alkyl chain, e.g. stearic acid) was used, their poor solubility in acetonitrile makes it impossible to track the reaction process by HPLC method. This suggests that there is a need to develop an alternative method to track reaction process when higher fatty acid is used.

3.2 Tracking fatty anhydride preparation by ATR-FTIR

Figure 3.4a shows the ATR-FTIR spectrum of pure heptanoic acid. Peaks around 2800 cm^{-1} are assigned to $–CH_2$ and $–CH_3$ groups in its long fatty alkyl chain, peak at 1706.6 cm^{-1} is assigned to the carboxyl groups. Figure 3.4b shows the ATR-FTIR spectrum of pure acetic anhydride. The two peaks for pure acetic anhydride at 1752.9 cm^{-1} and 1826.3 cm^{-1} are assigned to stretching vibration of aldehyde

carbonyl groups. Figure 3.4c shows the ATR-FTIR spectrum of equal moles mixture of heptanoic acid and acetic anhydride where all peaks assigned to both heptanoic acid and acetic anhydride are seen.

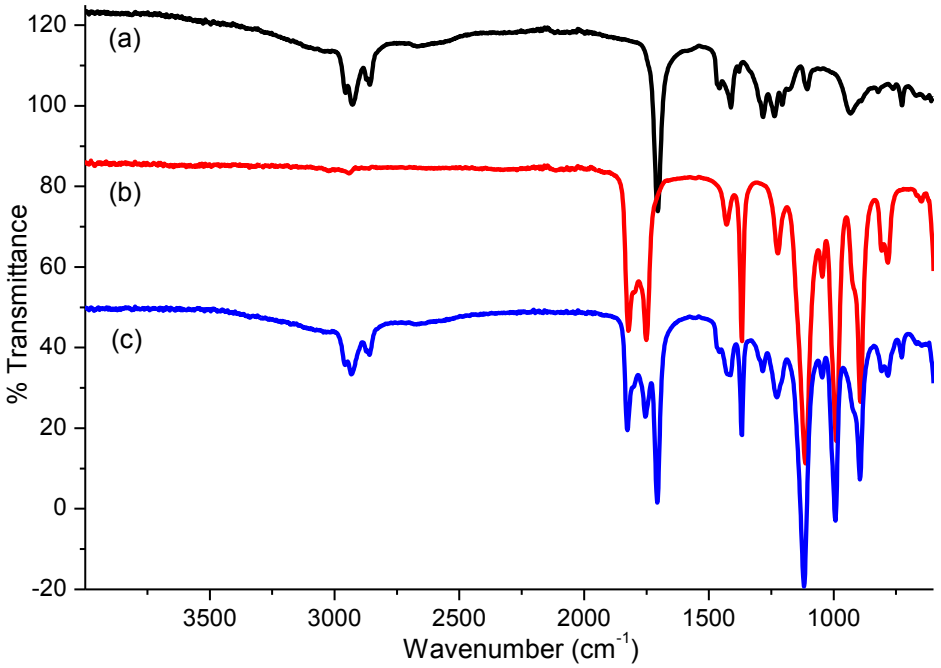

Figure 3.4: ATR-FTIR spectra a) pure heptanoic acid; b) pure acetic anhydride; c) mixture of heptanoic acid and acetic anhydride without microwave heating

As discussed in section 3.1, HPLC method had shown that at the end of the acetic anhydride-heptanoic acid reaction, heptanoic acid was mostly consumed either through the reaction or by evaporation and heptanoic-acetic anhydride and heptanoic anhydride remained. Same conclusion can be reached based on ATR-FTIR analysis discussed above. Figure 3.5a shows ATR-FTIR spectrum of as-mixed equal moles of acetic anhydride and heptanoic acid, as was shown in Figure 3.4c. Figure 3.5b shows ATR-FTIR spectrum of reaction mixture after microwave heating at 100% power for 8 min. As can be seen the intensity of 1706.6 cm^{-1} peak has been significantly reduced. Since 1706.6 cm^{-1} peak is assigned to carboxyl group, the reduced peak intensity means a significant reduction in the presence of heptanoic acid. With further microwave heating to 15 min, as shown in Figure 3.5c, the carboxyl peak at

1706.6 cm^{-1} disappeared from the spectrum, indicating the complete absence of the acid group. However, the intensity of two aldehyde peaks (1752.9 cm^{-1} and 1826.3 cm^{-1}) remained unchanged. Based on Figure 3.5c, we can conclude that the formation of a new compound which contains alkyl chain and anhydride carbonyl group, and in this case, heptanoic-acetic anhydride and heptanoic anhydride. However, from the ATR-FTIR spectra it is difficult to distinguish between heptanoic-acetic anhydride mixture and heptanoic anhydride. As a result, end point of the reaction can only conclude on complete consumption of heptanoic acid and the formation of anhydride.

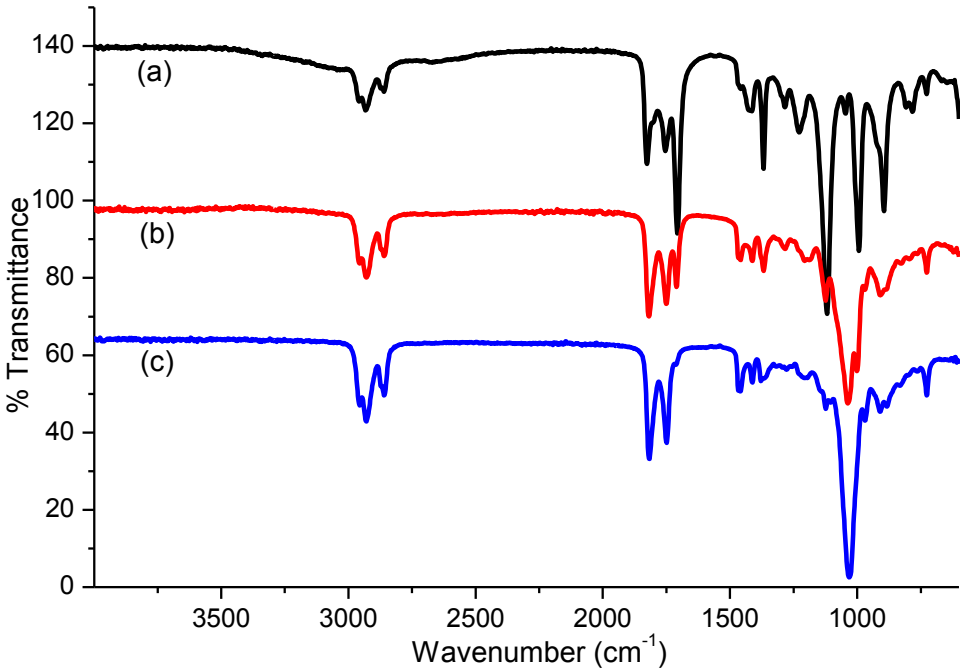

Figure 3.5: ATR-FTIR spectra of a) mixture of heptanoic acid and acetic anhydride before microwave heating; b) mixture of heptanoic acid and acetic anhydride after 100% power/8 min microwave heating; c) mixture of heptanoic acid and acetic anhydride after 100% power/15 min microwave heating

Similar process was used to track the chemical reaction when stearic acid was used in place of heptanoic acid. Figure 3.6a shows ATR-FTIR spectrum for a mixture of equal moles of acetic anhydride and stearic acid. When the reactant mixture was microwave heated for 8 min and at 100% power level,

intensity of carboxylic carbonyl peaks (1706.6 cm^{-1}) underwent a significant drop as can be seen in Figure 3.6b. However, with further heating to 15 min, carboxylic acid peak was still present in the spectrum as shown in Figure 3.6c. This clearly indicates the presence of stearic acid. Stearic acid (boiling point = 382 ℃) has a much higher boiling point than heptanoic acid (boiling point = 223 ℃) and with same microwave heating temperature, less stearic acid can be expected to evaporate from the reaction mixture. It's worth to mention here that, it's not clear whether the higher fatty acid requires a higher temperature for the reaction to go in the desired direction.

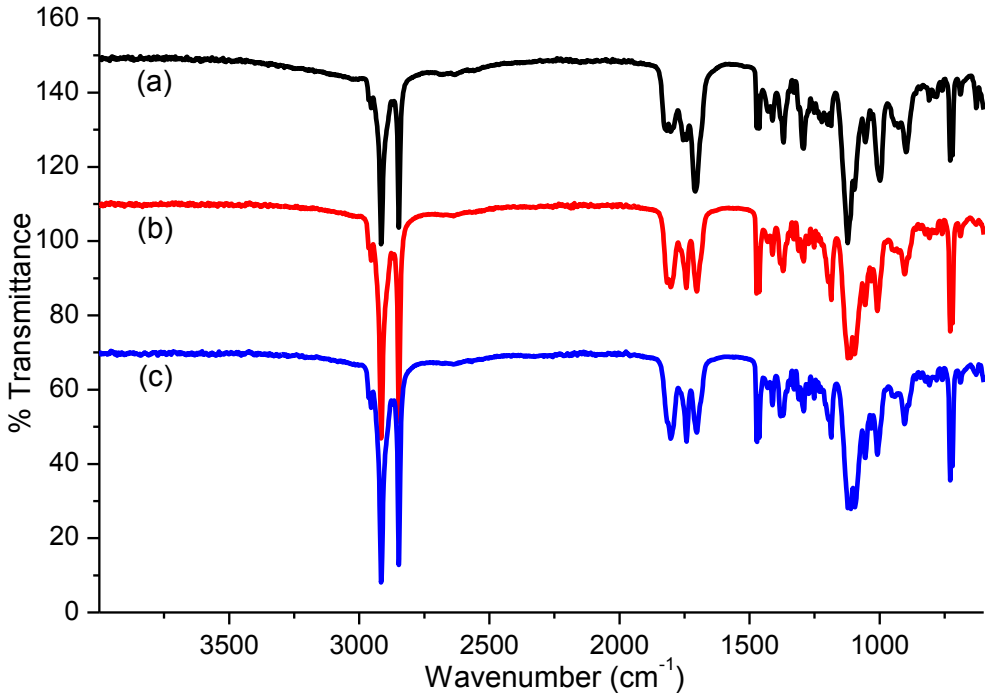

Figure 3.6: ATR-FTIR spectra a) mixture of stearic acid and acetic anhydride before microwave heating; b) mixture of stearic acid and acetic anhydride after 100% power/8 min microwave heating; c) mixture of stearic acid and acetic anhydride after 100% power/15 min microwave heating

3.3 ATR-FTIR analysis of hydrophobic treated cotton fabrics

ATR-FTIR was used to determine the ester formation and qualitatively compare the amount of ester groups present on cotton fabric treated to obtain hydrophobic characteristic. Figure 3.7 shows

ATR-FTIR spectra of cotton fabrics with different hydrophobic treatment conditions. When 100% power level of the microwave was applied, increase in heating time from 3 min to 15 min resulted in larger peak intensity at 1728 cm^{-1}, indicating larger amount of fatty acyl groups grafted on cotton (cellulose).

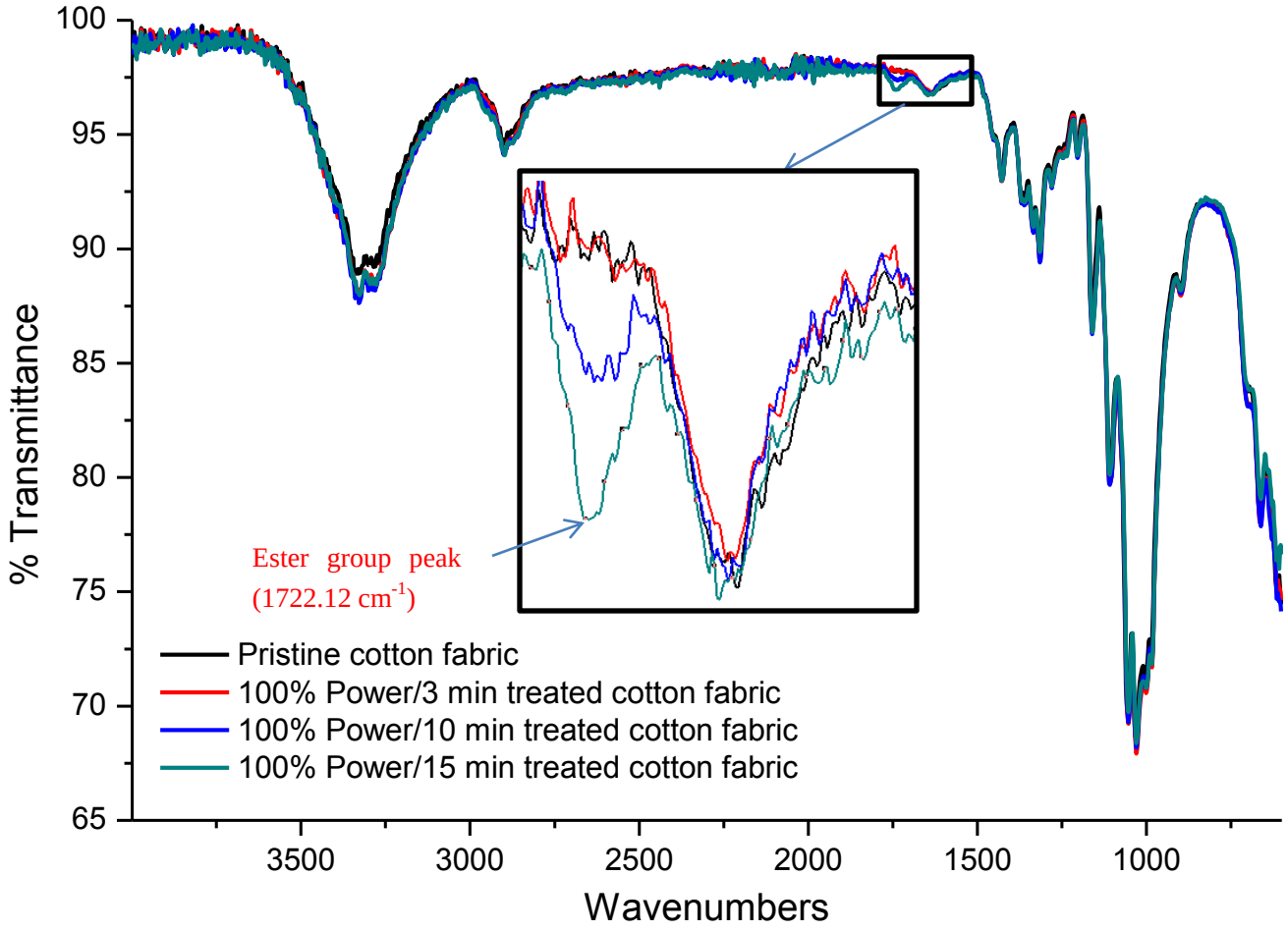

Figure 3.7: ATR-FTIR spectra of unmodified and hydrophobic treated cotton fabric treated under different conditions

Table 3.1 summarizes the assignment of ATR-FTIR peaks particularly for cellulose and its derivatives. After 3 min heating at 100% power, the resulting cotton fabric shows no difference with pristine cotton fabric, which implies that there are only a trace amount of fatty acyl groups grafted or the amount is below the sensitivity of ATR-FTIR. However, spectra for cotton fabric after 10 min

microwave heating shows newly emerged carbonyl peak at 1728 cm^{-1}. The cotton fabric, with further heating time to 15 min, showed an even stronger carbonyl peak than one obtained for 10 min treatment.

Table 3.1: Assignment of ATR-FTIR spectra peaks for cellulose (Heinze *et al.*, 2006)

Wavenumber (cm^{-1})	Assignment	Wavenumber (cm^{-1})	Assignment
3450–3570	OH stretch	1315–1317	CH_2 tip vibration
3200–3400	OH stretch	1277–1282	CH deformation
2933–2981	CH_2 antisymmetric stretch	1225–1235	OH in-plane deformation, also in COOH groups
2850–2904	CH_2 symmetric stretch	1200–1205	OH in-plane deformation
1725–1730	C=O stretch from acetyl- or COOH groups	1125–1162	C–O–C antisymmetric stretch
1635	Adsorption of water	1107–1110	Ring antisymmetric stretch
1455–1470	CH_2 symmetric ring stretch at pyrane ring; OH in-plane deformation	1015–1060	C–O stretch
1416–1430	CH_2 scissors vibration	925–930	Pyran ring stretch
1374–1375	CH deformation	892–895	C-anomeric groups stretch, C_1–H-deformation; ring stretch
1335–1336	OH in-plane deformation	800	Pyran ring stretch

3.4 Effect of different modification conditions on water contact angle of cotton fabrics

3.4.1 Effect of microwave power level and heating time

Hydrophobicity of the modified cotton fabric was evaluated by measuring water contact angle with water. The ethanol washed pristine (untreated) cotton fabric has a water contact angle of 0^o since it spreads and/or absorbs water immediately. Figure 3.8a shows that with fixed microwave heating time of 15 min, and the presence of fatty anhydride (preparation procedures described in section 2.3). Cotton fabric treated in a higher power level resulted in a higher water contact angle. For example, for hydrophobic treatment at 30% power level, the corresponding treated cotton fabric has a water contact angle of 123.7^o. When the power level was increased to 100%, the corresponding water contact angle reached 135.51^o, an increase of about 12^o. Both these treatments can be considered to have made the cotton fabric hydrophobic, though not superhydrophobic.

Water contact angle measurements were also used to evaluate the effect of microwave treatment time for cotton fabrics treated at 100% power level. The corresponding water contact angles are shown in Figure 3.8b. When the microwave treatment was carried out for 3 min the treatment resulted in a hydrophobic cotton fabric with 125.64^o water contact angle. The water contact angle increased with longer treatment time and reached 137.48^o for 15 min of microwave heating time.

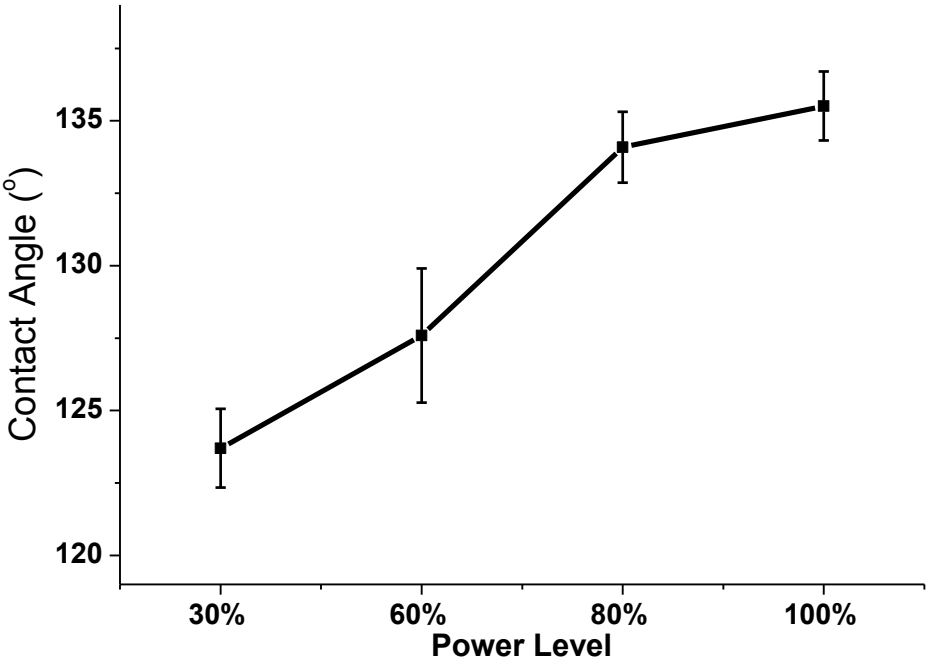

a)

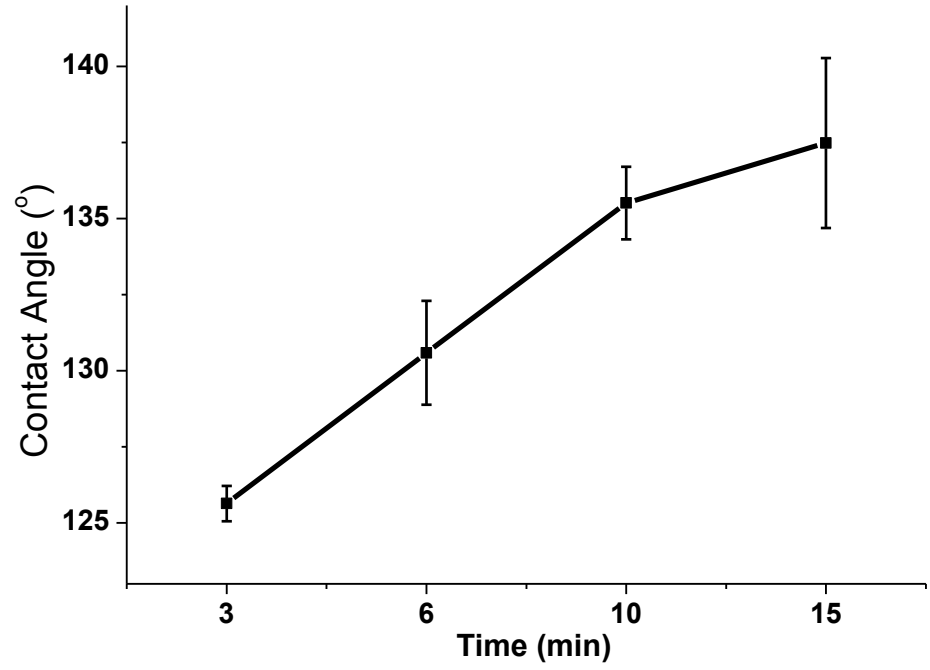

b)

Figure 3.8: Water contact angle measurement of modified cotton with different microwave heating conditions a) 10 min heating time was maintained; b) 100% power level was maintained

Based on the results seen in Figure 3.8, water contact angle shows a positive correlation with both power level and heating time. If the water contact angle is solely considered, one can assume that the value can increase further with a longer microwave treatment time. However, it's true that this will have a certain limitation as it will reach equilibrium under the experimental conditions. Microwave treatment is well known for its high energy efficiency for generating high temperature in a short time. However, both Figures 4.2 and 4.5 reveal that the reaction temperature, in some experiments, went beyond the boiling point of heptanoic acid (223℃). At such high temperature, the degradation of cellulose and loss of reactant due to evaporation can be significant, and hence, it is important to be careful and avoid such conditions.

3.4.2 Effect of fatty acid chain length

The effect of fatty chain length on water contact angle was characterized using fatty acids with different chain lengths. Microwave treatment condition was set at 100% power level for 15 min for these experiments. Fatty acids selected for this study were heptanoic acid, octanic acid, dodecanoic acid and stearic acid with carbon atoms in the alkyl chains of 7, 8, 12 and 18, respectively. It can be expected that fatty acid with a longer alkyl chain will have a lower surface energy because of the hydrophobicity of the alkyl chain itself. By grafting fatty acyl groups on the surface of cotton, its surface energy (or surface tension) can be significantly reduced. For similar surface roughness, the surface energy has negative relationship with water contact angle. Water contact angle values for these fatty acids grafted onto cotton are listed in Table 3.2. It is interesting to note that the water contact angle value only showed only a 3.3^{o} difference between them. This is probably due to the fact that only a small number of fatty acyl groups were grafted on to the cotton surface. As a result, the difference in surface energy and the water contact

angle is not significant. However, the data does indicate that there may be a correlation between the chain length and the water contact angle. If the process is optimized to obtain higher grafting level, higher water contact angles may be obtained. Figure 3.9 shows the histogram for the data listed in Table 3.2.

Unpaired *t*-test was used to determine if the water contact angle values are significantly different between the different fatty acids. Results shown that at 95% confidence interval, the two-tailed P value equals 0.1887, which means there is no statistically significant difference between heptanoic acid and stearic acid treatment.

Table 3.2: Effect of fatty chain length grafted onto cotton on water contact angle

Specimens	Number of Carbon in fatty chain	Water contact angle (^{o})	
		Mean	St. Dev.
Heptanoic acid	7	135.51	1.19
Octanic acid	8	135.42	2.31
Dodecanoic acid	12	136.26	2.71
Stearic acid	18	138.87	3.48

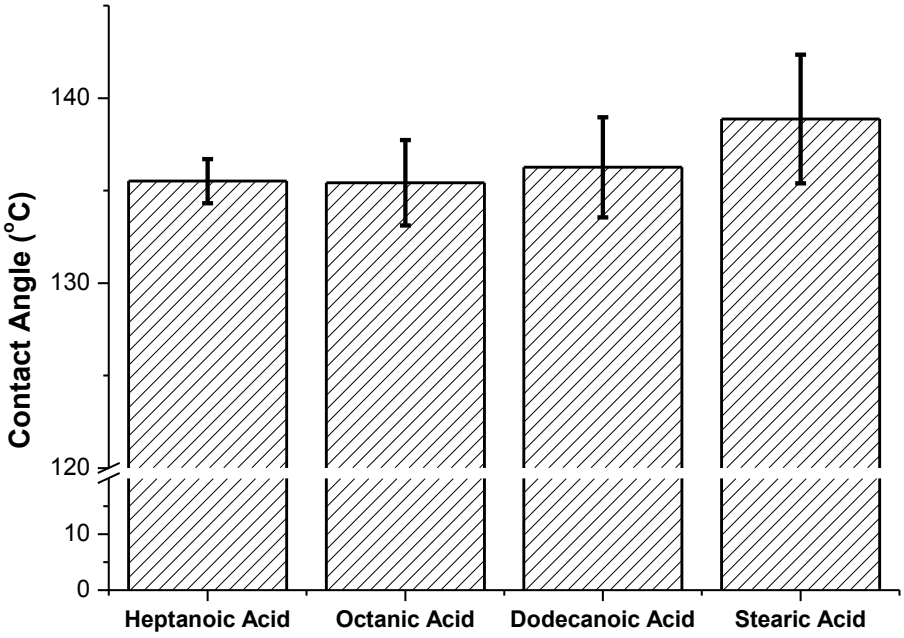

Figure 3.9: Effect of fatty chain length on water contact angle

3.5 Mechanical property results

As mentioned previously, the high temperature generated by microwave treatment can cause cellulose degradation. To study this, tensile properties of the cotton yarns, both warp and weft, were studied for fabrics treated under different conditions. The results of the tensile tests are shown in Table 3.3. Pristine (untreated) cotton yarn showed a tensile fracture stress at break (strength) of 733.43 MPa for warp and 630.15 MPa for weft. With 10 min microwave treatment but power levels ranging from 30% to 100%, the yarn tensile stress at break underwent a gradual decrease, confirming the cotton fiber degradation. For 100% power level and 10 min microwave treatment, the warp retained 80.3% of its original strength, i.e., lost 19.7%, whereas for weft it was 73.2% strength retention (loss of 26.8%).

For the treatment at 100% power level of microwave and with times ranging from 3 to 15 min, tensile stress at break initially underwent a gradual decrease. However, after 15 min treatment, a

significant drop was observed. For cotton yarn exposed to microwave treatment at 100% power level for 15 min, only 52.7% strength was retained (loss of 47.3%) for warp and 49.6% for weft (loss of 50.4%). These results imply that between the treatment time of 10 to 15 min, reaction temperature reaches a high point causing serious degradation of cellulose. Figure 3.10 shows the histogram of data presented in Table 3.3 for easy comparison.

Table 3.3: Tensile test results of cotton yarn

Specimens	Tensile Stress at Break (MPa)					
	Warp			Weft		
	Average	St. Dev.	% Retained	Average	St. Dev.	% Retained
Pristine cotton	733.4	49.2		630.1	37.8	
30% Power/10 min	729.4	59.9	99.4	604.1	56.1	95.8
60% Power/10 min	664.5	52.9	90.6	598.3	55.4	94.9
80% Power/10 min	649.9	35.4	88.6	545.3	42.3	86.5
100% Power/10 min	589.2	47.3	80.3	461.2	39.9	73.2
100% Power/3 min	692.3	43.9	94.3	611.7	59.2	97.0
100% Power/6 min	671.6	55.2	91.5	581.6	50.0	92.3
100% Power/15 min	381.9	16.2	52.0	312.5	12.7	49.6

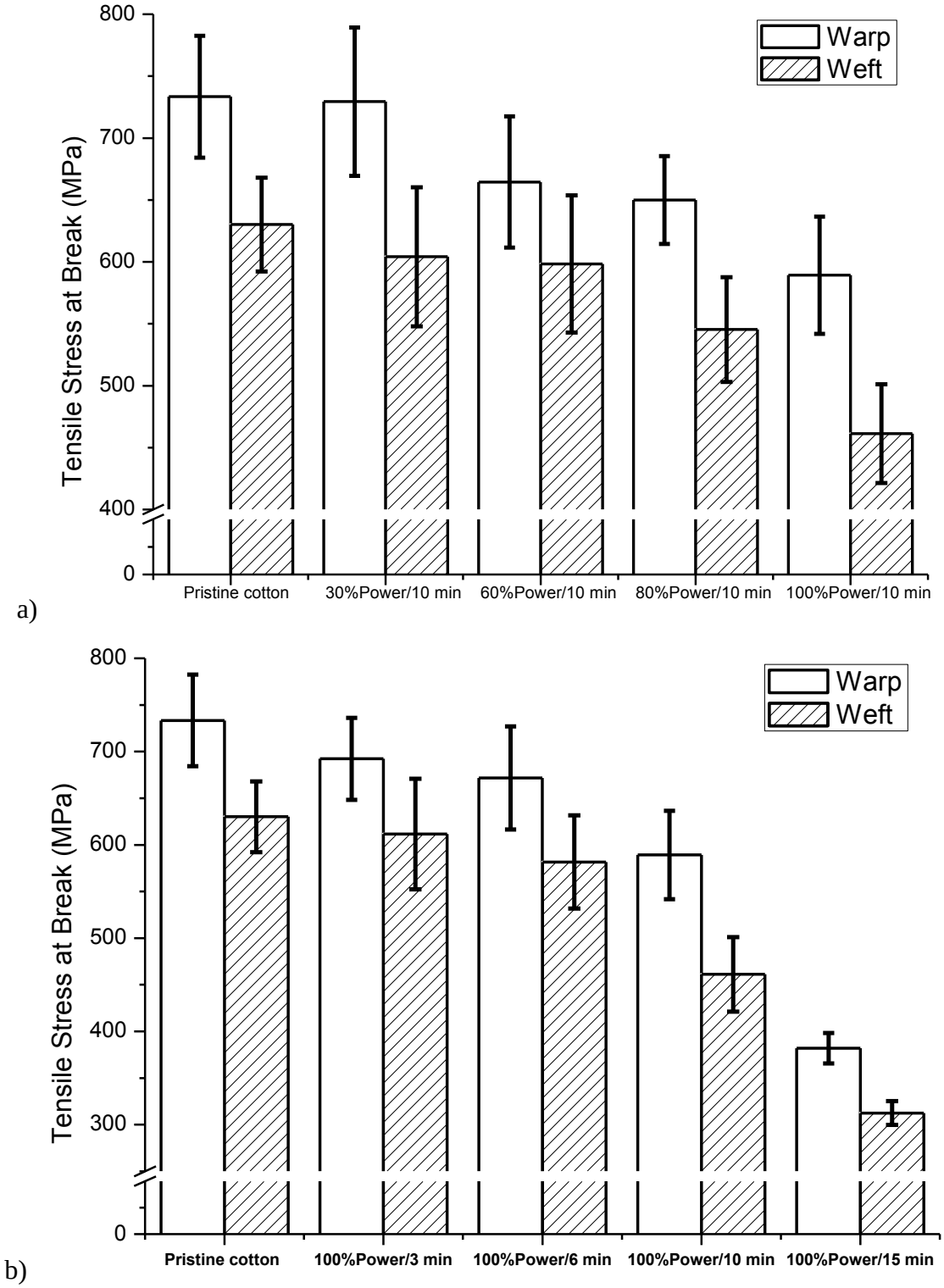

Figure 3.10: Histograms of tensile test results of cotton yarn a) hydrophobic treatment involved same microwave heating time and different power levels; b) hydrophobic treatment involved same power level with different heating times

3.6 Treatment durability after laundering

It is important that the hydrophobic treatment be durable and sustain many launderings without deteriorating. With a chemically grafted (covalently bonded) fatty acyl chain, the durability of this hydrophobic cotton fabric can be expected to be longer than any other physical coating methods. In the present study Tide® detergent was used to evaluate the laundry durability. The fabric was passed through several successive laundry cycles. As was expected, fabrics treated at higher microwave power level showed that more laundry cycles were needed before the fabric became hydrophilic. For a 10 min treatment applied at 30% microwave power level, the treated fabric only retained hydrophobicity for 3 laundry cycles. This number increased significantly to 31, when 100% power level was applied. Same phenomenon was observed in the case of 100% microwave power level but different treatment times. Fabrics treated for 3 min retained its hydrophobicity for only 3 laundry cycles. This number increased to over 35, when the microwave treatment was carried out for 15 min. Table 3.4 presents the laundry results of specimens treated with different microwave conditions.

Figure 3.11 shows the change in water contact angle as a function of laundry cycles. It can be seen that the water contact angle values decreased gradually with laundry cycles. When water contact angle approached 105^{o}, the cotton fabric could no longer retain water droplet for 10 seconds, the water droplet was absorbed by cotton fabric, so it was classified as non-hydrophobic. The decrease in water contact angle can be possibly explained by the hydrolysis of ester group with the presence of detergent. It may also be due to the cellulase enzymes used in the detergent to degrade and remove the top cellulose layer in cotton. In our case, unfortunately, the top layer is the one that is hydrophobic.

Table 3.4 Laundry durability of fabric hydrophobicity

Specimens	Cycle of laundry test			Average	St. Dev.
30% Power/10 min	3	3	3	3	0
60% Power/10 min	10	12	12	11.3	1.15
80% Power/10 min	23	22	24	23	1
100% Power/10 min	31	29	33	31	2
100% Power/3 min	2	3	3	2.67	0.57
100% Power/6 min	17	15	17	16.3	1.15
100%Power/15 min	35	35	37	35.7	1.15

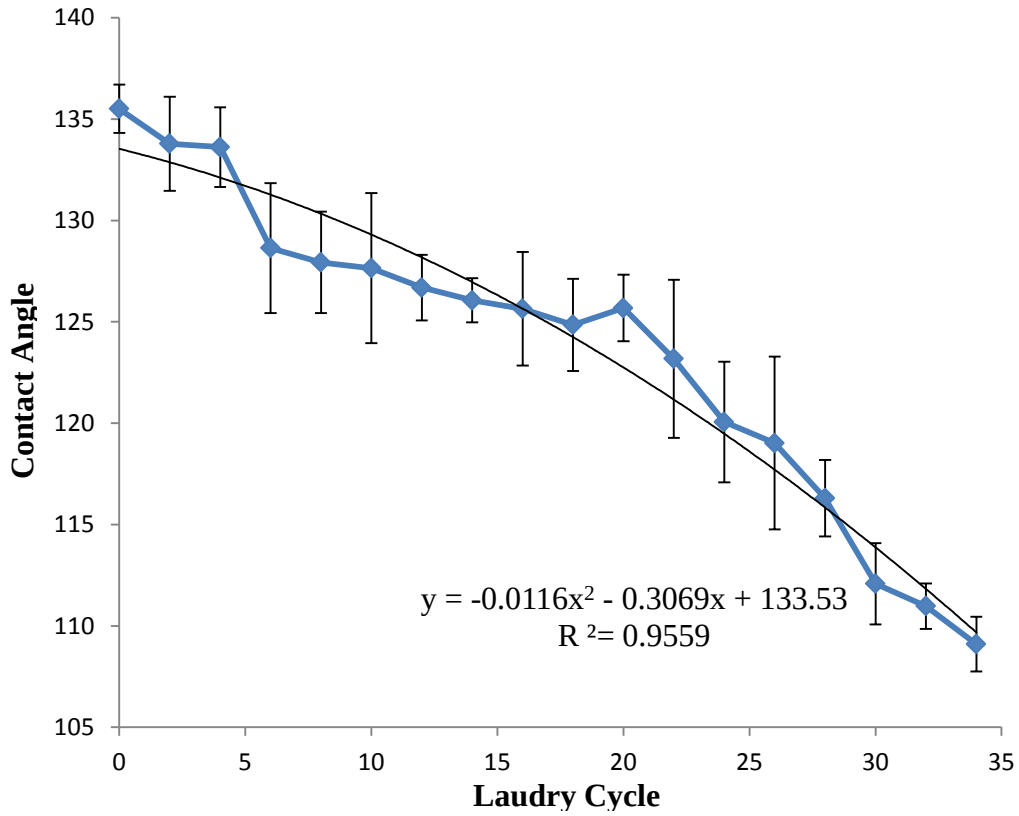

Figure 3.11: Change in water contact angle with different laundry cycles

3.7 Preparation of amine-silica particles

Amine-silica particles were prepared based on Stöber method (Stöber *et al.*, 1968). By changing reactant ratio, amine-silica particles with different sizes were obtained. Figure 3.12 shows SEM image of amine-silica particles. Average diameter of particles was calculated by randomly measuring 50 particles from SEM images. Results showed that the larger particles had an average diameter of 458 nm while the diameter of smaller particles was 107 nm. SEM analysis also revealed that the particles, particularly the larger ones, were uniformly spherical.

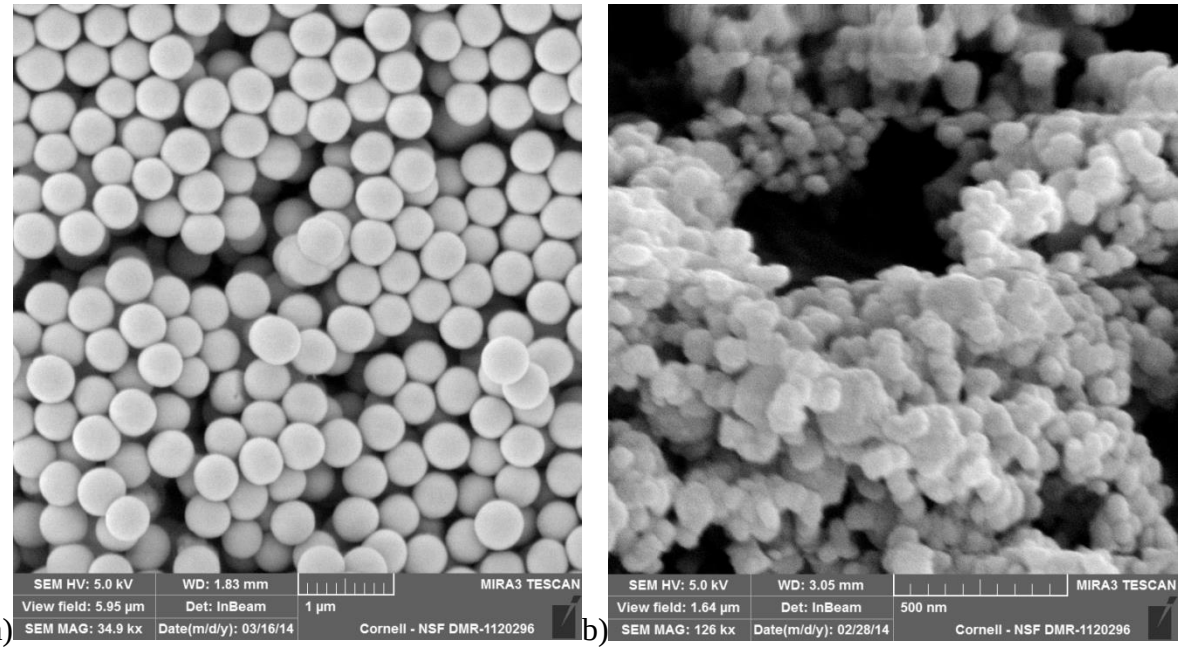

Figure 3.12: SEM images of amine-silica particles with diameter of a) 458 nm; b) 107 nm

ATR-FTIR technique was used to characterize the chemistry of amine-silica particles obtained in powder form. The ATR-FTIR spectra obtained for amine-silica particles and pure APTES are presented in Figure 3.13. APTES has one primary amine group in its chemical structure and the peak at 1552 cm^{-1} is assigned to that primary amine group and can been seen from ATR-FTIR spectrum of pure APTES. However, the amine group ($-NH_2$) peak at 1552 cm^{-1} was not detected in the case of amine-silica

particles (Chen *et al.*, 2008). The reasons why the amine group didn't appear in ATR-FTIR spectrum are not clear. However, the possible explanation is that the amine group content is blow the detection limit of ATR-FITR spectrometer.

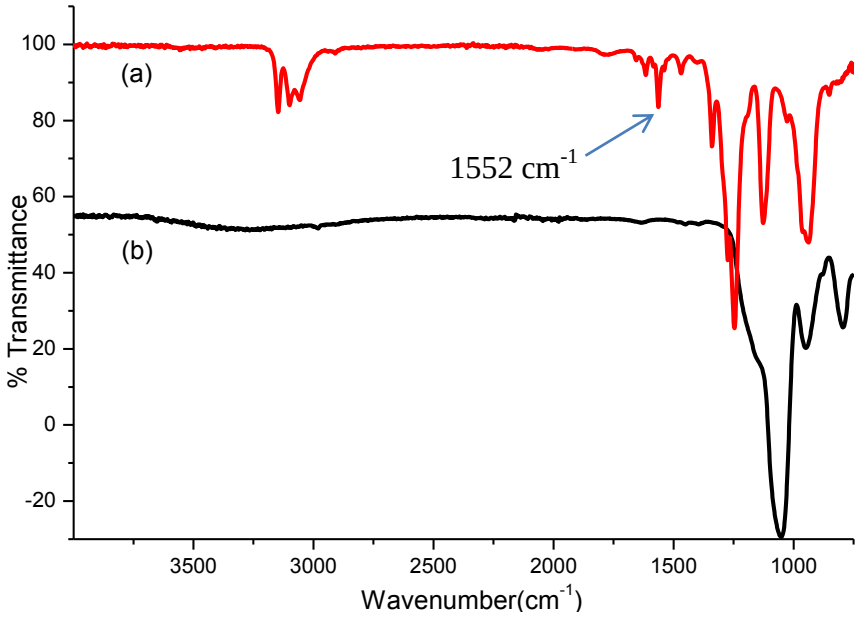

Figure 3.13: ATR-FTIR spectra of a) pure APTES; b) amine-silica particles

3.8 Amine content determination

Ninhydrin test was also used to detect the amine group. Ninhydrin can readily react with primary and secondary amines, and the resulting compound produces a purple color. With the help of UV-vis spectroscopy the purple color can be characterized to determine the amount of amine groups quantitatively. Figure 3.14 shows the reaction mechanism between ninhydrin and amine-silica particles.

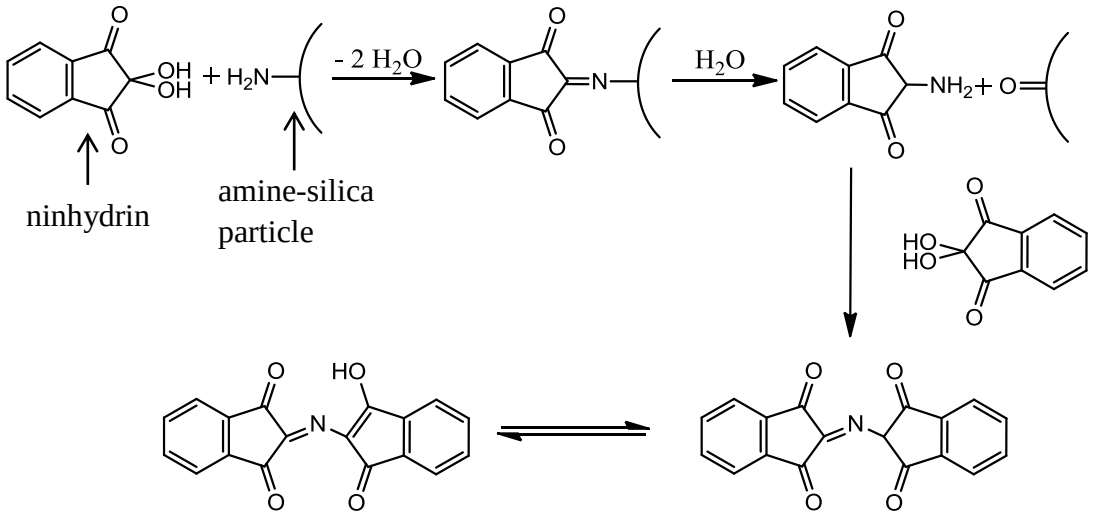

Figure 3.14: Reaction mechanism between ninhydrin and amine-silica particles

Calibration curve was constructed with different known concentrations of APTES solutions which were followed by ninhydrin reaction. APTES was used because it contains one primary amine group, and it's also a raw material for amine-silica particle synthesis in this research. Higher concentration of APTES resulted in a solution with denser purple color. Figure 3.15 shows different colors of the supernatant obtained after reacting ninhydrin with amine-silica particle specimens which were analyzed using UV-vis spectrometer.

Figure 3.16 shows UV-vis spectra of ninhydrin reacted APTES solutions with different concentrations (1.07 mM, 2.14 mM, 4.27 mM, respectively), the corresponding absorbance value at 568.11 nm was reported in Table 3.5. Based on the results presented in Table 3.5, calibration curve as shown in Figure 3.17 was constructed. It can be seen that the UV-vis absorbance (y) and APTES concentration (x) shows a linear relationship:

$$y = 0.2756x + 0.049 \quad (7)$$

With the help of the calibration curve, amine group concentration for amine-silica particles with

different preparation methods can be calculated. Three different amine-silica particles were prepared and their preparation procedures are summarized as follows:

Figure 3.15: Supernatant of amine-silica particle reacted with ninhydrin. The APTES concentration increases from left to right

With the help of the calibration curve, amine group concentration for amine-silica particles with different preparation methods can be calculated. Three different amine-silica particles were prepared and their preparation procedures are summarized as follows:

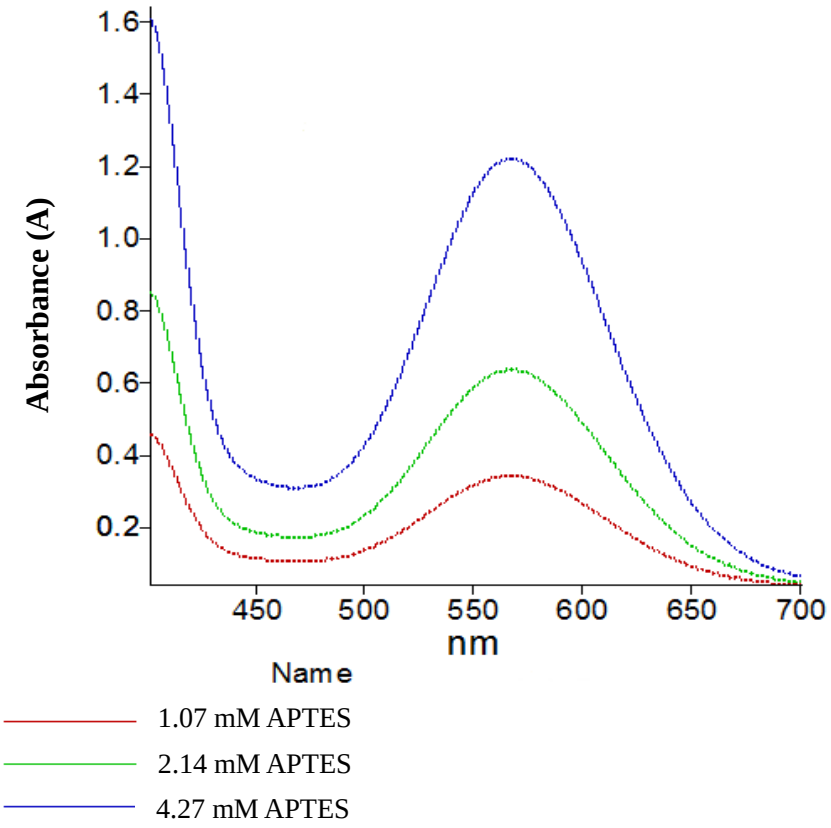

Figure 3.16: UV-vis spectra of different ninhydrin reacted APTES solutions

Table 3.5: Absorbance values from UV-vis spectroscopy measurement

Specimens	Absorbance at 568.11 nm
1.07 mM APTES solution	0.084789
2.14 mM APTES solution	0.52435
4.27 mM APTES solution	1.1954

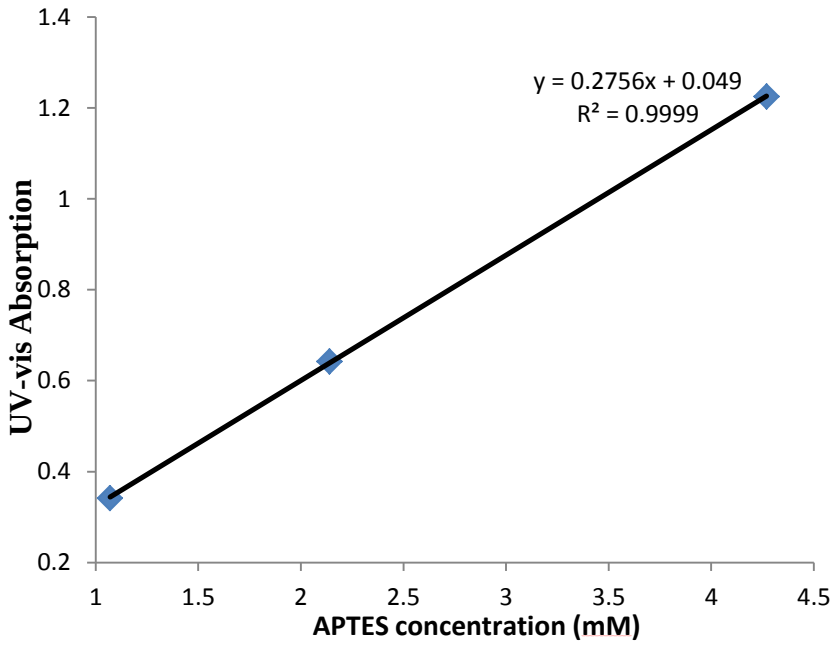

Figure 3.17: Calibration curve for amine group concentration determination

Since the only difference in the preparation method for amine-silica particles was the amount of APTES added, the resulting amine-silica particles have similar properties except the surface amine group content. Figure 3.18 shows the UV-vis spectra of those specimens, the corresponding absorbance values were recorded. Amine group concentration of the specimens can be calculated using Equation 7 and the results are shown in Table 3.6. Specimen ASP#2 had 1 g APTES added during the preparation step, 5 times more than ASP#1, surprisingly, amine group content in ASP#2 is 13 times more than ASP#1. However, with further increase of APTES amount to 3 g for ASP#3, about 2 times more amine groups were observed compared with ASP#2. Based on this result, it's expected that amine group concentration can be further increased. Presence of more amine groups on particle surface is highly preferred, since it means a higher possibility for the particles to be covalently bonded to the cotton surface.

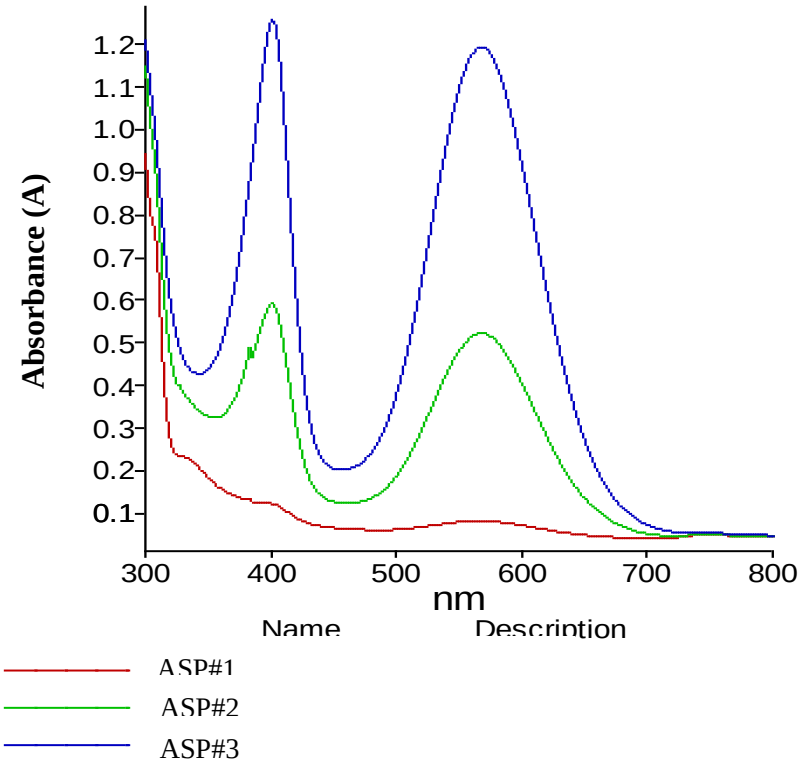

Figure 3.18: Uv-vis spectra of different ninhydrin reacted amine-silica particle dispersions

Table 3.6: Quantitative determination of amine concentration on silica particle surface

Specimens	Absorption (A)	Amine group conc. (mM)
ASP#1	0.084789	0.130
ASP#2	0.52435	1.725
ASP#3	1.1954	4.160

3.9 Cotton fabrics treated with single size particles

Single size amine-silica particle (small particle: 107 nm) containing dispersions with different concentrations, 0.5%, 0.1% and 0.02% (w/v), were prepared. Cotton fabrics with physically deposited particles using different particle concentrations were prepared as described in section 2.6.

SEM images of cotton fabrics with physically deposited amine-silica particles are shown in Figure 3.19. As can be seen in these images, particles are not evenly distributed on the fiber surface and their agglomerations result in different sizes. These uneven agglomerations were expected to further increase the surface roughness, as uniformly distributed particle layer will result in a flattened or smoother surface. As described in section 1.7, a rough surface is always preferred for enhanced hydrophobicity as it results in higher water contact angle.

In addition, particle dispersion with higher concentration results in higher particle loading on the fiber surface. There is a noticeable difference between the images shown in Figures 4.19b, 4.19c and 4.19d, where the corresponding amine-silica particle dispersion concentrations were 0.5%, 0.1% and 0.02%, respectively. Cotton fabric treated with 0.5% amine-silica particle dispersion showed the presence of more agglomeration than ones treated with 0.1% and 0.02%. This is due to the fact that dispersion with higher particle concentration is more likely to have problem of aggregation. Cotton fabric treated with 0.5% amine-silica particle dispersion also showed that the majority of cotton fiber surface was covered by amine-silica particles (Figure 3.19b). However, in Figure 3.19d, where cotton fabric treated with 0.02% amine-silica particles dispersion, majority of cotton fiber surface was exposed to the environment.

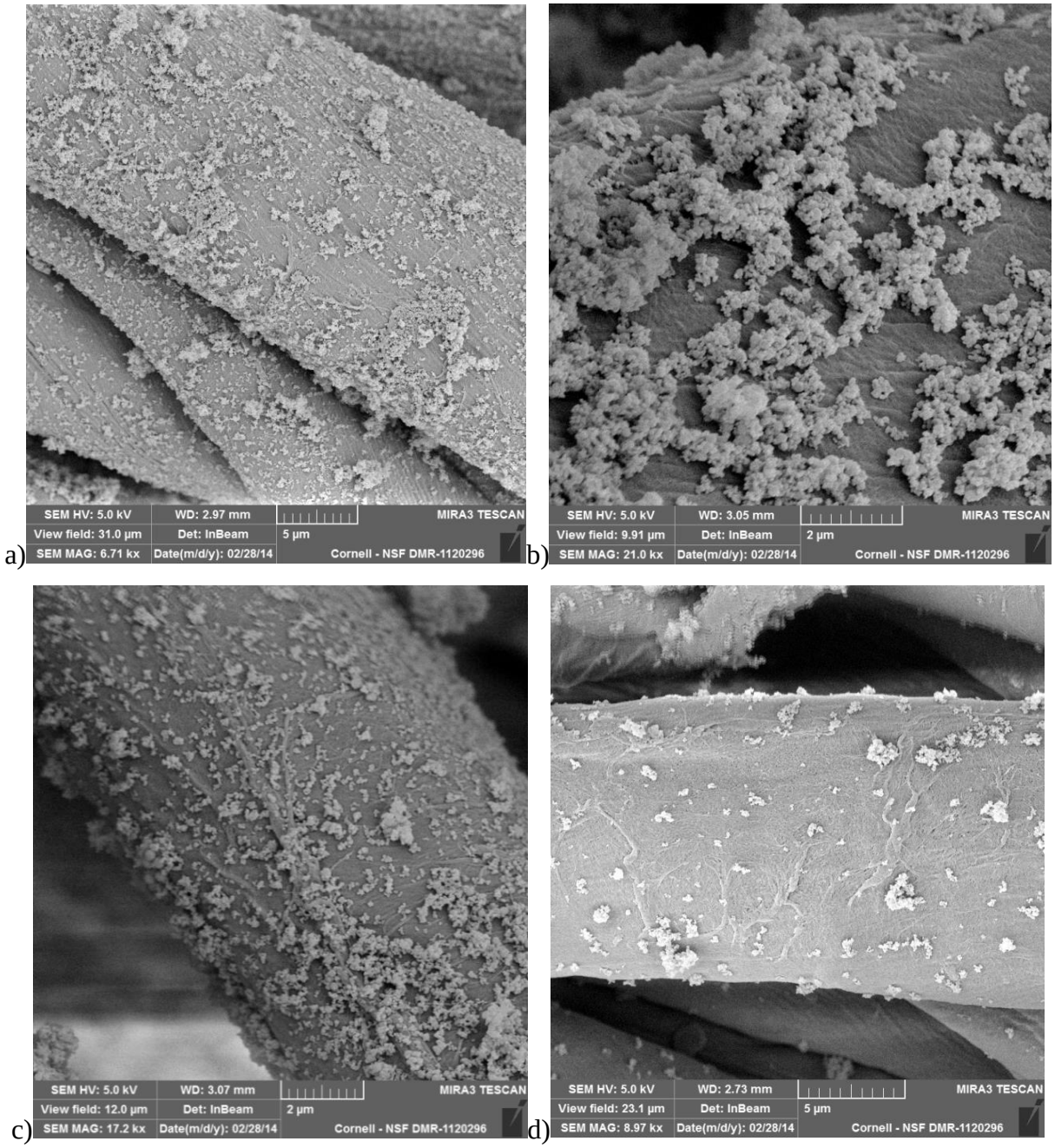

Figure 3.19: SEM images of small size amine-silica particles deposited on cotton fabric. Cotton fabric was first BTCA treated and activated, followed by immersing in a) and b) 0.5% amine-silica particle dispersion; c) 0.1% amine-silica particle dispersion; d) 0.02% amine-silica particle dispersion

3.10 Ultrasonication treatment of cotton fabric with physically adsorbed single size particles

Cotton fabric treated with 0.5% amine-silica particle dispersion (Figure 3.20a) was used to measure the effects of ultrasonication on removal of physically deposited particles. Cotton fabric with physically deposited particles was immersed in water for ultrasonication. Ultrasonication will cause physically adsorbed particles to vibrate, and eventually leave the fiber surface and diffuse into water phase. SEM images were taken after different ultrasonication durations to observe corresponding fiber surface morphology.

Figure 3.20 shows SEM images of cotton fabrics with physically deposited particles after different ultrasonication durations. There is no significant difference seen in the SEM images obtained for specimens before ultrasonication (Figure 3.20a and Figure 3.20b) and after 2 min ultrasonication treatment (Figure 3.20c and Figure 3.20d). However, after 5 min of ultrasonication (Figure 3.20e and Figure 3.20f), the amount of large agglomerations showed a noticeable decrease. Smaller agglomerations were still present on the fabric surface. After 10 min of ultrasonication, large agglomerations were completely removed and what remained was a single layer of small particles evenly distributed on cotton surface as seen in Figures 3.20g and Figure 3.20h.

From these results it may be concluded that ultrasonication removes majority physically adsorbed particles from cotton surface. Also, the large agglomerations are more likely to be removed than small agglomeration.

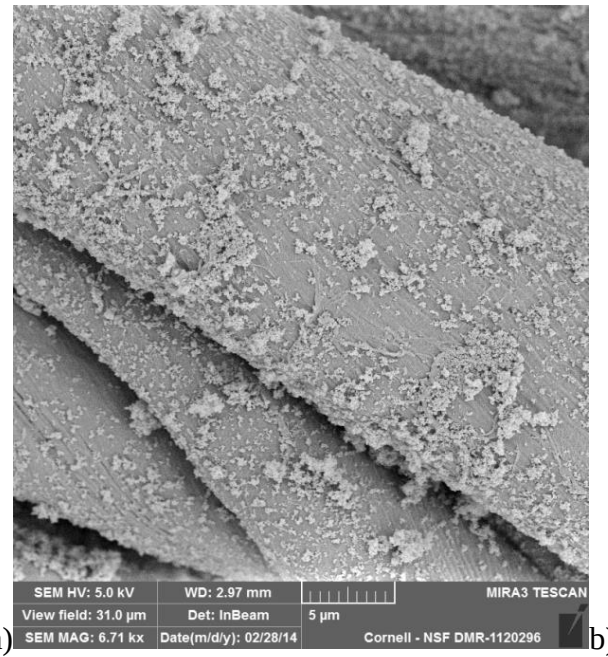
SEM HV: 5.0 kV
WD: 2.97 mm
MIRA3 TESCAN
View field: 31.0 µm
Det: InBeam
5 µm
SEM MAG: 6.71 kx
Date(m/d/y): 02/28/14
Cornell - NSF DMR-1120296

a)

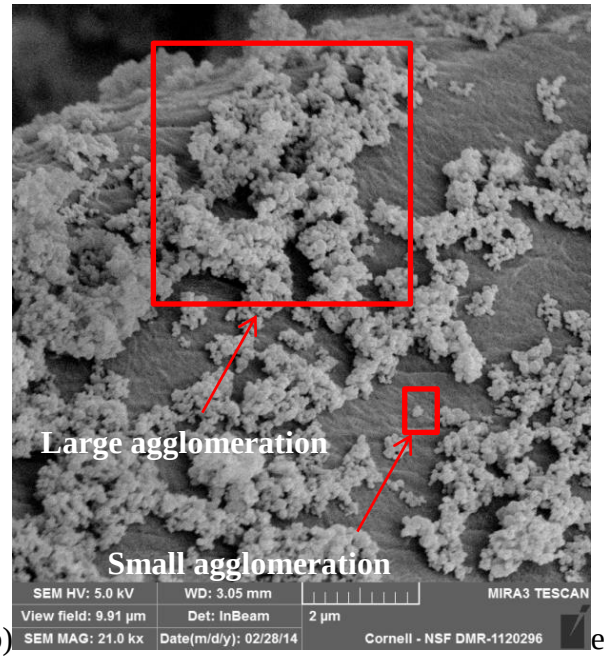
Large agglomeration
Small agglomeration
SEM HV: 5.0 kV
WD: 3.05 mm
MIRA3 TESCAN
View field: 9.91 µm
Det: InBeam
2 µm
SEM MAG: 21.0 kx
Date(m/d/y): 02/28/14
Cornell - NSF DMR-1120296

b)

e

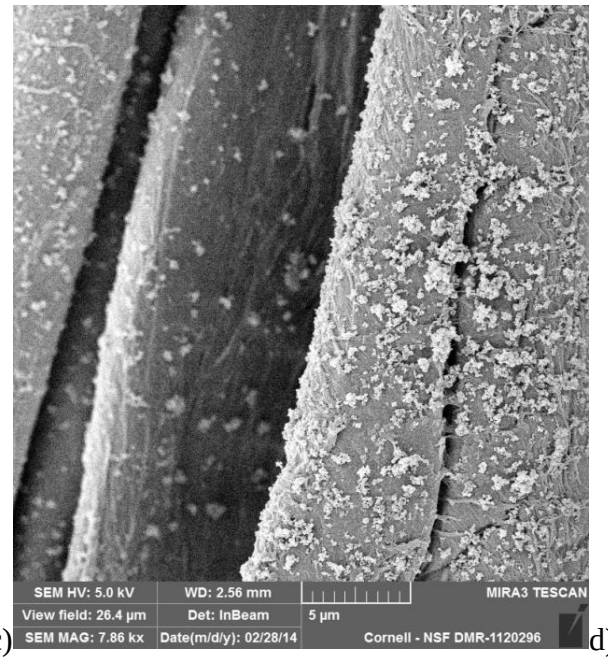
SEM HV: 5.0 kV
WD: 2.56 mm
MIRA3 TESCAN
View field: 26.4 µm
Det: InBeam
5 µm
SEM MAG: 7.86 kx
Date(m/d/y): 02/28/14
Cornell - NSF DMR-1120296

c)

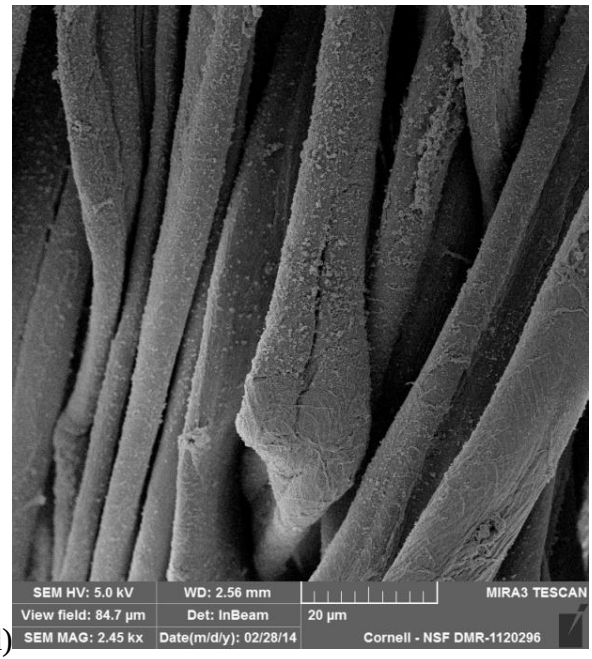
SEM HV: 5.0 kV
WD: 2.56 mm
MIRA3 TESCAN
View field: 84.7 µm
Det: InBeam
20 µm
SEM MAG: 2.45 kx
Date(m/d/y): 02/28/14
Cornell - NSF DMR-1120296

d)

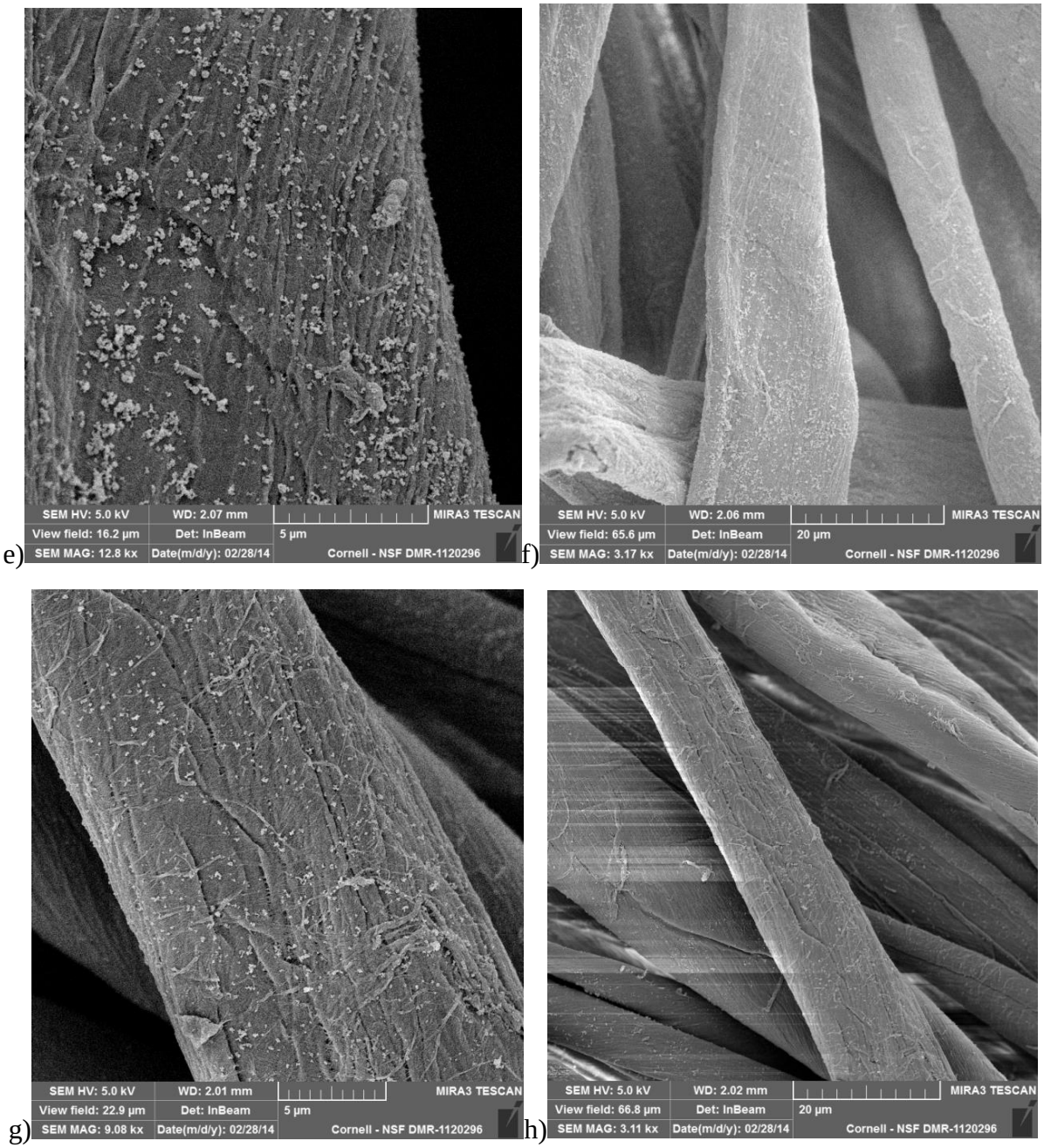

Figure 3.20: SEM image of ultrasonication treated cotton fabric with physically deposited particles a) and b) before ultrasonication; c) and d) after 2 min of ultrasonication; e) and f) after 5 min of ultrasonication; g) and h) after 10 min of ultrasonication

3.11 Hydrophobicity of cotton fabrics with physically deposited particles

Cotton fabric with physically deposited amine-silica particles increased the surface roughness. However, in order to obtain hydrophobicity, cotton fabric still needs to undergo hydrophobic treatment. Surface roughness and hydrophobicity together can result in superhydrophobicity as discussed earlier. The procedures described in section 2.6 were used to obtain hydrophobic cotton fabric. The treatment conditions used were 100% microwave power and 10 min of heating. During the treatment, fatty anhydride would react with hydroxyl groups on cellulose and amine groups on amine-silica particles forming ester and amide bonds, respectively.

The influence of hydrophobic treatment on the surface morphology of cotton fabric was characterized using SEM. Figure 3.21 shows SEM images of cotton fabric before and after hydrophobic treatment. No significant difference could be observed between these two images. The cotton fabric surface showed similar small and large agglomerations. This suggests that the hydrophobic treatment does not influence the surface morphology of physically deposited particles on cotton fabric.

Water contact angle of hydrophobic treated cotton fabrics were measured and the results are presented in Table 3.7. All hydrophobic cotton fabrics with deposited particles exhibited a higher water contact angle value than the control fabric for those with no particles deposited on cotton surface. After the treatment with amine-silica particle deposition on the cotton fabric surface higher degree of surface roughness was achieved. Dispersions with higher amine-silica particles resulted in increased surface roughness. These fabrics with higher surface roughness resulted in higher water contact angle as was expected.

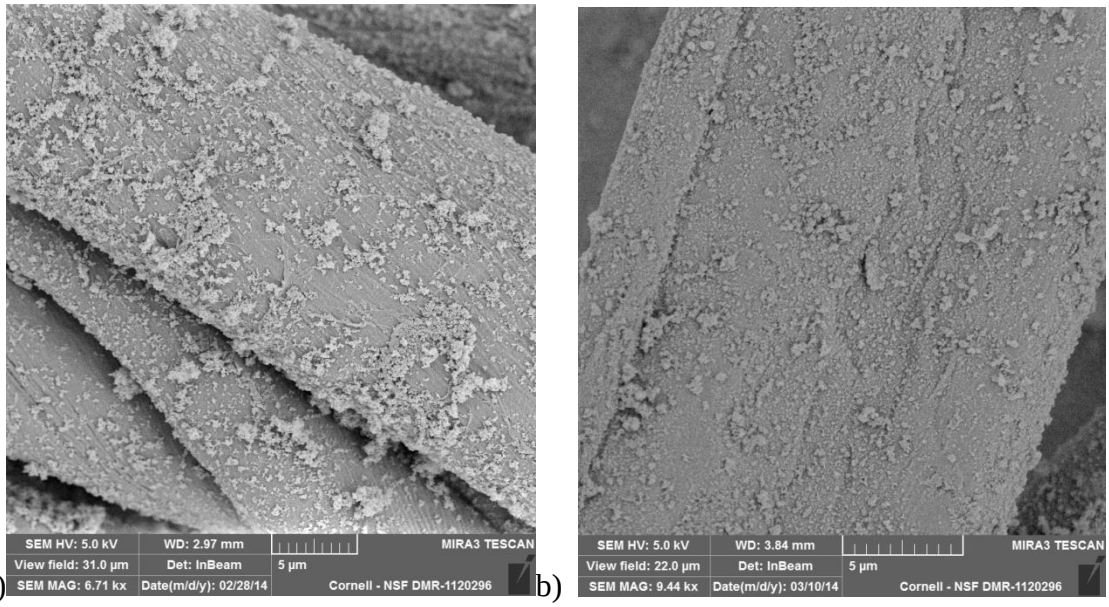

a) b)

Figure 3.21: SEM images of a) cotton fabric with physically deposited amine-silica particles; b) cotton fabric with physically deposited amine-silica particles followed by hydrophobic treatment

Cotton fabric treated with 0.02% amine-silica particle dispersion showed a 5.78^{o} increase in water contact angle than 135.5^{o} obtained for the control specimen. When 0.1% amine-silica particle dispersion was used, a 10.12^{o} increase in water contact angle to 143.6^{o} was obtained. With further increase in amine-silica particle dispersion to 0.5%, the water contact angle increased to 144.9^{o}, a 12.37^{o} increase in water contact angle than that obtained for the control specimen. Based on these results, it's expected that further increase in concentration of amine-silica particle dispersion will result in even higher water contact angle. While it is not clear how high a water contact angle can be obtained by this method, particle dispersion with high concentration will have difficulty in dispersing the particles. In addition, a very high loading of particles onto surface may cause the initially roughened surface to be smoothened. Flattened surface would then reduce the water contact angle.

Unpaired *t*-test was used to determine if the water contact angle values are significantly different from each other. Results showed that at 95% confidence interval, there is no statistically significant

difference between the control cotton fabric and that treated in 0.02% amine-silica particle dispersion. The two-tailed P value for this case was 0.0935. In addition, at 95% confidence interval, the difference was not considered to be statistically significant between cotton fabric treated with 0.02% amine-silica particle dispersion and the one treated with 0.5% amine-silica particle dispersion. The two-tailed P value for this case was 0.5874. The highest water contact angle of 144.9 is close to what is conventionally considered to be superhydrophobic, 150^{o}.

Table 3.7: Water contact angle results of hydrophobic cotton fabric with physically deposited particles

Specimens	Water contact angle (^{o})	St. Dev. (^{o})
Control (no particle)	135.5	1.1
Treated in 0.02% amine-silica particle dispersion	139.3	2.7
Treated in 0.1% amine-silica particle dispersion	143.6	2.9
Treated in 0.5% amine-silica particle dispersion	144.9	2.2

3.12 Effect of BTCA treatment on cotton fabrics

The cotton fabrics were also treated with BTCA to create pendent carboxyl groups on the surface of the cotton fabric. Those carboxyl groups can then be activated by EDC/NHS coupling reaction and the activated carboxyl groups will readily react with amine groups on the surface of amine-silica particle to form amide bond. As a result, amine-silica particles can be covalently bonded onto the surface of cotton fabric unlike in the previous case where the amine-silica particles were physically present. The chemically bonded particles can be expected to give permanent hydrophobicity and will not be washed off easily during laundering.

ATR-FTIR spectra of BTCA treated cotton fabric is shown in Figure 3.22. The newly appeared peak

at 1720 cm^{-1} was assigned to both ester carbonyl group and carboxyl group as it is impossible to distinguish between these two groups due to their overlapping. It's worthy to mention here that there is a minor peak that appears at 1564 cm^{-1}, which is assigned to carboxylate group (Yang, 1991); (Sricharussin *et al.*, 2004). By immersing BTCA treated cotton fabric in 0.1 M NaOH solution, the free carboxyl groups react with NaOH to form carboxylate groups. The ATR-FTIR spectra of 0.1 M NaOH solution treated cotton fabric is shown in Figure 3.23 and the peak intensity at 1564 cm^{-1} significantly increased indicating that the BTCA treated cotton fabric has large amount of free carboxyl groups. More free carboxyl groups are preferred in this situation, after activation by EDC/NHS coupling agent as they will result in a higher probability for attachment of the particles.

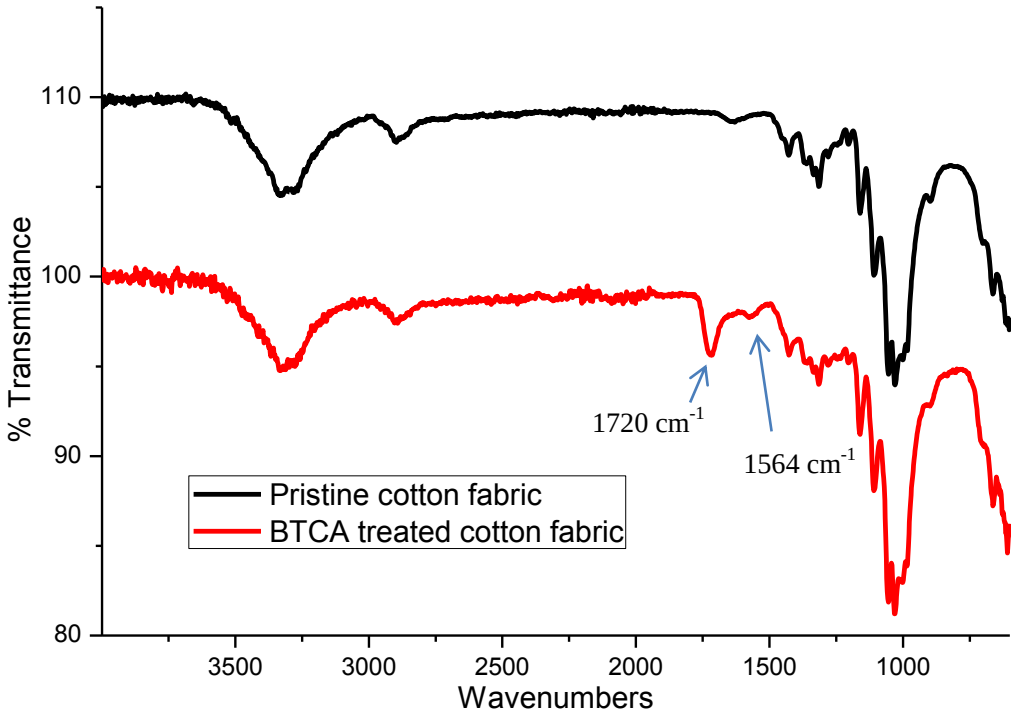

Figure 3.22: ATR-FTIR spectra of pristine cotton fabric and BTCA treated cotton fabrics

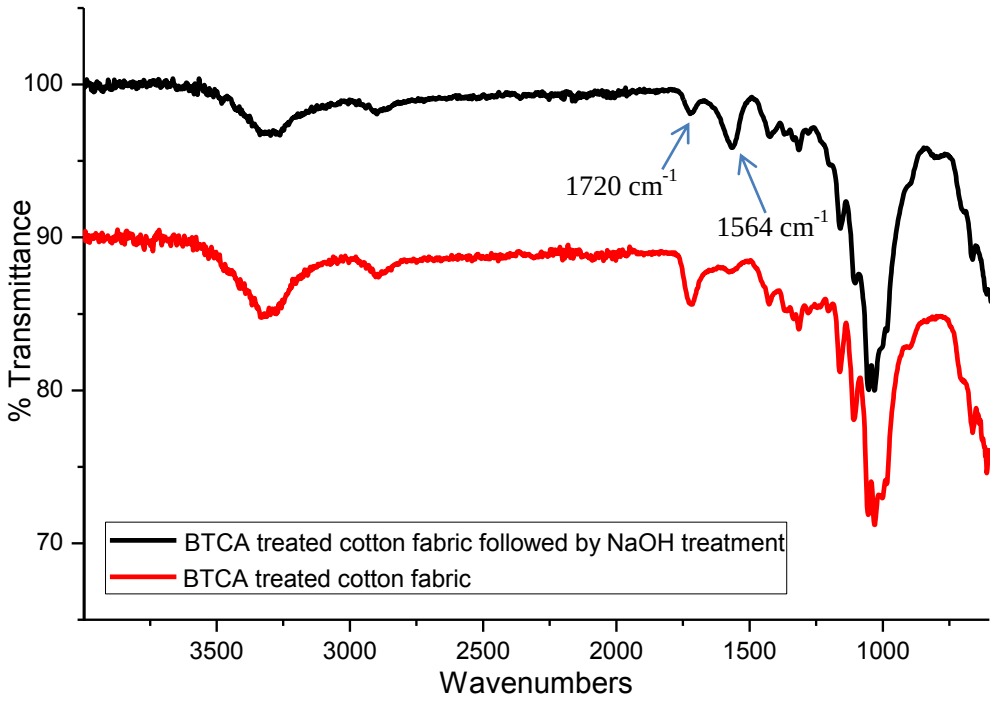

Figure 3.23: ATR-FTIR spectra of BTCA treated cotton fabric and BTCA treated cotton fabric followed by NaOH treatment

3.13 Effect of particle deposition on BTCA treated and activated cotton fabrics

BTCA treated cotton fabric has free carboxyl groups on the surface and after EDC/NHS coupling reaction those free carboxyl groups are activated. Once activated carboxyl groups should readily react with amine groups on amine-silica particles. Amine-silica particle dispersion with different concentrations, 0.5%, 0.1% and 0.02% (w/v), were prepared as described earlier and BTCA treated cotton fabrics were immersed in the dispersions. Three hrs of stirring the mixture at room temperature was needed for reaction to reach completion.

SEM images of cotton fabrics with covalently bonded amine-silica particles are shown in Figure 3.24. Surface morphology was similar to that obtained earlier with cotton fabric with physically deposited nanoparticles. Agglomerations of different sizes were evenly distributed on fiber surface. Amine-silica particle dispersions with three different concentrations gave a considerably similar surface morphology. This may due to the fact that covalent bonding method involves 3 hrs of immersing time in amine-silica particle dispersion, much longer than physical deposition method (30 min). It is possible that 3 hrs is long enough for particles to be adsorbed onto surface.

While the particles are covalently bonded in this method, the major drawback is that only the bottom layer of amine-silica particles are covalently bonded to the fiber surface. Beside the bottom layer, all other particles in the agglomerations stay in their position simply by physical attraction.

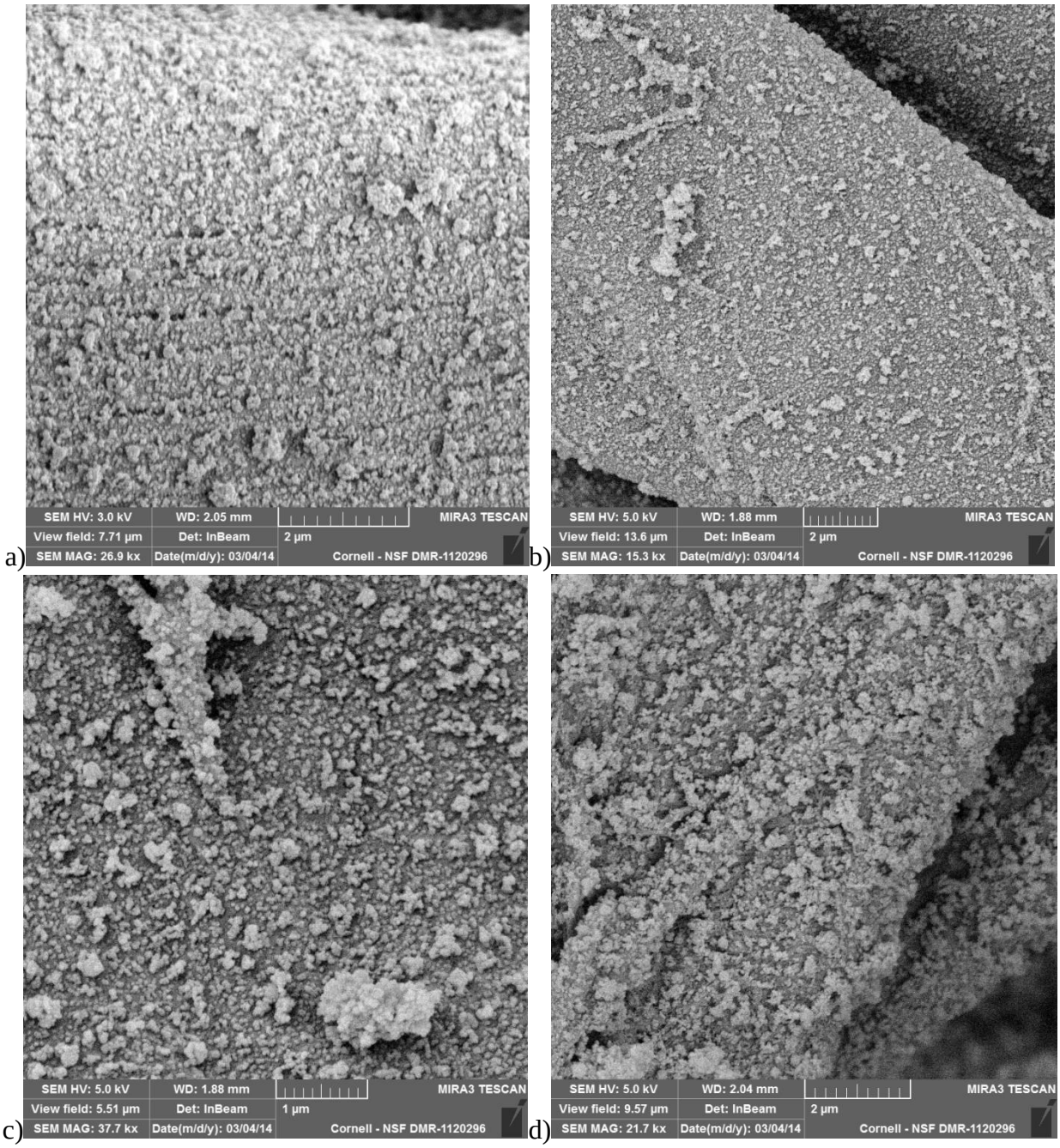

Figure 3.24: SEM images of cotton fabric treated with covalently bonding method. a) 0.5% amine-silica particle dispersion; b) and c) 0.1% amine-silica particle dispersion; d) 0.02% amine-silica particle dispersion

3.14 Hydrophobic treatment of cotton fabric with covalently bonded particles

Cotton fabric with covalently bonded particles was further treated with fatty anhydride to obtain higher hydrophobicity, if possible, and the detailed procedures have been described in section 2.4. Conditions were set to 100% microwave power and 10 min of microwave heating. During the treatment, fatty anhydride reacted with the hydroxyl groups on cellulose and amine groups on amine-silica particles to form ester bonds and amide bonds, respectively.

Water contact angle of hydrophobic treated cotton fabrics were measured and the results are shown in Table 3.8. For comparison water contact angles obtained for fabrics on which particles were physically deposited are also included. Hydrophobic treated cotton fabrics with covalently bonded particles all exhibited higher water contact angle values than the control (no particles deposited). This can be simply explained by the increased roughness brought about by amine-silica particle deposition.

Interestingly, hydrophobic treated cotton fabrics with covalently bonded particles showed higher water contact angle values than those treated with physical deposition method. By comparing the SEM images of those two methods, cotton fabrics treated with covalent bonding method showed a higher degree of roughness than those with physical deposition method. There may be two reasons for this. Covalent bonding method involved a longer particle deposition time to allow amide formation to be completed. As a result, this process allowed more particles to be deposited on to fiber surface. Also, in the physical deposition method the particles have the freedom to get back into the liquid phase even after being deposited on the fiber surface.

Cotton fabric treated in 0.02% amine-silica particle dispersion showed a water contact angle of 145.84^{o}, a 10.33^{o} increase than that obtained for control fabric specimen (135.51^{o}). When 0.1%

amine-silica particle dispersion was used the water contact angle was 149.77^{o}, a 14.3^{o} increase than control specimen. With further increase in amine-silica particle dispersion concentration to 0.5%, the water contact angle with water was 148.82^{o}, an increase of 13.3^{o} compared to that obtained for control fabric specimen. Cotton fabric treated in 0.5% amine-silica particle dispersion concentration showed a slightly lower water contact angle than fabric treated in 0.1% dispersion concentration. However, unpaired *t*-test showed that at 95% confidence level, there is no statistically significant difference between water contact angle values obtained from 0.5% particle dispersion and 0.1% particle dispersion. In this case the two-tailed P value equals 0.2705.

Table 3.8: Water contact angle results of hydrophobic cotton fabric with covalently bonded particles

Specimens	Water contact angle (^{o})	St. Dev. (^{o})
Control (no particles)	135.51	1.19
Treated in 0.02% amine-silica particle dispersion	145.84	2.74
Treated in 0.1% amine-silica particle dispersion	149.77	4.57
Treated in 0.5% amine-silica particle dispersion	148.82	3.54

3.15 Laundry durability test for hydrophobic cotton fabric with covalently bonded particles

Hydrophobic cotton fabric with covalently bonded particles was washed with Tide® detergent to test its laundering durability. The laundering process has been discussed earlier in section 2.11. After 13 laundry cycles, cotton fabric absorbed water droplet within 10 s, meaning the hydrophobicity was lost after washing.

SEM images of cotton fabrics with different laundry washing conditions are shown in Figure 3.25. SEM image in Figure 3.25a was obtained before the laundry wash, Figure 3.25b was obtained after 7

laundry cycles and Figure 3.25c was obtained after 13 laundry cycles. No significant decrease in surface particle concentration was observed by comparing Figures 3.25a and 4.25b. However, Figure 3.25c did show a significant decrease in surface particles. In addition, increasing in cotton fiber surface splitting or fibrillation also could be detected.

As stated earlier the hydrophobic cotton fabric lost its water repellency after 13 wash cycles. This perhaps can be explained by the decrease in the amount of hydrophobic silica particles. During the laundry wash, top layer of hydrophobic silica particles do wash away from the fiber surface, because they can be physically removed by the agitation during washing. Once the hydrophobic silica particles, in the top layer are removed the inner layer of particles are exposed to the environment. While those inner layer particles may be hydrophilic, they may not have had the chance to react with the fatty anhydride, keeping them non-hydrophobic. While this is a possibility, there is no scientific evidence to support this idea.

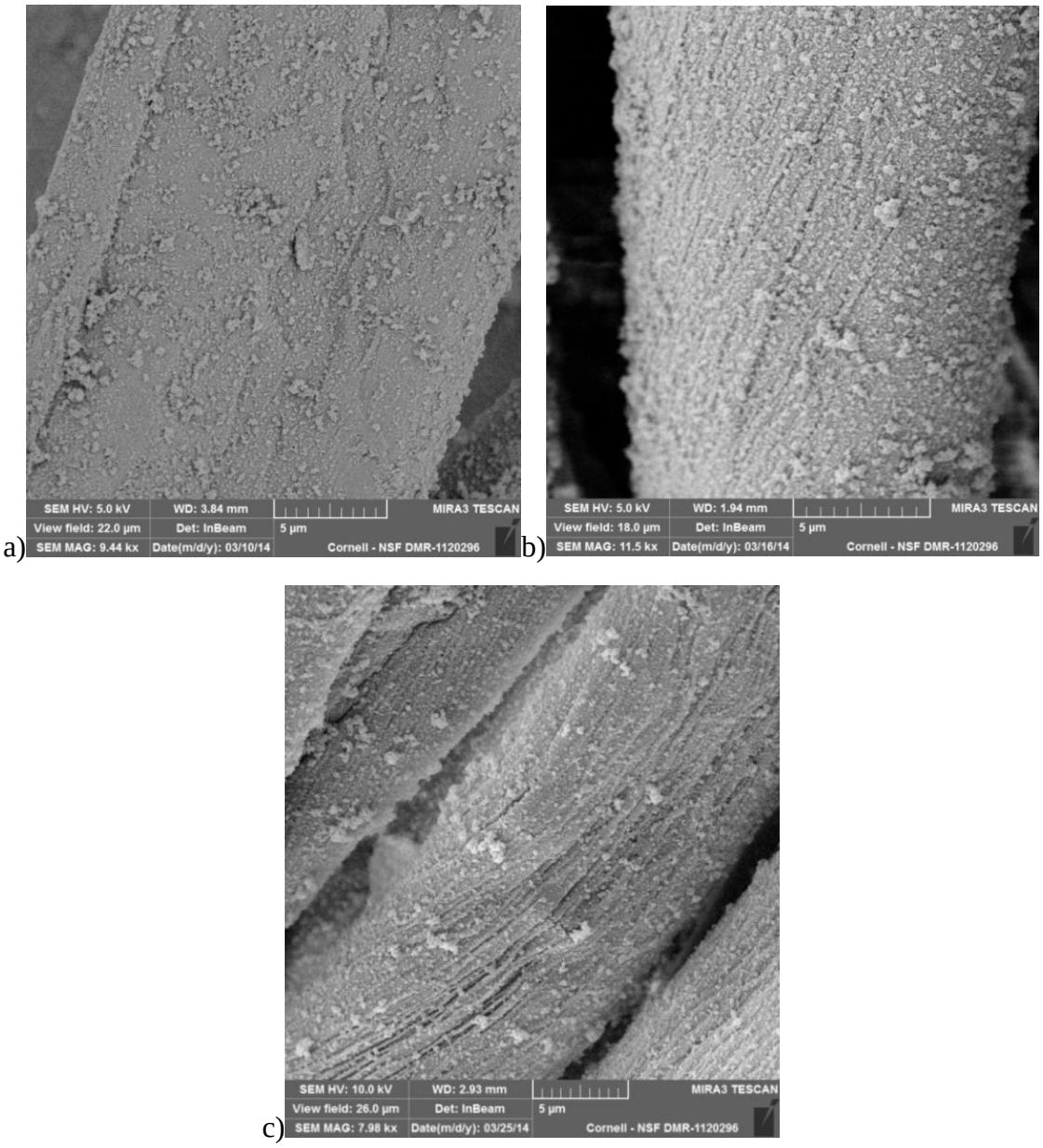

Figure 3.25: SEM image of hydrophobic treated cotton fabric a) taken before laundering; b) taken after 7 laundry cycles; c) taken after 13 laundry cycles

Water contact angle of hydrophobic treated cotton fabric was measured during laundry durability test. Figure 3.26 shows the water contact angle after every two wash cycles. A constantly minor decrease in water contact angle was observed within 8 laundry cycles. After that significant decrease was seen until the cotton fabric was no longer hydrophobic. After 12 laundry cycles, water contact angle decreased to 97.4^{o}, a decrease of about 50^{o} when compared with the unlaundered hydrophobic cotton fabric.

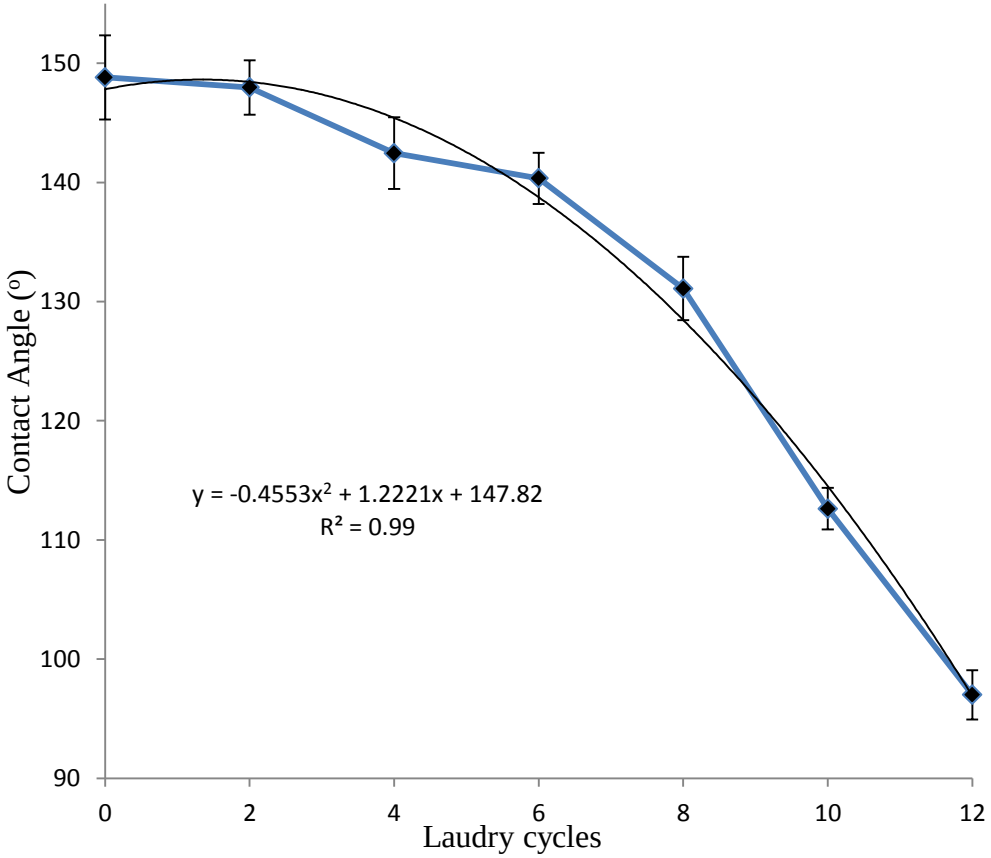

Figure 3.26: Change in water contact angle with laundry cycles

3.16 Cotton fabric with dual-size particles treatment

Previously described methods involve the use of single size particle and only the smaller size amine-silica particles were used (nominal diameter size = 107 nm). In this section, both large (nominal

diameter size = 458 nm) and small size amine-silica particles (nominal diameter size = 107 nm) were deposited onto cotton surface at the same time. 0.1 g of large particles and 0.1 g small particles were dispersed in 50 mL of absolute ethanol. In this case 1 hr of ultrasonication was used to form uniformly dispersed particle dispersion.

Different strategies were used to deposit particles onto cotton surface, namely, physical deposition, crosslinking and green crosslinking methods. Similar procedures as described in section 2.6 were used for particle deposition. Figure 3.27 shows SEM images of cotton fabric with physically deposited dual size particles. Both large and small amine-silica particles are deposited onto the surface of the cotton fabric. Small size particles are evenly distributed on the fiber surface. However, large particles are not completely separated and in most cases, they are connected with each others forming agglomerations.

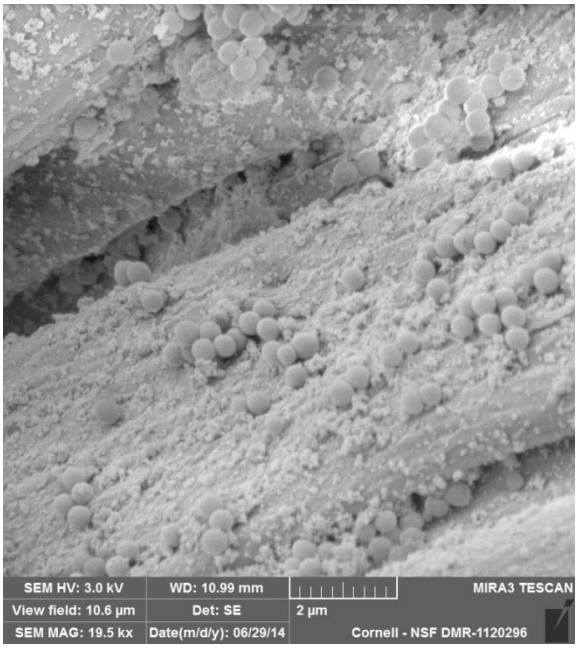

Figure 3.27: SEM image of cotton fabric treated in dual size particle dispersion

Ultrasonication was used to study the removal of dual size particles from cotton surface. It should be noted here that ultrasonication is considered to be much more severe than washing or laundering with

detergent because of the power it has to shake and remove the particles. SEM images of specimens after 10 and 20 min of ultrasonication treatment are shown in Figure 3.28a and Figure 3.28b, respectively. The results were similar to those observed for single size particles. After 10 min of ultrasonication, majority of particles were removed from fiber surface. With further increase in ultrasonication time to 20 min, all large size particles were completely removed. However, one layer of small particles was still present on the fiber surface.

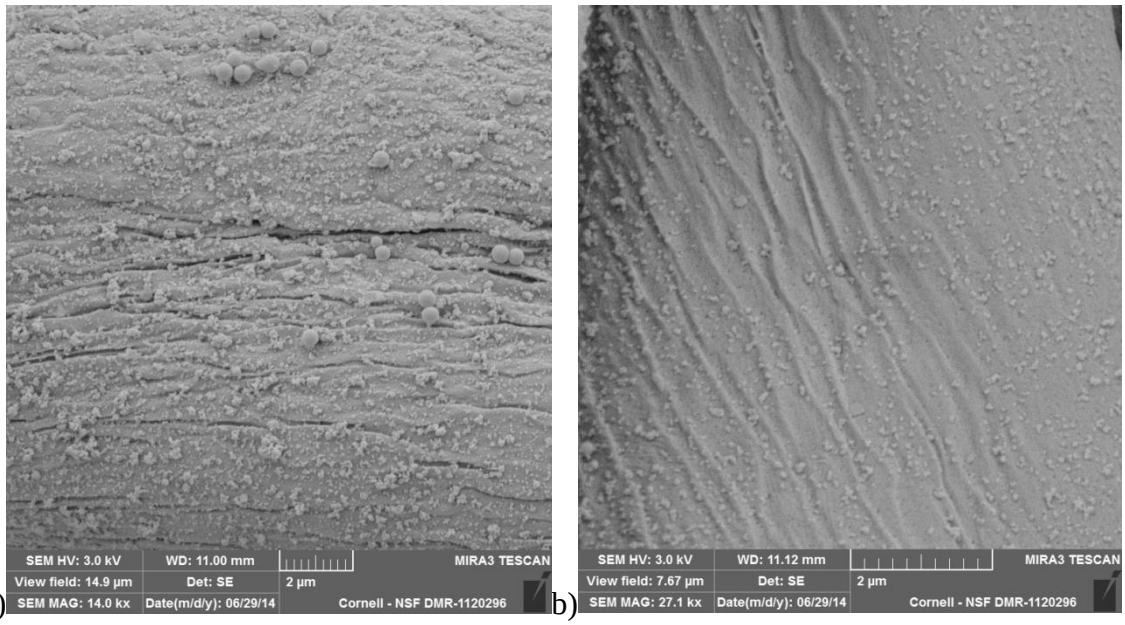

a) b)

Figure 3.28: SEM images of dual size particle deposited cotton fabric surface a) after 10 min ultrasonication; b) after 20 min ultrasonication

3.17 XPS analysis

X-ray photoelectron spectroscopy (XPS) was used to study the surface elemental composition of washed pristine cotton fabric as well as cotton fabric deposited with dual size particles. The XPS spectra of washed pristine cotton fabric and cotton fabrics deposited with dual size particles are shown in Figure 3.29a and Figure 3.29b, respectively. The corresponding XPS elemental composition data are presented in Table 3.9.

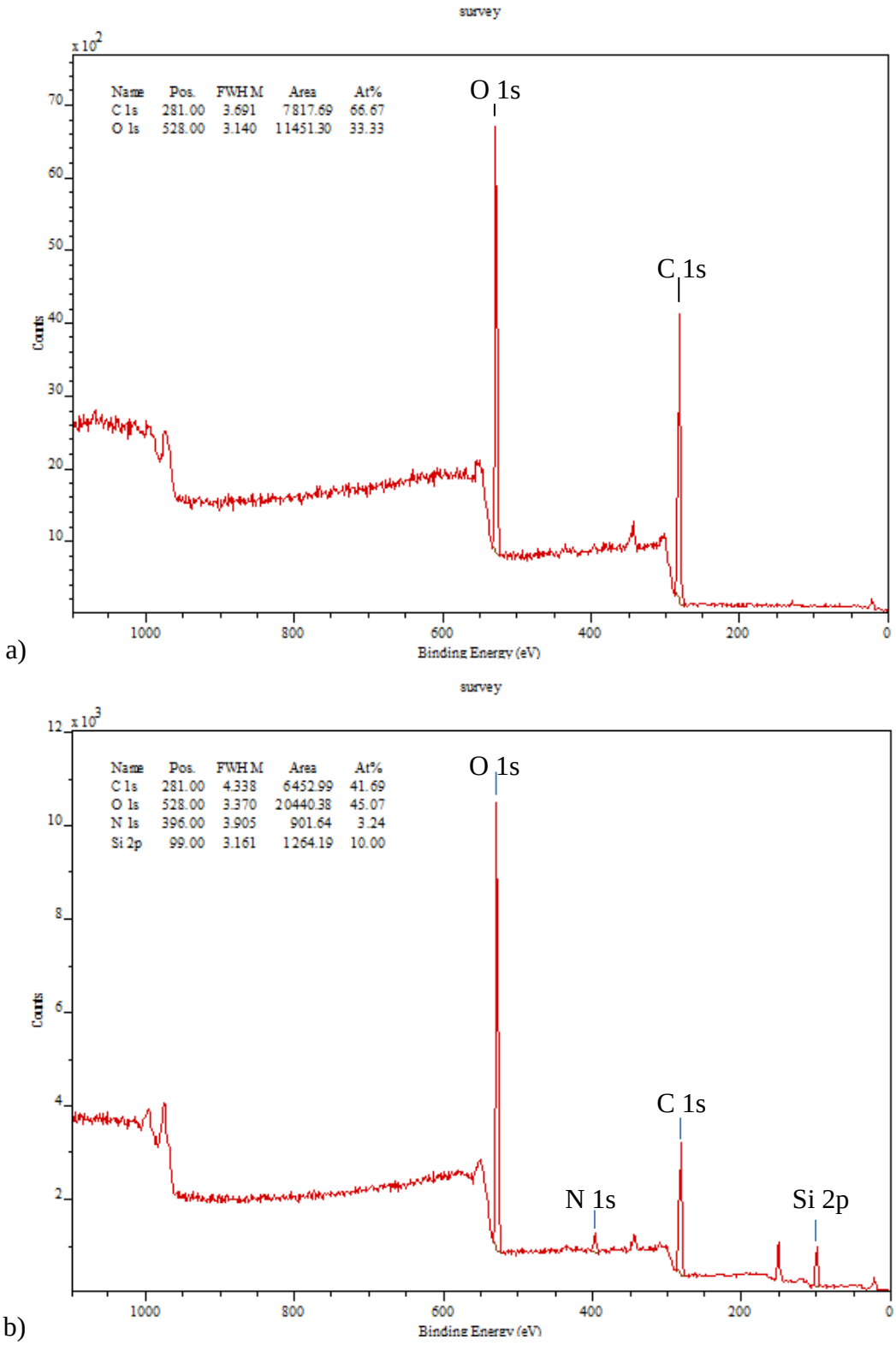

Figure 3.29: XPS spectra of a) washed pristine cotton fabric; b) cotton fabric deposited with amine-silica particles

The pure cellulose (cotton) should have an oxygen-to-carbon atomic ratio (O/C) value of 0.83 based on the chemistry. XPS results, however, showed that O/C value of washed pristine cotton fabric to be only 0.45. Other researchers also have found very similar results (Topalovic *et al.*, 2007); (Xu *et al.*, 2003). After amine-silica deposition, two new peaks appeared on the XPS spectrum for nitrogen and silica. These two new peaks confirmed the successful grafting of amine groups onto silica particles. O/C value also increased after particle deposition because oxygen is a major element in silica particles. Oxygen in amine-silica particles is mainly contained in two bonds: Si-O-Si and Si-OH.

Table 3.9: Results of XPS elemental composition of washed pristine cotton fabric and cotton fabric deposited with amine-silica particles

Element	Washed pristine cotton fabric (%)	Cotton fabric with particles (%)
C	66.67	41.69
O	33.33	45.07
Si	0	3.24
N	0	10.00
O/C	0.45	1.08

3.18 Crosslinking cotton fabric with dual size particles

Cotton fabric with dual size amine-silica particles was also treated with two different crosslinkers as well as BTCA which was used as a green crosslinker. Detailed crosslinking procedures have been described earlier in section 2.6. As mentioned during the crosslinking reaction, both cotton and amine-silica particles can be crosslinked. In addition, crosslinkers act as a chemical bridge between

cellulose and amine-silica particles through covalent bond formation. BTCA reacts with cellulose to form ester bond and with amine groups on amine-silica particle surface to form amide bonds.

Figure 3.30 shows the ATR-FTIR spectra of green crosslinker, i.e., the oxidized sucrose as well as pure sucrose. ATR-FTIR spectrum of oxidized sucrose shows a new peak at 1716 cm^{-1} which is assigned to carbonyl group from aldehyde, carboxyl and, possibly ketone groups generated through oxidation. The desired oxidized form, however, is aldehyde which readily reacts with both amine and hydroxyl groups. The aldehyde-amine reaction is known as Maillard reaction. Carboxyl group is considered to have moderate reactivity and usually requires co-reactant, EDC/NHS to facilitate the reaction (Grabarek and Gregely, 1990). Ketone group does not react with hydroxyl or amine group and, hence, not a desired group.

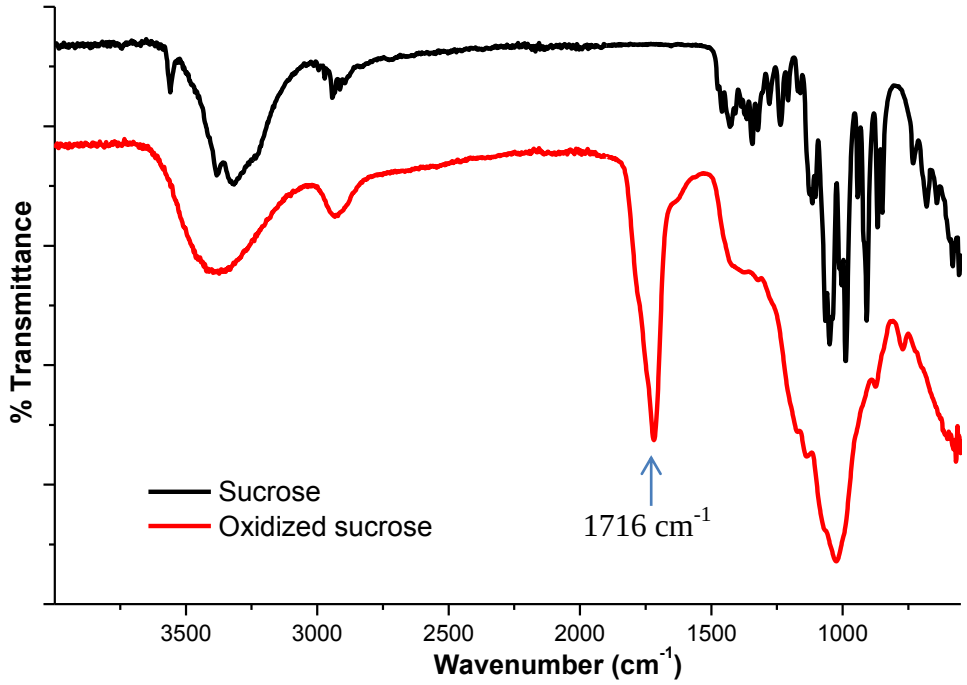

Figure 3.30: ATR-FTIR spectra of sucrose and oxidized sucrose

Hydroxylamine agent was used to quantitatively determine the aldehyde content in oxidized sucrose. Details of this procedure are described in section 2.13. Figure 3.31 shows the chemical structure of sucrose. As it can be seen it contains three primary hydroxyl groups and four secondary hydroxyl groups. The primary hydroxyl groups can be oxidized into aldehyde and carboxyl groups. However, it's not clear whether the secondary hydroxyl groups can be oxidized into ketone groups. Since hydroxylamine can react with both aldehyde and ketone, it is necessary to assume that secondary hydroxyl group cannot be oxidized in this case.

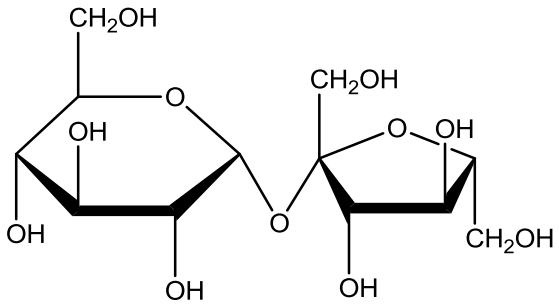

Figure 3.31: Chemical structure of sucrose

Titration results showed that 30.89% of primary hydroxyl groups were oxidized into aldehyde groups. This means that on an average there is one aldehyde group in one oxidized sucrose molecule. As mentioned earlier the oxidized sucrose with two or more aldehyde groups is the desired product as it can crosslink at those locations. Both cellulose and amine-silica nanoparticles, also act as chemical bridge to covalently bonded cellulose and amine-silica particles.

Cotton fabric with dual size amine-silica particles was treated with either BTCA or oxidized sucrose as crosslinker. SEM images of cotton fabric crosslinked by BTCA or oxidized sucrose are shown in Figure 3.32a and Figure 3.32b, respectively. Similar surface morphology was obtained on cotton fabric as compared to physically deposited dual size particles. As can be seen, fiber surface was covered by

both large and small amine-silica particles creating the desired roughness. However, certain degree of agglomeration was obtained in both cases.

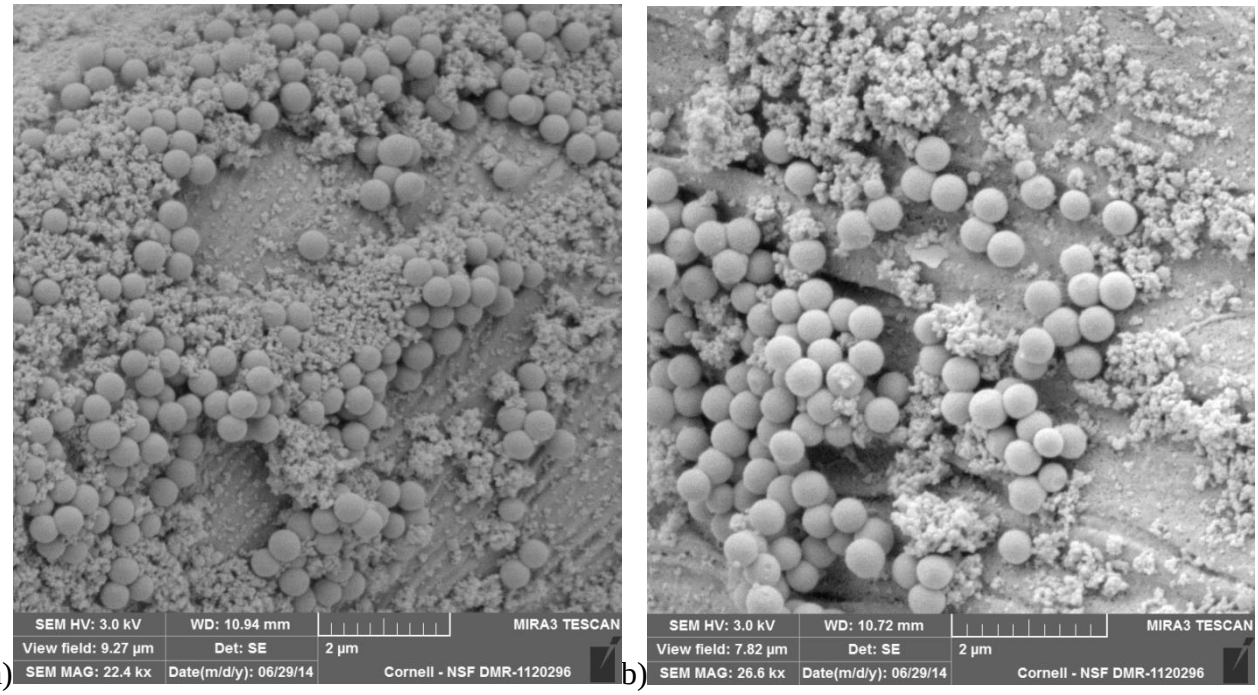

a) b)

Figure 3.32: SEM images of cotton fabric with dual size particles crosslinked by a) BTCA; b) oxidized sucrose

3.19 Ultrasonication treatment of crosslinked cotton fabric with dual size particles

Ultrasonication treatment was used to remove any physically adsorbed or loosely bonded particles. The remaining particles were assumed (or expected) to be crosslinked or covalently bonded to fiber surface. SEM images of crosslinked cotton fabric after ultrasonication treatment are shown in Figure 3.33. Both images show that ultrasonication caused a significant loss of particles on cotton fiber surface. However, BTCA crosslinked specimen (Figure 3.33a) showed more residual particles than the one crosslinked with oxidized sucrose (Figure 3.33b).This is not a surprise since the same weight of crosslinker was used during crosslinking step. While every BTCA molecule, with four carboxyl groups,

can involve in crosslinking, not all oxidized sucrose can be used for crosslinking. Only those oxidized sucrose with two or more aldehyde groups have the crosslinking capability.

a) 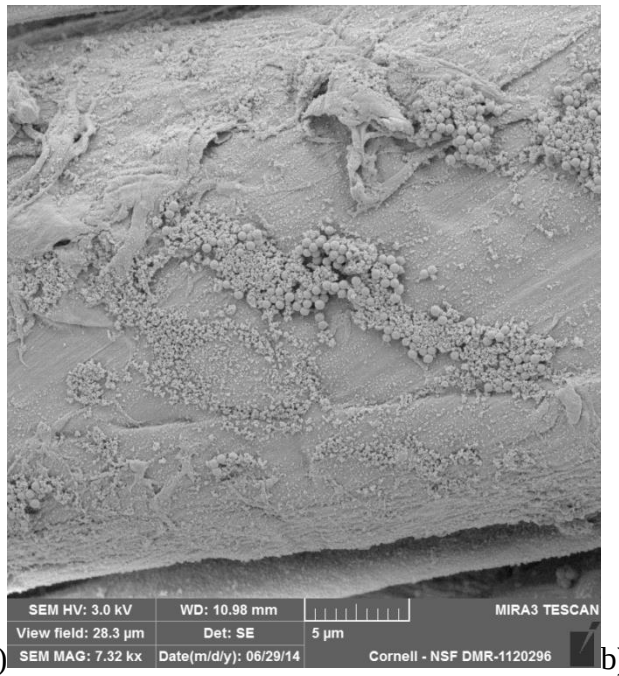

b) 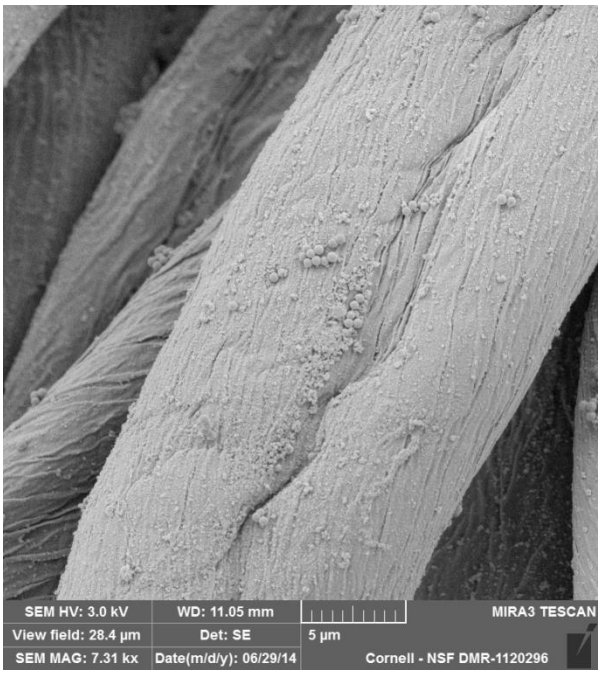

Figure 3.33: SEM images of crosslinked cotton fabric with dual size amine-silica particles after ultrasonication treatment a) BTCA crosslinked; b) oxidized sucrose crosslinked

3.20 Hydrophobic treatment of crosslinked cotton fabric with dual size particles

Cotton fabric with dual size amine-silica particles increased the surface roughness, however, in order to obtain hydrophobicity, cotton fabric still needed to undergo hydrophobic treatment. The procedures described in section 2.4 were used for the hydrophobic treatment. Conditions were set to 100% microwave power and 10 min heating treatment. During the treatment, fatty anhydride was expected to react with both cellulose and amine-silica particles. Fatty anhydrides when reacted with hydroxyl groups on cellulose formed ester bonds, and when formed amide bonds reacted with amine groups on amine-silica particles.

Water contact angle of hydrophobic treated cotton fabrics were measured and the results are presented in Table 3.10. Due to the increased surface roughness and hydrophobicity, all cotton fabrics with surface deposited particles exhibited much higher water contact angles compared to the control (no particle deposited) fabrics as was expected.

Table 3.10: Water contact angle results of hydrophobic cotton fabric with dual size amine-silica particles

Specimen	Water contact angle (^{o})	St. Dev. (^{o})
Control (no particle)	135.51	1.19
BTCA crosslinked cotton fabric with dual sized particles	150.81	3.81
Oxidized sucrose crosslinked cotton fabric with dual sized particles	152.73	3.09
Cotton fabric with physically deposited dual sized particles	153.41	2.33

*all specimens underwent hydrophobic treatment.

Unpaired t-test was used to determine if the water contact angle values were significantly different from one another. Interestingly, at 95% confidence interval, highest and lowest water contact angle values were statistically not different (with the two-tailed P value of 0.3703). In other words, despite the fact that three specimens were treated with different conditions, they had same particle deposition and hydrophobic treatment process (100% microwave power level and 10 min heating). Similar surface roughness as well as same surface energy resulted in identical water contact angle.

3.21 Laundry durability test for cotton fabric with dual size amine-silica particles

Hydrophobic cotton fabrics with dual size amine-silica particles were washed with Tide® detergent to test its laundry durability. Table 3.11 shows the number of laundry cycles needed to lose their hydrophobicity. Hydrophobic cotton fabric treated with physical deposition method lost its hydrophobicity after 5 laundry cycles. Hydrophobic cotton fabric after crosslinking treatment showed a higher durability than physical deposition method. Oxidized sucrose crosslinked specimen showed 11 laundry cycle durability, and BTCA crosslinked specimen showed 24 laundry cycles durability. However, all these three specimens exhibited lower laundry durability than the control (no particle but hydrophobic treated), which lost its hydrophobicity after 31 cycles of laundry.

Table 3.11: Laundry durability test for hydrophobic cotton fabric with dual size particles

Specimen	Laundry cycle
Control (no particle)	31
Cotton fabric with physically deposited dual sized particles	5
BTCA crosslinked cotton fabric with dual sized particles	24
Oxidized sucrose crosslinked cotton fabric with dual sized particles	11

*all specimens underwent hydrophobic treatment.

The possible reasons contributing to the loss of hydrophobicity during laundry durability test listed as followings: 1) Detergent will aid removal of particles during washing. Also, the cellulase can remove the top layer of the molecules. 2) Chemical bonding between particles and cellulose may be hydrolyzed by detergent.

4. CONCLUSIONS

Fatty acid was converted into more reactive form, fatty anhydride, by using acetic anhydride as co-reactant. HPLC and ATR-FTIR spectroscopy were used to successfully track the fatty anhydride conversion process.

With the presence of fatty anhydride, longer microwave heating time and higher power level resulted in higher contact angles of hydrophobic cotton fabrics. Cotton fabric treated in 100% microwave power and 15 min along with fatty anhydride resulted in a water contact angle of over 137^{o} making it hydrophobic

Fatty anhydride prepared by either heptanoic acid or stearic acid showed no statistical difference in the hydrophobicity of treated cotton fabrics.

100% power level and 15 min microwave treated cotton fabrics showed laundering durability of up to 37 cycles. However, the yarns showed significant reduction in strength under these conditions; about 50% strength was retained. 37 laundering cycles are equivalent to 185 normal home washings.

Fatty acid hydrophobic treatment showed no significant effect to fiber surface topography.

Silica particles with two different sizes (450 nm and 100 nm) were prepared based on Stöber method. APTES was used to attach amine group onto silica particles.

Ninhydrin test was successfully used to determine the amine content on silica particles. XPS analysis results confirmed the presence of nitrogen in amine-silica particles. However, ATR-FTIR spectra of amine-silica particles didn't show peak for amine group because of its lower sensitivity.

Ultrasonication was shown to remove the physically adsorbed amine-silica particles on cotton fibers. Ultrasonication was shown to remove large size particles agglomeration more than the small particles.

Water contact angle of 144.9^{o} was achieved by deposition of single size amine-silica particles (d = 107 nm) onto cotton fabrics that was followed by hydrophobic treatment (100% Power/10 min). About 10^{o} increase of water contact angle was obtained when compared with control fabric with same hydrophobic treatment but with no particles deposited. This was due to the surface roughness generated by the particles.

BTCA crosslinked cotton fabrics with dual size amine-silica particles which underwent ultrasonication showed majority of particles to remain on the fiber surface. Resulting crosslinked and hydrophobic cotton fabric allowed 24 cycles of laboratory laundering without the loss of hydrophobicity.

Water contact angle of over 153^{o} (superhydrophobicity) was achieved when cotton fabric dual size particles were physically adsorbed on to the fabric and followed by hydrophobic treatment (100% Power/10 min).

5. FUTURE SUGGESTIONS

In the present study fatty anhydride was prepared by mixing fatty acid and acetic anhydride under microwave heating. The fatty anhydride was further reacted with cotton fabric to allow esterification to take place, using microwave heating. It is, perhaps, necessary to prepare fatty anhydride using microwave heating because the evaporation of fatty acid and fatty-acetic anhydride require high temperature. Boiling points of heptanoic acid and stearic acid are 223 ℃ and 382 ℃, respectively. Their mix anhydride forms are expected to have even higher boiling point. However, in the case of reacting the fatty anhydride with cotton fabric, temperatures around 120 – 150 ℃ may be adequate for the reaction to take place. In this case, conventional thermal heating method may give better result than microwave heating. The major advantages of thermal heating are that the reaction temperature can be controlled and high temperature, which will cause the degradation of cellulose, can be avoided.

The amine-silica particles used in this study were prepared based on Stöber method, which use TEOS and APTES as initial materials. Both TEOS and APTES are petroleum based materials. However, recent studies have shown that silica nanoparticles can be prepared from rice husk, a material that is sustainable and very inexpensive (Liu et al., 2013); (Wang et al., 2012). By replacing the current amine-silica particle method with rice husk method the process can be made much 'greener'. However, silica particles will not react with fatty anhydride or BTCA. This means silica particles prepared by rice husk method will need further surface functionalization. It can be challenging to find an appropriate 'green' chemical for the surface functionalization.

Oxidized sucrose, as a 'green' crosslinker was used to crosslink amine-silica particles and cotton fabric. In this case about 31% of primary hydroxyl groups of sucrose were oxidized into aldehyde

groups. This means there is on an average one aldehyde group in each oxidized sucrose molecule. For crosslinking a minimum of two aldehyde groups are required. A method is needed to maximize the aldehyde groups.

Hydrogen peroxide was used to oxidize sucrose, once the reaction is finished. Once the reaction is complete, it's necessary to remove hydrogen peroxide before the oxidized sucrose solution is dried in an oven at around 50^{o}C for about 2 days. It's possible that the remaining hydrogen peroxide will cause further oxidation of hydroxyl or aldehyde groups. Few methods are available for the effective removal of hydrogen peroxide. As example, catalase, an enzyme to decompose hydrogen peroxide to water and oxygen (Chance et al., 1955), may be used. Another example may be ferric ion catalyzed decomposition of hydrogen peroxide (Walling and Goosen, 1973).

6. REFERENCES

Antova, Ginka, Palmira Vasvasova, and Magdalen Zlatanov. "Studies upon the synthesis of cellulose stearate under microwave heating." *Carbohydrate Polymers* 57, no. 2 (2004): 131-134.

Athauda, Thushara J., Wesley Williams, Kenneth P. Roberts, and Ruya R. Ozer. "On the surface roughness and hydrophobicity of dual-size double-layer silica nanoparticles." *Journal of Materials Science* 48, no. 18 (2013): 6115-6120.

Barthlott, Wilhelm, and Christoph Neinhuis. "Purity of the sacred lotus, or escape from contamination in biological surfaces." *Planta* 202, no. 1 (1997): 1-8.

Bellanger, Hervé, Thierry Darmanin, Elisabeth Taffin de Givenchy, and Frédéric Guittard. "Chemical and physical pathways for the preparation of superoleophobic surfaces and related wetting theories." *Chemical Reviews* 114, no. 5 (2014): 2694-2716.

Bhat, N. V., A. N. Netravali, A. V. Gore, M. P. Sathianarayanan, G. A. Arolkar, and R. R. Deshmukh. "Surface modification of cotton fabrics using plasma technology." *Textile Research Journal* (2011): 0040517510397574.

Bico, José, Uwe Thiele, and David Quéré. "Wetting of textured surfaces." *Colloids and Surfaces A: Physicochemical and Engineering Aspects* 206, no. 1 (2002): 41-46.

Blossey, Ralf. "Self-cleaning surfaces—virtual realities." *Nature Materials* 2, no. 5 (2003): 301-306.

Byun, Doyoung, Jongin Hong, Jin Hwan Ko, Young Jong Lee, Hoon Cheol Park, Bong-Kyu Byun, and Jennifer R. Lukes. "Wetting characteristics of insect wing surfaces." *Journal of Bionic Engineering* 6, no. 1 (2009): 63-70.

Cassie, A. B. D., and S. Baxter. "Wettability of porous surfaces." *Transactions of the Faraday Society* 40 (1944): 546-551.

Chauvelon, G., L. Saulnier, A. Buleon, J‐F. Thibault, C. Gourson, R. Benhaddou, R. Granet, and P. Krausz. "Acidic activation of cellulose and its esterification by long‐chain fatty acid." *Journal of Applied Polymer Science* 74, no. 8 (1999): 1933-1940.

Chen, Song, Akiyoshi Osaka, Satoshi Hayakawa, Kanji Tsuru, Eiji Fujii, and Koji Kawabata. "Novel one-pot sol-gel preparation of amino-functionalized silica nanoparticles." *Chemistry Letters* 37, no. 11 (2008): 1170-1171.

Christie, William W. "Preparation of ester derivatives of fatty acids for chromatographic analysis." *Advances in Lipid Methodology* 2, no. 69 (1993): e111.

Dankovich, Theresa A., and You-Lo Hsieh. "Surface modification of cellulose with plant triglycerides for hydrophobicity." *Cellulose* 14, no. 5 (2007): 469-480.

Dastidar, Trina Ghosh, and Anil N. Netravali. "A soy flour based thermoset resin without the use of any external crosslinker." *Green Chemistry* 15, no. 11 (2013): 3243-3251.

Deng, Bo, Ren Cai, Yang Yu, Haiqing Jiang, Chunlei Wang, Jiang Li, Linfan Li. "Laundering durability of superhydrophobic cotton fabric." *Advanced Materials* 22, no. 48 (2010): 5473-5477.

Edgar, Kevin J., Charles M. Buchanan, John S. Debenham, Paul A. Rundquist, Brian D. Seiler, Michael C. Shelton, and Debra Tindall. "Advances in cellulose ester performance and application." *Progress in Polymer Science* 26, no. 9 (2001): 1605-1688.

Gao, Xuefeng, and Lei Jiang. "Biophysics: water-repellent legs of water striders." *Nature* 432, no. 7013 (2004): 36-36.

Grabarek, Zenon, and John Gergely. "Zero-length crosslinking procedure with the use of active esters." *Analytical Biochemistry* 185, no. 1 (1990): 131-135.

Guo, Zhiguang, and Weimin Liu. "Biomimic from the superhydrophobic plant leaves in nature: Binary structure and unitary structure." *Plant Science* 172, no. 6 (2007): 1103-1112.

Hansen, W. R., and K. Autumn. "Evidence for self-cleaning in gecko setae." *Proceedings of the National Academy of Sciences of the United States of America* 102, no. 2 (2005): 385-389.

Heinze, Thomas, Tim Liebert, and Andreas Koschella. *Esterification of polysaccharides*. Springer, 2006.

Heinze, Thomas, and Wolfgang G. Glasser. *Cellulose derivatives: modification, characterization, and nanostructures.* Vol. 688. An American Chemical Society Publication, 1998.

Heinze, Th, and T. Liebert. "Unconventional methods in cellulose functionalization." *Progress in Polymer Science* 26, no. 9 (2001): 1689-1762.

Heinze, U., and W. Wagenknecht. "Comprehensive cellulose chemistry: functionalisation of cellulose." (1998).

Hekster, Floris M., Remi WPM Laane, and Pim de Voogt. "Environmental and toxicity effects of

perfluoroalkylated substances." In *Reviews of Environmental Contamination and Toxicology*, pp. 99-121. Springer New York, 2003.

Hikita, Masaya, Keiji Tanaka, Tetsuya Nakamura, Tisato Kajiyama, and Atsushi Takahara. "Super-liquid-repellent surfaces prepared by colloidal silica nanoparticles covered with fluoroalkyl groups." *Langmuir* 21, no. 16 (2005): 7299-7302.

Hoefnagels, H. F., Di Wu, G. De With, and W. Ming. "Biomimetic superhydrophobic and highly oleophobic cotton textiles." *Langmuir* 23, no. 26 (2007): 13158-13163.

Hon, David N-S., ed. *Chemical modification of lignocellulosic materials*. CRC Press, 1995.

Jandura, Peter, Bohuslav V. Kokta, and Bernard Riedl. "Fibrous long‐chain organic acid cellulose esters and their characterization by diffuse reflectance FTIR spectroscopy, solid‐state CP/MAS ^{13}C‐NMR, and X‐ray diffraction." *Journal of Applied Polymer Science* 78, no. 7 (2000): 1354-1365.

Ji, Jian, Jinhong Fu, and Jicong Shen. "Fabrication of a superhydrophobic surface from the amplified exponential growth of a multilayer." *Advanced Materials* 18, no. 11 (2006): 1441-1444.

Klemm, Dieter, Brigitte Heublein, Hans‐Peter Fink, and Andreas Bohn. "Cellulose: fascinating biopolymer and sustainable raw material." *Angewandte Chemie International Edition* 44, no. 22 (2005): 3358-3393.

Lai, Yue-Kun, Zhong Chen, and Chang-Jian Lin. "Recent progress on the superhydrophobic surfaces with special adhesion: from natural to biomimetic to functional." *Journal of Nanoengineering and Nanomanufacturing* 1, no. 1 (2011): 18-34.

Li, Xue-Mei, David Reinhoudt, and Mercedes Crego-Calama. "What do we need for a superhydrophobic surface? A review on the recent progress in the preparation of superhydrophobic surfaces." *Chemical Society Reviews* 36, no. 8 (2007): 1350-1368.

Li, Yang, Shanshan Chen, Mengchun Wu, and Junqi Sun. "All Spraying Processes for the Fabrication of Robust, Self‐Healing, Superhydrophobic Coatings." *Advanced Materials* 26, no. 20 (2014): 3344-3348.

Liebert, Tim F., and Thomas Heinze. "Tailored cellulose esters: synthesis and structure determination." *Biomacromolecules* 6, no. 1 (2005): 333-340.

Ma, Minglin, and Randal M. Hill. "Superhydrophobic surfaces." *Current Opinion in Colloid & Interface Science* 11, no. 4 (2006): 193-202.

Maim, C. J., J. W. Mench, D. L. Kendall, and G. D. Hiatt. "Aliphatic acid esters of cellulose: preparation by acid-chloride-pyridine procedure." *Industrial & Engineering Chemistry* 43, no. 3 (1951): 684-688.

Martines, Elena, Kris Seunarine, Hywel Morgan, Nikolaj Gadegaard, Chris DW Wilkinson, and Mathis O. Riehle. "Superhydrophobicity and superhydrophilicity of regular nanopatterns." *Nano letters* 5, no. 10 (2005): 2097-2103.

Navard, Patrick ed. *The European Polysaccharide Network of Excellence (EPNOE)*, Springer-Verlag Wien, 2012.

Nishino, Takashi, Masashi Meguro, Katsuhiko Nakamae, Motonori Matsushita, and Yasukiyo Ueda. "The lowest surface free energy based on-CF3 alignment." *Langmuir* 15, no. 13 (1999): 4321-4323.

Oliveira, Nuno M., Rui L. Reis, and João F. Mano. "Superhydrophobic surfaces engineered using diatomaceous earth." *ACS Applied Materials & Interfaces* 5, no. 10 (2013): 4202-4208.

Peydecastaing, Jerome, Carlos Vaca‐Garcia, and Elisabeth Borredon. "Consecutive reactions in an oleic acid and acetic anhydride reaction medium." *European Journal of Lipid Science and Technology* 111, no. 7 (2009): 723-729.

Qian, Baitai, and Ziqiu Shen. "Fabrication of superhydrophobic surfaces by dislocation-selective chemical etching on aluminum, copper, and zinc substrates." *Langmuir* 21, no. 20 (2005): 9007-9009.

Ramaratnam, Karthik, Volodymyr Tsyalkovsky, Viktor Klep, and Igor Luzinov. "Ultrahydrophobic textile surface via decorating fibers with monolayer of reactive nanoparticles and non-fluorinated polymer." *Chemical Communications* 43 (2007): 4510-4512.

Roach, Paul, Neil J. Shirtcliffe, and Michael I. Newton. "Progress in superhydrophobic surface development." *Soft Matter* 4, no. 2 (2008): 224-240.

Romei, Francesca. *Leonardo Da Vinci*. The Oliver Press, Inc., 2008.

Samaranayake, Gamini, and Wolfgang G. Glasser. "Cellulose derivatives with low DS. I. A novel acylation system." *Carbohydrate Polymers* 22, no. 1 (1993): 1-7.

Saito, Akira. "Material design and structural color inspired by biomimetic approach." *Science and Technology of Advanced Materials* 12, no. 6 (2011): 064709.

Satge, C., B. Verneuil, P. Branland, R. Granet, P. Krausz, J. Rozier, and C. Petit. "Rapid homogeneous esterification of cellulose induced by microwave irradiation." *Carbohydrate Polymers* 49, no. 3 (2002): 373-376.

Shirtcliffe, Neil J., Glen McHale, Michael I. Newton, Carole C. Perry, and Paul Roach. "Porous materials show superhydrophobic to superhydrophilic switching." *Chemical Communications* 25 (2005): 3135-3137.

Soto-Cantu, Erick, Rafael Cueto, Jerome Koch, and Paul S. Russo. "Synthesis and rapid characterization of amine-functionalized silica." *Langmuir* 28, no. 13 (2012): 5562-5569.

Sricharussin, W., W. Ryo-Aree, W. Intasen, and S. Poungraksakirt. "Effect of boric acid and BTCA on tensile strength loss of finished cotton fabrics." *Textile Research Journal* 74, no. 6 (2004): 475-480.

Stöber, Werner, Arthur Fink, and Ernst Bohn. "Controlled growth of monodisperse silica spheres in the micron size range." *Journal of Colloid and Interface Science* 26, no. 1 (1968): 62-69.

Sun, Taolei, Lin Feng, Xuefeng Gao, and Lei Jiang. "Bioinspired surfaces with special wettability." *Accounts of Chemical Research* 38, no. 8 (2005): 644-652.

Topalovic, Tatjana, Vincent A. Nierstrasz, Lorenzo Bautista, Dragan Jocic, Antonio Navarro, and Marijn MCG Warmoeskerken. "XPS and water contact angle study of cotton surface oxidation by catalytic bleaching." *Colloids and Surfaces A: Physicochemical and Engineering Aspects* 296, no. 1 (2007): 76-85.

Tuteja, Anish, Wonjae Choi, Minglin Ma, Joseph M. Mabry, Sarah A. Mazzella, Gregory C. Rutledge, Gareth H. McKinley, and Robert E. Cohen. "Designing superoleophobic surfaces." *Science* 318, no. 5856 (2007): 1618-1622.

Vaca-Garcia, C., S. Thiebaud, M. E. Borredon, and Giuseppe Gozzelino. "Cellulose esterification with fatty acids and acetic anhydride in lithium chloride/N, N-dimethylacetamide medium." *Journal of the American Oil Chemists' Society* 75, no. 2 (1998): 315-319.

Wang, Pinglang, and Bernard Y. Tao. "Synthesis and characterization of long‐chain fatty acid cellulose ester (FACE)." *Journal of Applied Polymer Science* 52, no. 6 (1994): 755-761.

Wang, Weixing, Jarett C. Martin, Xiaotian Fan, Aijie Han, Zhiping Luo, and Luyi Sun. "Silica nanoparticles and frameworks from rice husk biomass." *ACS Applied Materials & Interfaces* 4, no. 2 (2012): 977-981.

Wenzel, Robert N. "Resistance of solid surfaces to wetting by water." *Industrial & Engineering Chemistry* 28, no. 8 (1936): 988-994.

Wolfs, Melanie, Thierry Darmanin, and Frederic Guittard. "Superhydrophobic fibrous polymers."

Polymer Reviews 53, no. 3 (2013): 460-505.

Wooh, Sanghyuk, Jai Hyun Koh, Soojin Lee, Hyunsik Yoon, and Kookheon Char. "Trilevel‐Structured Superhydrophobic Pillar Arrays with Tunable Optical Functions." *Advanced Functional Materials* (2014).

Wu, Jin, Jun Zhang, Hao Zhang, Jiasong He, Qiang Ren, and Meili Guo. "Homogeneous acetylation of cellulose in a new ionic liquid." *Biomacromolecules* 5, no. 2 (2004): 266-268.

Xu, Bi, and Zaisheng Cai. McCord, M. G., Y. J. Hwang, Y. Qiu, L. K. Hughes, and M. A. Bourham. "Surface analysis of cotton fabrics fluorinated in radio‐frequency plasma." *Journal of Applied Polymer Science* 88, no. 8 (2003): 2038-2047.

Xue, Chao-Hua, Shun-Tian Jia, Jing Zhang, and Li-Qiang Tian. "Superhydrophobic surfaces on cotton textiles by complex coating of silica nanoparticles and hydrophobization." *Thin Solid Films* 517, no. 16 (2009): 4593-4598.

Yan, Y. Y., N. Gao, and W. Barthlott. "Mimicking natural superhydrophobic surfaces and grasping the wetting process: A review on recent progress in preparing superhydrophobic surfaces." *Advances in Colloid and Interface Science* 169, no. 2 (2011): 80-105.

Yang, Charles Q. "FT-IR spectroscopy study of the ester crosslinking mechanism of cotton cellulose." *Textile Research Journal* 61, no. 8 (1991): 433-440.

Yang, Shuai, Jie Ju, Yuchen Qiu, Yaxu He, Xiaolin Wang, Shixue Dou, Kesong Liu, and Lei Jiang. "Peanut leaf inspired multifunctional surfaces." *Small* 10, no. 2 (2014): 294-299.

Yu, Minghua, Guotuan Gu, Wei-Dong Meng, and Feng-Ling Qing. "Superhydrophobic cotton fabric coating based on a complex layer of silica nanoparticles and perfluorooctylated quaternary ammonium silane coupling agent." *Applied Surface Science* 253, no. 7 (2007): 3669-3673.

Zhou, Hua, Hongxia Wang, Haitao Niu, Adrian Gestos, Xungai Wang, and Tong Lin. "Fluoroalkyl silane modified silicone rubber/nanoparticle composite: A super durable, robust superhydrophobic fabric coating." *Advanced Materials* 24, no. 18 (2012): 2409-2412.

Zimmermann, Jan, Felix A. Reifler, Giuseppino Fortunato, Lutz‐Christian Gerhardt, and Stefan Seeger. "A Simple, One‐Step Approach to Durable and Robust Superhydrophobic Textiles." *Advanced Functional Materials* 18, no. 22 (2008): 3662-3669.